「The study of radiation-induced chromosome aberrations in humans and mice for the improvement of cytogenetic biodosimetry and furthered understanding of low dose-rate ionizing radiation」

「細胞遺伝学的線量評価法の改善のためのヒトとマウスにおける放射線誘発染色体異常に関する研究および低線量率電離放射線のさらなる理解」

弘前大学大学院保健学研究科保健学専攻

提出者氏名：Valerie Goh Swee Ting

所　　属：　生体検査科学領域

指導教員：　三浦富智

Page of Contents

Introduction (Overall thesis)

Ionizing radiation exposure causes various types of DNA damage in cells depending on radiation dose and linear energy transfer (LET). High LET radiation such as α particles and high dose/dose-rate radiation primarily induce DNA damage by direct action, by directly depositing energy into DNA. Low LET radiation such as X-rays and γ-rays can also induce DNA damage by indirect action, where free radicals and reactive oxygen species, produced by the photolysis of water molecules, oxidize DNA bases[1)]. Non-targeted radiation effects are also possible, especially in low dose/dose-rate radiation. As opposed to the traditional theory of DNA damage induction in irradiated cells only, non-targeted cells surrounding irradiated cells could also show DNA damage caused by radiation-induced bystander effects (RIBE)[2)].

In the 1960s, classical cytogenetic biodosimetry was established after a clear dose-response relationship between chromosome aberration frequency and increasing radiation dose was observed[3)]. Cytogenetic biodosimetry is the use of established cytogenetic endpoints to estimate dose exposed in an individual suspected of prior radiation exposure, usually after a radiation accident[4)]. The four cytogenetic endpoints, as recommended by the International Atomic Energy Agency (IAEA) in EPR-Biodosimetry, are dicentric chromosomes (Dic) (chromosomes with two centromeres), micronuclei (MN) (small nuclei formed), translocations (Tr) (transfer of genetic material within or between chromosomes) and prematurely condensed chromosome (PCC) rings[5)] (Figure 1). These cytogenetic endpoints indicate the presence of DNA damage caused by ionizing radiation.

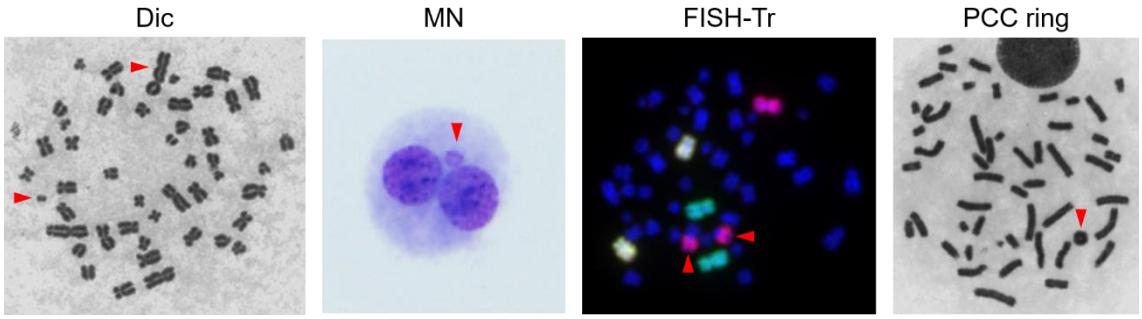

Figure 1: Established chromosome aberrations for cytogenetic biodosimetry (red arrows). From left to right: dicentric chromosome (Dic) and its associated acentric fragment, micronucleus (MN), translocation detected with fluorescence *in situ* hybridization (FISH-Tr) and ring chromosome in prematurely condensed chromosomes (PCC ring).

DNA damage in human peripheral blood lymphocytes is analyzed as peripheral blood is easy to access, the dose to lymphocyte nuclei is a good approximation to the dose

to soft tissue for photons and neutrons, and whole body dose can be estimated[5]. Both whole blood (WB) and peripheral mononuclear cells (PBMCs) isolated from WB with density centrifugation are used for cell culture[5]. The type of aberration used for cytogenetic biodosimetry depends on various factors such as half-life, detectable dose range, minimum dose estimated, type of dose exposure, radiation specificity and the presence of internationally standardized manuals[5-6]. For acute dose estimation for partial and whole-body exposures from 0.1 to 5 Gy, Dic is usually used as it is often regarded as the gold standard of cytogenetic biodosimetry due to its high radiation specificity and very low background frequency[7]. In contrast, MN can be used for acute whole-body dose estimation from 0.3 to 4 Gy, but background MN frequency is influenced by donor age, sex and lifestyle[8]. On the other hand, Tr analysis is useful for retrospective dosimetry[9-10] due to its long half-life in cells without unstable aberrations[11]. Lastly, the analysis of PCC rings is useful for acute high doses of 5 to 20 Gy as chromosome condensation for PCC analysis is independent of cells entering mitosis[12].

Dose estimation with cytogenetic biodosimetry proved to be useful in previous cases of accidental radiation exposures, such as the Goiânia incident in Brazil[13], the radiological accident in Istanbul, Turkey[14], the Nueva Aldea incident in Chile[15] and the JCO Tokai-Mura incident in Japan[16]. It can also be used to analyze excess radiation damage and possible excess cancer risk in residents living in high background radiation areas[17-18] or in areas with previous nuclear accidents[19-20], and in occupational exposure of medical radiologists[21] and nuclear radiation clean-up workers[22-23]. Furthermore, cytogenetic biodosimetry can be used in a mass-casualty event caused by radiation exposures from accidents or malicious acts for triage assessment[24]. In such an event, rapid and reliable identification of individuals exposed to ≥ 2 Gy whole-body equivalent dose from the worried-well is necessary for fast medical response[25].

For dose estimation to be reliably performed, a well-established dose-response calibration curve (DRC) must be constructed with acutely irradiated human peripheral blood from multiple healthy donors. For low LET radiation, a linear-quadratic relationship between aberration yield and increasing dose is seen ($Y = C + \alpha D + \beta D^2$, where C, α, β are coefficients, Y is aberration yield and D is dose) (Figure 2).

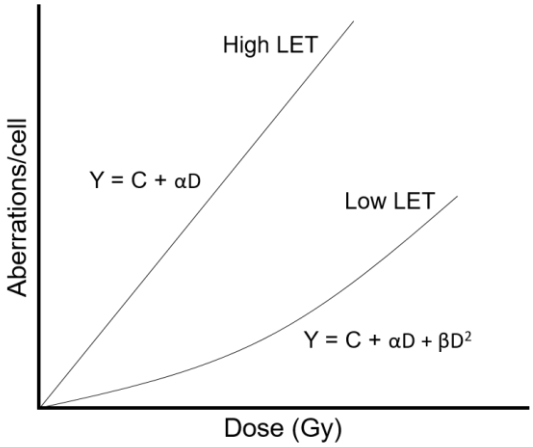

Figure 2: Dose-response calibration curves (DRC) of each radiation quality. For radiation with high linear energy transfer (LET), a linear relationship $Y = C + \alpha D$ is seen between aberration frequency and dose. For low LET radiation, a linear-quadratic equation $Y = C + \alpha D + \beta D^2$ is seen between aberration frequency and dose. [Adapted from EPR-Biodosimetry[5)]]

Dic and other aberrations are assumed to be formed as a result of a DNA double-strand break (DSB). Thus, components of the DRC equation correspond to background frequency of aberrations (C), DSBs formed by a single ionizing track traversing two double helices (αD) and DSBs formed by two different ionizing tracks traversing two double helices (βD^2) (Figure 3). In sparsely ionizing low-LET radiation, βD^2 dominates αD as DSB formation is likely caused by multiple different tracks[26)].

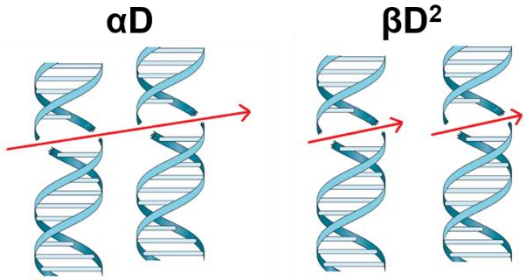

Figure 3: Ionizing radiation tracks causing DNA double-strand breaks (DSB), corresponding to αD and βD^2 of the DRC equation. For αD, a single ionizing track traverses both sides of the double helix to cause DSB. For βD^2, two double helices are broken by two different tracks for DSB formation. [Adapted from IAEA Module 8 Part 1[26)]]

Poisson distribution is often assumed for aberration distribution, especially for Dic[27)]. As the probability of ionizing radiation tracks traversing cell nuclei is considered as a discrete event (Figure 4), DSBs and chromosome aberrations arising from ionizing radiation are hence also discrete.

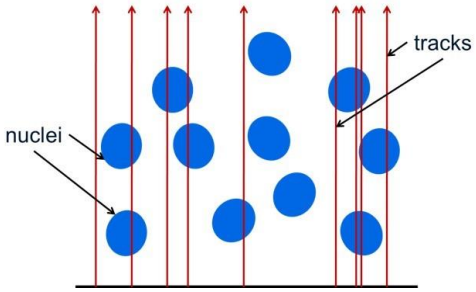

Figure 4: Ionizing radiation tracks traversing cell nuclei as random discrete events. [Adapted from IAEA Module 8 Part 1[26)]]

As such, the aberration distribution of each dose point for DRC construction should always be verified first for a Poisson distribution. If Poisson assumption is rejected, weighting factors should be corrected according to the dispersion index, or a different regression model (e.g. Quasipoisson, Negative Binomial, Hermite distribution) should be used[26)]. According to the documents (17099[28)]; 19238[29)]; 20046[30)]) published by the International Organization of Standardization (ISO), ≥ 5 dose points should be used for 0 to 1 Gy, while ≥ 7 dose points should be used for the entire curve. For statistical reliability, a high number of cells should also be analyzed, especially in lower doses as chromosome aberration frequency is low. Lastly, information related to DRC construction should be comprehensively reported by each laboratory, such as the DRC coefficients and their standard errors and *p*-values, goodness-of-fit results with Pearson's chi-squared test[31)] and DRC validation with blind or known doses[32)].

Similarly, dose estimation is performed by directly solving the DRC equation with the aberration yield of the individual suspected of radiation exposure (Figure 5). Decision threshold, detection limit and minimum detectable dose (MDD) should be reported for each individual. Dose estimation is only reliable if the aberration yield is higher than the decision threshold. MDD can be easily calculated by solving the DRC equation with detection limit. Decision threshold and detection limit are both dependent on background aberration frequency and number of cells scored[30)]. In addition to estimated dose, uncertainties related to the estimated dose should also be reported, to account for the uncertainties related to the DRC and uncertainties of the aberration yield[5, 33-34)]. In other words, the estimated dose and its lower and upper dose limits should be reported.

There are currently four methods commonly used for dose uncertainty estimation: Method A[33)], Method C[34)], Simplified Method C[5)] and Bayesian method[35)]. A 95 %

confidence limit (CL) is often used to "encompass the true doses for at least 95 % of all occasions"[5], though an 83 % CL can be used to reduce the risk of over-estimation of upper and lower dose limits[36]. Method A can be difficult to perform manually as it involves partial derivatives[37]. Method C is hence often used due to its simplicity, as upper and lower dose limits can be easily calculated when the upper and lower Poisson CL intersect the lower and upper 95 % CL curves respectively (Figure 5). Simplified Method C estimates upper and lower dose limits when the upper and lower Poisson CL intersect the DRC, and is only recommended if many cells were scored. Instead of the frequentist approach used by the above 3 methods, where conclusions are drawn based on the frequency of data in one event, the Bayesian framework draws conclusions by additionally considering previous events and uncertainties. Estimated dose and its upper and lower dose limits can be easily obtained with the "radir" package in R[35]. Due to a variety of uncertainty estimation methods available, a Monte-Carlo stimulated study of uncertainty estimation with Dic was performed to evaluate the best option for dose estimation. The Bayesian Method was chosen as the most optimal method to report upper and lower dose limits for both high and low doses[38].

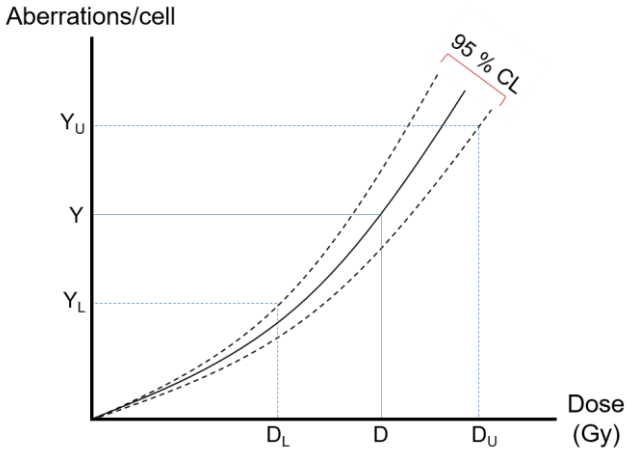

Figure 5: Dose estimation and its uncertainties with Method C. Dose (D) can be easily estimated by solving the DRC equation $Y = C + \alpha D + \beta D^2$ with the measured aberration yield (Y). Uncertainties associated with estimated dose can be obtained with Method C. 95 % confidence limit (CL) is usually chosen to "define an interval that will encompass the true dose on at least 95 % of occasions". Lower 95 % CL (D_L) is obtained when the lower 95 % CL yield (Y_L) crosses the upper curve. Upper 95 % CL (D_U) is obtained when the upper 95 % CL yield (Y_U) crosses the lower curve. [Adapted from EPR-Biodosimetry[5]]

As the process of DRC construction, dose estimation and their uncertainties and can be quite complicated, several easy-to-use software have been developed to aid researchers, such as CABAS[39], Dose Estimate[40] and Biodose Tools[41]. Each software

should be used with conscious knowledge of the statistical methods behind DRC construction and dose estimation, as Poisson distribution is always assumed to be true by default. Furthermore, different uncertainty estimations are reported by each software. For example, CABAS uses Simplified Method C with Poisson assumption. Dose Estimate uses Method A and Method C, and automatically adjusts Poisson CL if Poisson distribution is violated. Depending on the type of aberrations modelled, some aberration distributions tend to violate Poisson assumptions, such as MN and Tr. In such a case, adjustments to the weights or a change in the regression model should be performed. Likewise, Poisson CL should be adjusted based on the dispersion index if Method C is used.

In addition to classical chromosome aberration endpoints used in cytogenetic biodosimetry, other biomarkers such as γH2AX foci[42], proteins[43-44], gene expression[45-46] and miRNA[47] have also been evaluated as potential alternatives for biodosimetry, especially in triage assessment. However, cytogenetic endpoints still remain as one of the more accurate and reliable methods for biodosimetry. Technological developments in cytogenetic biodosimetry have improved triage response in the event of a mass-casualty radiological accident. High throughput processing of cell culture, harvest and staining can be performed in a fully automated robotic system using fingerprick blood samples with Rapid Automated Biodosimetry Tool (RABiT)[48]. Likewise, automated imaging and scoring with imaging flow cytometry integrated with RABiT has also been proposed[49]. Automated and semi-automated slide-based scoring systems for Dic[50-51] and MN[52-53] were also developed to reduce the time taken for scoring. In this thesis, however, we will be focusing on manual scoring with light microscopy on Giemsa-stained slides as a low-cost alternative and as a baseline for comparison with other computerized methods.

As mentioned earlier, various comprehensive documents have been published by IAEA and ISO to ensure standardization among multiple laboratories around the world. These documents are also updated every 5 to 10 years to account for new findings and techniques evaluated in cytogenetic biodosimetry. Even though these established methods were used for dose estimation in many radiation-related incidents in the past, there is always room to improve for such a multi-disciplinary field. Cytogenetic biodosimetry assumes a similar level of radiation sensitivity for all individuals. In reality, inter-individual differences in radiation responses are often observed after different types of

ionizing radiation, type of dose exposure, amount of dose exposed, period of dose exposure, dose-rate, existing health conditions, prior exposure to carcinogenic chemicals, smoking and alcohol intake, and most importantly, age and sex, resulting in many factors that could affect the reliability of dose estimation with cytogenetic biodosimetry[54-57].

The first part of this cumulative dissertation aims to improve on current cytogenetic biodosimetry techniques to report a more reliable dose estimation and its uncertainty, particularly in the CBMN and FISH-Tr assays. Multiple comparisons were performed in experimental protocols of cell culture and harvest, scoring of cytogenetic endpoints, DRC construction, dose estimation and their different methods of uncertainty estimation.

In Chapter 1, ISO standardization of FISH-Tr DRC construction and dose estimation was recently published in 2019 (ISO 20046:2019)[30], even though the first editions of ISO documents for DCA and CBMN assay were available from 2004 (ISO 19238)[29] and 2014 (ISO 17099)[28] respectively. Despite the lack of ISO standardization, there were over previous 20 attempts in FISH-Tr DRC construction, used for various applications in retrospective biodosimetry, such as occupational dose exposure estimation[58] and monitoring of exposed victims many years after initial radiation exposure[59]. However, when various factors in previous FISH-Tr DRC construction attempts were compared with ISO recommendations, it was clear that many laboratories were not aware of the statistical requirements and the initial raw data manipulation. In addition, there was no easy-to-use software available to reliably construct FISH-Tr DRCs and report enough statistical results according to ISO recommendations, as software such as CABAS[39] and Dose Estimate[40] were mainly developed for Dic DRCs. Thus, in this study, a DRC with Tr scored with 1, 2, 4-FISH was constructed with a modified R-script initially published by H. Braselmann[5]. Observed Tr frequency was age-adjusted to remove background Tr, using the Sigurdson's equation[60]. Cells scored were converted to cell-equivalents (CE) separately for males and females as chromosome lengths are sex-specific[61]. CE conversion is also necessary as different laboratories stain different chromosomes for Tr analysis, which affects the percentage of genome analyzed for Tr scoring[62]. The FISH-Tr DRC was constructed with IRLS at a dispersion index of 1.0 assuming Poisson distribution, and a linear-quadratic relationship was seen between age-adjusted Tr/CE and increasing dose. Our FISH-Tr DRC was also compared with

previously published DRCs from 0 to 1 Gy. Various factors affecting the reliability of FISH-Tr DRC were also discussed. This study was published in the International Journal of Radiation Biology[63].

In Chapter 2, CBMN assay can be performed in both whole blood (WB) and peripheral blood mononuclear cells (PBMCs) isolated from WB[5, 28]. Cytochalasin B (Cyt-B) is used to arrest dividing cells at cytokinesis to obtain binucleated cells (BNC). Based on the MN scoring criteria compiled by the Human MicroNucleus (HUMN) project, MN should only be scored in unruptured BNC with clear cytoplasmic boundaries[64]. Thus, a high frequency of unruptured scorable BNC with intact cytoplasm is key for efficient MN scoring. In addition, the nuclear division index (NDI) is often reported as a cell proliferation indicator, which also requires viable cells with intact cytoplasm to be counted[65]. For cell harvest with WB cultures, hypotonic treatment and fixation with methanol and acetic acid are required to remove erythrocytes for CBMN analysis. On the other hand, as lymphocytes in PBMC cultures are susceptible to cell rupture, cytocentrifugation of fresh cells was proposed by M. Fenech[66] and is the recommended method for PBMC harvest by IAEA[5] and ISO[28]. However, PBMC cell suspensions are unable to be stored for long-term as the cells are not fixed, and equipment like cytocentrifuges are not commonly found in cytogenetic laboratories. In this chapter, the Chromosome Research Group (CRG) in Hirosaki University developed an alternative method of harvest to cytocentrifugation, where the CRG protocol can be used to harvest and fix cells from CBMN assay performed with PBMC cultures. In addition, NDI and MN frequency were compared between WB and PBMC cultures, scoring all (cells with and without intact cytoplasm) or scorable cells (only cells with intact cytoplasm), and low and high humidity during cell spreading. 0 and 2 Gy peripheral blood from four males and four females from their 20s to 50s were evaluated. This study was published in the International Journal of Radiation Biology[67].

In Chapter 3, as higher NDI and lower MN frequency was seen in 2 Gy PBMCs than WB, we hypothesized that some soluble component(s) present in WB but absent in PBMCs could be responsible for the differences seen. Thus, we used a 6 well transwell co-culture system with different combinations of 0 and 2 Gy WB and PBMC co- and mono-cultures in 4 healthy donors (M, 25 y.o.; M, 51 y.o.; F, 23 y.o.; F, 26 y.o.). Co-cultures were separated with a 0.4 μm transwell membrane insert to allow soluble factors

to pass through, but not cells. Although co-culture systems are often used to evaluate RIBE[68] or interactions between two cell lines after irradiation[69], this set-up of a co-culture system to evaluate parameters in CBMN assay with WB and PBMCs has not yet been performed. 3 scorers manually evaluated NDI and MN frequency on Giemsa-stained slides. NDI and MN frequency were compared in swapped wells with the same condition (e.g. PBMC [w/ WB] upper & PBMC [w/ WB] lower) and wells of the same condition at the same level (e.g. PBMC [w/ WB] upper & PBMC [w/ WB-IR] upper). In addition, the possibility of different culture vessels (15 ml polypropylene tubes, 6-well polystyrene plates) affecting NDI and MN frequency was explored in a similar donor population. NDI and MN frequency of donors of the same age-group and sex were compared in mono-cultures in upper and lower wells of the co-culture system, and single cultures previously performed in 15 ml tubes of Chapter 2.

In Chapter 4, a rapid and accurate triage assessment of individuals exposed to whole-body equivalent of ≥ 2 Gy is essential for effective medical treatment. Dic is recommended for triage assessment due to its short culture time of 48 h. However, manual scoring of 50 metaphases/30 Dic in each individual can take up to 150 min[70]. On the other hand, manual MN scoring in 200 BNC/200 MN for triage[28] can be quickly completed. In this study, a shortened 48 h CBMN assay was proposed for triage as opposed to the conventional 72 h CBMN assay, using manual MN scoring on Giemsa-stained slides. NDI, % BNC, MN frequency and MN distributions for both triage and conventional modes were first evaluated in WB and PBMC cultures of three healthy donors (F, 26 y.o.; M, 34 y.o.; M, 52 y.o.) irradiated with 0, 2 and 4 Gy X-ray. Three conditions of CBMN assay were compared: 48 h culture (24 h @ Cyt-B), 72 h culture (24 h @ Cyt-B) and 72 h culture (44 h @ Cyt-B). Time taken for triage MN scoring was also evaluated. DRCs for WB and PBMC cultures in three other healthy donors (F, 23 y.o.; M: 25 y.o.; M, 29 y.o.) were also constructed for 48 h culture (24 h @ Cyt-B) and 72 h culture (44 h @ Cyt-B). Dose estimation with triage and conventional MN frequency was also compared.

In the second part of this cumulative thesis, the same type of chromosome aberrations analyzed in the metaphases of primary human lymphocytes can also be used to analyze radiation-induced chromosome damage in primary murine splenocytes. The effects of high dose-rate ionizing radiation (HDR-IR) are well-known to be biologically

damaging[71]. In contrast, the effects of low dose-rate ionizing radiation (LDR-IR) of ≥ 6 mSv/h[72] have been shown to be both beneficial and damaging[73]. Furthermore, previous LDR-IR experiments conducted in mice focused more on the effects after irradiation in adults[74-76], effects after *in utero* irradiation in pregnant mice[77-78] and trans-generational effects after irradiation of the F_0 generation[79-80]. Experiments comparing HDR-IR and LDR-IR effects in neonatal mice are not as common[81]. To comprehensively compare radiation effects in the short-term and long-term, unstable and stable splenocyte chromosome aberration kinetics were examined together with physical parameters and histology.

In Chapter 5, a large-scale mouse study was performed in 420 B6C3F1 mice, in collaboration with the National Institutes for Quantum and Radiological Science and Technology (QST). At least 5 male and 5 female mice were analyzed at each condition. Neonatal mice at 7 days old were irradiated to a total of 4 Gy, at LDR-IR of 6 mGy/h for 22 h or HDR-IR of 30 Gy/h. For short-term effects, mice at 14, 21, 28 and 35 d were analyzed. For long-term effects, mice at 14, 21, 28, 35, 42, 75, 100, 200, 300, 400 and 500 d were analyzed. Physical parameters of body weight, absolute spleen mass and spleen index were measured. Spleen histology was evaluated in hematoxylin and eosin-stained sections. Unstable (Dic, excess acentric fragments [Ace]) and stable (marker chromosomes) chromosome aberrations were scored in Giemsa-stained metaphases from mitogen-stimulated murine splenocytes. Q-banding was also performed for additional chromosome karyotyping. More than 89,000 metaphases have been analyzed.

References (Overall thesis)

1. Dale WM: Direct and indirect effects of ionizing radiations. In: Zuppinger A. (ed) Strahlenbiologie [Radiation Biology]. Handbuch der Medizinischen Radiologie [Encyclopedia of Medical Radiology]. Vol. 2/1, pp. 1–38, Springer, Berlin, Heidelberg, 1966.
2. Mothersill C, Seymour C: Radiation-induced bystander effects and adaptive responses–the Yin and Yang of low dose radiobiology? Mutat Res, 568(1):121–128, 2004.
3. Bender MA, Gooch PC: Somatic chromosome aberrations induced by human whole-body irradiation: the "Recuplex" criticality accident. Radiat Res, 29(4):568-582,

1966.

4. Bauchinger M: Cytogenetic effects in human lymphocytes as a dosimetry system. In: Eisert WG, Mendelsohn ML. (ed) Biological dosimetry. pp. 15–24, Springer, Berlin, Heidelberg, 1984.
5. International Atomic Energy Agency. Cytogenetic dosimetry: applications in preparedness for and response to radiation emergencies. EPR-Biodosimetry. IAEA, Vienna, Austria, 2011.
6. Rojas-Palma C, Liland A, Jerstad AN, Etherington G, del Rosarlo Pérez M, Rahola T, Smith K: TMT handbook, triage, monitoring and treatment of people exposed to ionizing radiation following a malevolent act. Norwegian Radiation Protection Authority, Norway, 2009.
7. Hoffmann W, Schmitz-Feuerhake I: How radiation-specific is the dicentric assay? J Expo Anal Environ Epidemiol, 9(2):113–133, 1999.
8. Fenech M, Bonassi S: The effect of age, gender, diet and lifestyle on DNA damage measured using micronucleus frequency in human peripheral blood lymphocytes. Mutagenesis, 26(1):43–49, 2011.
9. Edwards AA, Lindholm C, Darroudi F, Stephan G, Romm H, Barquinero J, Barrios L, Caballin MR, Roy L, Whitehouse CA, Tawn EJ, Moquet J, Lloyd DC, Voisin P: Review of translocations detected by FISH for retrospective biological dosimetry applications. Radiat Prot Dosimetry, 113(4):396–402, 2005.
10. Grégoire E, Roy L, Buard V, Delbos M, Durand V, Martin-Bodiot C, Voisin P, Sorokine-Durm I, Vaurijoux A, Voisin P, Baldeyron C, Barquinero JF: Twenty years of FISH-based translocation analysis for retrospective ionizing radiation biodosimetry. Int J Radiat Biol, 94(3):248–258, 2018.
11. Cho MS, Lee JK, Bae KS, Han EA, Jang SJ, Ha WH, Lee SS, Barquinero JF, Kim WT: Retrospective biodosimetry using translocation frequency in a stable cell of occupationally exposed to ionizing radiation. J Radiat Res, 56(4):709–716, 2015.
12. Puig R, Barrios L, Pujol M, Caballín MR, Barquinero JF: Suitability of scoring PCC rings and fragments for dose assessment after high-dose exposures to ionizing radiation. Mutat Res, 757(1):1–7, 2013.
13. Ramalho AT, Nascimento AC: The fate of chromosomal aberrations in 137Cs-exposed individuals in the Goi^ania radiation accident. Health Phys, 60(1):67–70,

1991.
14. International Atomic Energy Agency: The radiological accident in Nueva Aldea. IAEA, Vienna, Austria, 2009.
15. International Atomic Energy Agency: The radiological accident in Istanbul. Vienna, IAEA, Vienna, Austria, 2000.
16. Hayata I, Kanda R, Minamihisamatsu M, Furukawa M, Sasaki MN: Cytogenetical dose estimation for 3 severely exposed patients in the JCO criticality accident in Tokai-mura. J Radiat Res, 42(Suppl):S149–S155, 2001.
17. Jiang T, Hayata I, Wang C, Nakai S, Yao S, Yuan Y, Dai L, Liu Q, Chen D, Wei L, et al.: Dose-effect relationship of dicentric and ring chromosomes in lymphocytes of individuals living in the high background radiation areas in China. J Radiat Res. 41(Suppl):S63–S68, 2000.
18. Zakeri F, Rajabpour MR, Haeri SA, Kanda R, Hayata I, Nakamura S, Sugahara T, Ahmadpour MJ: Chromosome aberrations in peripheral blood lymphocytes of individuals living in high background radiation areas of Ramsar, Iran. Radiat Environ Biophys, 50(4):571–578, 2011.
19. Scarpato R, Lori A, Panasiuk G, Barale R: FISH analysis of translocations in lymphocytes of children exposed to the Chernobyl fallout: preferential involvement of chromosome 10. Cytogenet Cell Genet, 79(1–2):153–156, 1997.
20. Akiba S: Epidemiological studies of Fukushima residents exposed to ionising radiation from the Fukushima Daiichi Nuclear Power Plant prefecture—a preliminary review of current plans. J Radiol Prot, 32(1):1–10, 2012.
21. Jang S, Lee JK, Cho M, Yang SS, Kim SH, Kim WT: Consecutive results of blood cell count and retrospective biodosimetry: useful tools of health protection regulation for radiation workers. Occup Environ Med, 73(10):694–700, 2016.
22. Snigiryova G, Braselmann H, Salassidis K, Shevchenko V, Bauchinger M: Retrospective biodosimetry of Chernobyl clean-up workers using chromosome painting and conventional chromosome analysis. Int J Radiat Biol, 71(2):119–127, 1997.
23. Littlefield LG, McFee AF, Salomaa SI, Tucker JD, Inskip PD, Sayer AM, Lindholm C, Mäkinen S, Mustonen R, Sorensen K, et al.: Do recorded doses overestimate true doses received by Chernobyl cleanup workers? Results of cytogenetic analyses of

Estonian workers by fluorescence in situ hybridization. Radiat Res, 150(2):237–249, 1998.

24. Sullivan JM, Prasanna PG, Grace MB, Wathen LK, Wallace RL, Koerner JF, Coleman CN: Assessment of biodosimetry methods for a mass-casualty radiological incident: medical response and management considerations. Health Phys, 105(6):540–54, 2013.
25. Radiation Emergency Medical Management: Suggested triage categories after a nuclear detonation when resources are limited. https://www.remm.nlm.gov/triagecategories.htm. (Last updated: 27 Oct 2020; Last accessed: 17 Nov 2020).
26. International Atomic Energy Agency: IAEA Module 8 Part 1: Applied statistics for biological dosimetry.
27. Edwards AA, Lloyd DC, Purrott RJ: Radiation induced chromosome aberrations and the Poisson distribution. Radiat Environ Biophys, 16(2):89–100, 1979.
28. International Organization for Standardization: Radiological protection – Performance criteria for laboratories using the cytokinesis block micronucleus (CBMN) assay in peripheral blood lymphocytes for biological dosimetry. ISO 17099, 2014.
29. International Organization for Standardization: Radiological protection – Performance criteria for service laboratories performing biological dosimetry by cytogenetics. ISO 19238, 2014.
30. International Organization for Standardization: Radiological protection – Performance criteria for laboratories using Fluorescence In Situ Hybridization (FISH) translocation assay for assessment of exposure to ionizing radiation. ISO 20046, 2019.
31. Merkle W: Poisson goodness-of-fit tests for radiation-induced chromosome aberrations. Int J Radiat Biol Relat Stud Phys Chem Med, 40(6):685–692, 1981.
32. Barquinero JF, Barrios L, Caballín MR, Miró R, Ribas M, Subias A, Egozcue J: Establishment and validation of a dose-effect curve for gamma-rays by cytogenetic analysis. Mutat Res, 326(1):65–69, 1995.
33. Savage JRK, Papworth DG: Constructing a 2B calibration curve for retrospective dose reconstruction, Radiat Prot Dosimetry, 88(1):69–76, 2000.
34. Merkle W: Statistical methods in regression and calibration analysis of chromosome

aberration data. Radiat Environ Biophys, 21(3):217–233, 1983.

35. Higueras M, Puig P, Ainsbury EA, Rothkamm K: A new inverse regression model applied to radiation biodosimetry. Proc Math Phys Eng Sci. 471(2174):20140588, 2015.
36. Schenker N, Gentleman JF: On judging the significance of differences by examining the overlap between confidence intervals. Am Stat, 55(3):182–186, 2001.
37. International Atomic Energy Agency: Cytogenetic analysis for radiation dose assessment. Technical reports series No. 405. IAEA, Vienna, Austria, 2001.
38. Ainsbury EA, Higueras M, Puig P, Einbeck J, Samaga D, Barquinero JF, Barrios L, Brzozowska B, Fattibene P, Gregoire E, et al.: Uncertainty of fast biological radiation dose assessment for emergency response scenarios. Int J Radiat Biol, 93(1):127–135, 2017.
39. Deperas J, Szluinska M, Deperas-Kaminska M, Edwards A, Lloyd D, Lindholm C, Romm H, Roy L, Moss R, Morand J, Wojcik A: CABAS: a freely available PC program for fitting calibration curves in chromosome aberration dosimetry. Radiat Prot Dosimetry, 124(2):115–23, 2007.
40. Ainsbury EA, Lloyd DC: Dose estimation software for radiation biodosimetry. Health Phys, 98(2):290–295, 2010.
41. Hernández A, Endesfelder D, Einbeck J, Puig P, Benadjaoud A, Higueras M, Ainsbury E, Gaëtan G, Kulka U, Barrios L, Barquinero JF: Biodose Tools: An R Shiny Application for Biological Dosimetry, 2020. https://biodosetools-team.github.io/biodosetools/
42. Moquet J, Barnard S, Rothkamm K: Gamma-H2AX biodosimetry for use in large scale radiation incidents: comparison of a rapid '96 well lyse/fix' protocol with a routine method. PeerJ, 2, e282, 2014.
43. Ossetrova NI, Sandgren DJ, Blakely WF: Protein biomarkers for enhancement of radiation dose and injury assessment in nonhuman primate total-body irradiation model. Radiat Prot Dosimetry, 59(1-4):61–76, 2014.
44. Balog RP, Bacher R, Chang P, Greenstein M, Jammalamadaka S, Javitz H, Knox SJ, Lee S, Lin H, Shaler T, Shura L, Stein P, Todd K, Cooper DE: Development of a biodosimeter for radiation triage using novel blood protein biomarker panels in humans and non-human primates. Int J Radiat Biol, 96(1):22–34, 2020.

45. Port M, Ostheim P, Majewski M, Voss T, Haupt J, Lamkowski A, Abend M: Rapid high-throughput diagnostic triage after a mass radiation exposure event using early gene expression changes. Radiat Res, 192(2):208–218, 2019.
46. Macaeva E, Mysara M, De Vos WH, Baatout S, Quintens R: Gene expression-based biodosimetry for radiological incidents: assessment of dose and time after radiation exposure. Int J Radiat Biol, 95(1):64–75, 2019.
47. Menon N, Rogers CJ, Lukaszewicz AI, Axtelle J, Yadav M, Song F, Chakravarti A, Jacob NK: Detection of Acute Radiation Sickness: A feasibility study in non-human primates circulating miRNAs for triage in radiological events. PLoS One. 11(12):e0167333, 2016.
48. Repin M, Pampou S, Brenner DJ, Garty G: The use of a centrifuge-free RABiT-II system for high-throughput micronucleus analysis. J Radiat Res, 61(1):68–72, 2020.
49. Wang Q, Rodrigues MA, Repin M, Pampou S, Beaton-Green LA, Perrier J, Garty G, Brenner DJ, Turner HC, Wilkins RC: Automated triage radiation biodosimetry: Integrating imaging flow cytometry with high-throughput robotics to perform the cytokinesis-block micronucleus assay. Radiat Res,191(4):342–351, 2019.
50. Shirley B, Li Y, Knoll JHM, Rogan PK: Expedited radiation biodosimetry by automated dicentric chromosome identification (ADCI) and dose estimation. J Vis Exp. 127:56245, 2017.
51. Romm H, Ainsbury E, Barnard S, Barrios L, Barquinero JF, Beinke C, Deperas M, Gregoire E, Koivistoinen A, Lindholm C, Moquet J, Oestreicher U, Puig R, Rothkamm K, Sommer S, Thierens H, Vandersickel V, Vral A, Wojcik A: Automatic scoring of dicentric chromosomes as a tool in large scale radiation accidents. Mutat Res, 756(1-2):174–183, 2013.
52. Willems P, August L, Slabbert J, Romm H, Oestreicher U, Thierens H, Vral A: Automated micronucleus (MN) scoring for population triage in case of large scale radiation events. Int J Radiat Biol, 86(1):2–11, 2010.
53. Decordier I, Papine A, Vande Loock K, Plas G, Soussaline F, Kirsch-Volders M: Automated image analysis of micronuclei by IMSTAR for biomonitoring. Mutagenesis, 26(1):163–168, 2011.
54. Léonard A, Rueff J, Gerber GB, Léonard ED: Usefulness and limits of biological dosimetry based on cytogenetic methods. Radiat Prot Dosimetry, 115(1-4):448–454,

2005.

55. Pinto MM, Santos NF, Amaral A: Current status of biodosimetry based on standard cytogenetic methods. Radiat Environ Biophys, 49(4):567–581, 2010.
56. Pajic J, Rakic B, Rovcanin B, Jovicic D, Novakovic I, Milovanovic A, Pajic V: Inter-individual variability in the response of human peripheral blood lymphocytes to ionizing radiation: comparison of the dicentric and micronucleus assays. Radiat Environ Biophys, 54(3):317–325, 2015.
57. Mosse I, Kilchevsky A, Nikolova N, Zhelev N: Some problems and errors in cytogenetic biodosimetry. Biotechnol Biotechnol Equip, 31(3):460–468, 2017.
58. Beaton-Green LA, Barr T, Ainsbury EA, Wilkins RC: Retrospective biodosimetry of an occupational overexposure-case study. Radiat Prot Dosimetry, 172(1-3):254–259, 2016.
59. Natarajan AT, Santos SJ, Darroudi F, Hadjidikova V, Vermeulen S, Chatterjee S, Berg M, Grigorova M, Sakamoto-Hojo ET, Granath F, Ramalho AT, Curado MP: 137Cesium-induced chromosome aberrations analyzed by fluorescence in situ hybridization: eight years follow up of the Goiânia radiation accident victims. Mutat Res, 400(1-2):299–312, 1998.
60. Sigurdson AJ, Ha M, Hauptmann M, Bhatti P, Sram RJ, Beskid O, Tawn EJ, Whitehouse CA, Lindholm C, Nakano M, et al.: International study of factors affecting human chromosome translocations. Mutat Res, 652(2):112–121, 2008.
61. Morton NE: Parameters of the human genome. Proc Natl Acad Sci USA. 88(17):7474–7476, 1991.
62. Lucas JN, Awa A, Straume T, Poggensee M, Kodama Y, Nakano M, Ohtaki K, Weier HU, Pinkel D, Gray J: Rapid translocation frequency analysis in humans decades after exposure to ionizing radiation. Int J Radiat Biol, 62(1):53–63, 1992.
63. Goh VST, Fujishima Y, Abe Y, Sakai A, Yoshida MA, Ariyoshi K, Kasai K, Wilkins RC, Blakely WF, Miura T. Construction of fluorescence in situ hybridization (FISH) translocation dose-response calibration curve with multiple donor data sets using R, based on ISO 20046:2019 recommendations. Int J Radiat Biol, 95(12):1668–1684, 2019.
64. Bonassi S, Fenech M, Lando C, Lin YP, Ceppi M, Chang WP, Holland N, Kirsch-Volders M, Zeiger E, Ban S, et al.: HUman MicroNucleus project: international

database comparison for results with the cytokinesis-block micronucleus assay in human lymphocytes: I. Effect of laboratory protocol, scoring criteria, and host factors on the frequency of micronuclei. Environ Mol Mutagen, 37(1):31-45, 2001.

65. Eastmond DA, Tucker JD: Identification of aneuploidy-inducing agents using cytokinesis-blocked human lymphocytes and an antikinetochore antibody. Environ Mol Mutagen, 13(1):34–43, 1989.
66. Fenech M: Cytokinesis-block micronucleus cytome assay. Nat Protoc. 2(5):1084–1104, 2007.
67. Goh VST, Nakayama R, Blakely WF, Abe Y, Chua CEL, Chew ZH, Nakata A, Fujishima Y, Yoshida MA, Kasai K, Ariyoshi K, Miura T: Improved harvest and fixation methodology for isolated human peripheral blood mononuclear cells in cytokinesis-block micronucleus assay. Int J Radiat Biol, 97(2):194–207, 2021.
68. Hill MA, Stevens DL, Kadhim M, Blake-James M, Mill AJ, Goodhead DT: Experimental techniques for studying bystander effects in vitro by high and low-LET ionising radiation. Radiat Prot Dosimetry, 122(1-4):260–265, 2006.
69. Haubner F, Leyh M, Ohmann E, Pohl F, Prantl L, Gassner HG: Effects of external radiation in a co-culture model of endothelial cells and adipose-derived stem cells. Radiat Oncol, 8:66, 2013.
70. International Organization for Standardization: Radiation protection - Performance criteria for laboratories performing cytogenetic triage for assessment of mass casualties in radiological or nuclear emergencies - General principles and application to dicentric assay. ISO 21243, 2008.
71. Dainiak N: Medical management of acute radiation syndrome and associated infections in a high-casualty incident. J Radiat Res, 59(suppl_2):ii54-ii64, 2018.
72. United Nations Scientific Committee on the Effects of Atomic Radiation: Biological mechanisms of radiation actions at low doses. A white paper to guide the Scientific Committee's future programme of work. Report V.12-57831. 2012.
73. Tang FR, Loke WK, Khoo BC: Low-dose or low-dose-rate ionizing radiation-induced bioeffects in animal models. J Radiat Res, 58(2):165–182, 2017.
74. Tanaka K, Kohda A, Toyokawa T, Ichinohe K, Oghiso Y: Chromosome aberration frequencies and chromosome instability in mice after long-term exposure to low-dose-rate gamma-irradiation. Mutat Res, 657(1):19–25, 2008.

75. Seawright JW, Samman Y, Sridharan V, Mao XW, Cao M, Singh P, Melnyk S, Koturbash I, Nelson GA, Hauer-Jensen M, Boerma M: Effects of low-dose rate γ-irradiation combined with simulated microgravity on markers of oxidative stress, DNA methylation potential, and remodeling in the mouse heart. PLoS One, 12(7):e0180594, 2017.
76. Yamauchi K, Ono T, Ayabe Y, Hisamatsu S, Yoneya M, Tsutsumi Y, Komura JI: Life-shortening effect of chronic low-dose-rate irradiation in calorie-restricted mice. Radiat Res, 192(4):451–455, 2019.
77. Abramsson-Zetterberg L, Zetterberg G, Sundell-Bergman S, Grawé J: Absence of genomic instability in mice following prenatal low dose-rate gamma-irradiation. Int J Radiat Biol, 76(7):971–977, 2000.
78. Kato F, Ootsuyama A, Nomoto S, Kondo S, Norimura T: Threshold effect for teratogenic risk of radiation depends on dose-rate and p53-dependent apoptosis. Int J Radiat Bio, 77(1):13–19, 2001.
79. Mughal SK, Myazin AE, Zhavoronkov LP, Rubanovich AV, Dubrova YE: The dose and dose-rate effects of paternal irradiation on transgenerational instability in mice: a radiotherapy connection. PLoS One, 7(7):e41300, 2012.
80. Braga-Tanaka I 3rd, Tanaka S, Kohda A, Takai D, Nakamura S, Ono T, Tanaka K, Komura JI: Experimental studies on the biological effects of chronic low dose-rate radiation exposure in mice: overview of the studies at the Institute for Environmental Sciences. Int J Radiat Biol, 94(5):423–433, 2018.
81. Spalding JF, Thomas RG, Tietjen GL: Life span of C57 mice as influenced by radiation dose, dose rate, and age at exposure. LA-9528. Los Alamos National Laboratory, New Mexico, USA, 1982.

Chapter 1:

「Construction of fluorescence *in situ* hybridization (FISH) translocation dose-response calibration curve with multiple donor data sets using R, based on ISO 20046:2019 recommendations」

「ISO 20046:2019 に基づく R を使用した複数のドナーデータセットによる蛍光 *in situ* ハイブリダイゼーション（FISH）転座法用線量反応曲線の構築」

弘前大学大学院保健学研究科保健学専攻

提出者氏名：Valerie Goh Swee Ting

所　　属：　生体検査科学領域

指導教員：　三浦富智

List of Abbreviations (Chapter 1)

CBMN: cytokinesis-block micronucleus

CE: cell equivalent

CL: confidence limit

D_L: lower confidence dose limit

D_U: upper confidence dose limit

DAPI: 4′,6-diamidino-2-phenylindole

Dic: dicentric chromosome(s)

DRC: dose-response calibration curve

FISH: fluorescence *in situ* hybridization

IAEA: International Atomic Energy Agency

IRLS: iteratively reweighted least squares

ISO: International Organization for Standardization

MDD: minimum detectable dose

SE: standard error

Tr: translocation(s)

Tr/CE: translocation per cell equivalent

WCP: whole chromosome paint

Y_L: lower Poisson translocation yield

Y_U: upper Poisson translocation yield

ZIP: zero-inflated Poisson

Introduction (Chapter 1)

Cytogenetic biodosimetry is used to estimate doses in an individual suspected of radiation exposure. For dose estimation of acute partial or whole-body exposures from 0.1 to 5 Gy[1)], the construction of a dose-response calibration curve (DRC) using the gold standard dicentric chromosome assay is highly recommended by the International Atomic Energy Agency (IAEA)[2)]. However, in prolonged periods after the initial radiation exposure and in low dose protracted exposures, dose estimation with dicentric chromosomes (Dic) might be greatly underestimated due to its short half-life of between 13.5[3)] and 36 months[4)]. As a result, dose estimation with chromosome translocations (Tr) detected by fluorescence *in situ* hybridization (FISH) with whole chromosome paint (WCP) probes could be more representative for retrospective biodosimetry. Tr are highly persistent in lymphocytes after the initial radiation exposure[5)], with an expected half-life long after the normal human life expectancy in stable cells without unstable chromosome aberrations[6)].

Retrospective biodosimetry is used in follow-up examinations of radiation accident victims or to monitor chronic low dose occupational work exposure of medical officers and nuclear accident clean-up workers. Over 20 attempts of FISH-Tr DRC construction were made for retrospective dose estimation for various applications, such as accumulated dose estimation in Mayak nuclear power plant workers[7)] or to analyse factors that could affect the reliability of retrospective dosimetry[8)]. Standardization of a FISH-Tr DRC construction is hence essential as age-adjustment to remove spontaneous Tr, conversion of cells scored to their genomic or cell equivalents (CE), the recommended number of doses below 1 Gy and the recommended number of cells scored for calibration had been left out in previous attempts of DRC construction. Moreover, the types of Tr scored were inconsistent and there was no conclusive agreement if only stable or all unstable and stable aberrations should be scored. This could possibly lead to higher levels of uncertainty for DRC coefficients, ultimately affecting the accuracy of dose estimation. Thus, for consistency between multiple cytogenetic laboratories, internationally standardized guidelines and recommendations for FISH-Tr DRC and dose estimation were published recently in ISO 20046:2019[9)].

In this study, the steps recommended by ISO 20046:2019 for DRC construction and dose estimation using previously published Tr detected by three-color FISH from five

Japanese donors[10] were explored. Some potential considerations for future constructions of more statistically reliable FISH-Tr DRCs were also discussed. Although software such as Dose Estimate[11] and CABAS[12] are available for curve fitting and dose estimation, R[13] was used for DRC construction in this study. The code written by H. Braselmann in EPR-Biodosimetry[2], meant for Dic per cell, was modified to age-adjusted Tr per cell equivalent (Tr/CE).

Materials & Methods (Chapter 1)

Blood collection and irradiation, peripheral blood culture, WCP-FISH and centromere-FISH, image capturing and Tr scoring

Detailed information about blood collection and irradiation, cell culture, WCP-FISH and centromere-FISH, image capture and Tr scoring was previously published by Abe *et al.* [10]. Briefly, peripheral blood was collected in lithium-heparin tubes (BD Biosciences, San Jose, CA, USA) from five healthy individuals of four males (23, 35, 44 and 55 y.o.) and one female (33 y.o.) with their written informed consent. The blood was irradiated with γ-rays (Gamma cell 40, Best Theratonics, Ottawa, Ontario, Canada) at 0, 0.01, 0.02, 0.05, 0.1, 0.2, 0.5 and 1 Gy, at a dose rate of 0.263 Gy/min. Peripheral blood lymphocytes were isolated with BD Vacutainer CPT tubes (BD, NJ, USA), cultured and fixed according to IAEA's recommendations[2]. Chromosome painting with WCP probes for chromosomes 1, 2 and 4 (Customized XCP-Mix probe Mix-#1R-#2G-#4RG, MetaSystems GmbH, Altlussheim, Germany), centromere painting (Poseidon All Human Centromere probe, KREATECH, Amsterdam, the Netherlands) and nuclear counter-stain with DAPI were performed, as previously described[14-15]. Tr were scored on Isis FISH Imaging System (Ver 5.4, MetaSystems GmbH), by three trained, experienced observers without prior knowledge about the irradiation dose.

More than 5000 metaphases (> 2000 CE) were scored for each dose in each donor[9]. Tr analysis was only performed in metaphases with 45 or 46 centromeres containing all three pairs of differentially painted chromosomes (chromosome 1: red, chromosome 2: green, chromosome 4: yellow). Apparent one-way Tr and two-way Tr counts were included[16]. Each two-way Tr was counted as a single event. Similarly, each one-way Tr was also counted as a single event[17]. Complex Tr was converted to the equivalent number of simple Tr based on the number of color junctions[17]. No distinction

was made between cells with unstable and stable Tr, hence all simple Tr were scored and used for DRC construction.

FISH-Tr DRC construction with R

DRC construction and its associated statistical analyses were performed with R ver 3.5.3[13] and RStudio ver 1.1.463[18]. The additional package "readxl"[19] was used to import data sets from Microsoft Excel to RStudio. Before running the R-Script, observed Tr and number of cells scored were converted to age-adjusted Tr and their respective CEs for each dose.

For age adjustment, Equation (1), provided by Sigurdson *et al.*[20], was used to obtain background Tr frequency, due to the absence of Japanese population-specific background Tr. There was also good agreement between the background Tr frequency of the five donors and the background Tr frequency derived from Sigurdson *et al.* Age-adjusted Tr/CE was then obtained using Equation (2).

$$Background\ Tr/CE\ of\ x\ years\ old = e^{-7.925} + e^{-9.284}(x \cdot e^{x \cdot 0.01062}) \quad (1)$$

$$Age\text{-}adjusted\ Tr/CE = Observed\ Tr/CE - Background\ Tr/CE \quad (2)$$

The conversion of number of cells scored to CE is shown in Equation (3). The calculations are based on the formula proposed by Lucas *et al.*[21] and individual chromosome lengths derived by Morton[22].

$$F_G = F_{P(1+2+4)}/2.05[f_1(1-f_1) + f_2(1-f_2) + f_4(1-f_4) - (f_1f_2 + f_1f_4 + f_2f_4)] \quad (3)$$

F_G: Full genome aberration frequency
F_P: Tr frequency detected by FISH
f_P: Fraction of genome hybridized, taking into account the sex of the subject (female: $f_P = 0.2234$, male: $f_P = 0.2271$)

Chromosomes 1, 2 and 4 occupy about 23 % of the entire genome. Hence, the CE was calculated using Equation (4) for males and Equation (5) for females.

$$CE\ (male) = Total\ cells\ scored\ \times 0.3948 \quad (4)$$

$$CE\ (female) = Total\ cells\ scored\ \times 0.3896 \quad (5)$$

Briefly, after checking that the Tr yield followed a Poisson distribution, a constant dispersion index of 1 was subsequently used. Linear-quadratic curve fitting for low-LET

radiation was done by the method of iteratively reweighted least squares (IRLS). The upper and lower 95% confidence limits (CL) of the curve were calculated using Equation (6), as provided by ISO 20046:2019. Detection limit, decision threshold, upper (Y_U) and lower (Y_L) Poisson Tr yields, upper (D_U) and lower (D_L) confidence dose limits and minimum detectable dose (MDD) were also obtained based on ISO 20046:2019 and EPR-Biodosimetry.

$$Age\text{-}adjusted\ Tr/CE = C + \alpha D + \beta D^2 \pm \sqrt{R^2[var(C) + var(\alpha)D^2 + var(\beta)D^4 + 2covar(C,\alpha)D + 2covar(C,\beta)D^2 + 2covar(\alpha,\beta)D^3]} \quad (6)$$

D: Absorbed dose
C, α, β: Coefficients of the fitted linear-quadratic curve
R^2: Coefficient of determination, and is the 95 % confidence limit of a chi-square distribution, χ^2 (df, 95 %), with df = 2 or 3. For a linear-quadratic curve (df = 3), $\chi^2 = 7.81$
var: Variance of the coefficient in the bracket
covar: Covariance of the coefficients in the bracket

Other statistical tests

Poisson distribution was verified in the Dic distribution of the same cell population published previously[10], by evaluating dispersion index and performing a suite of tests (i.e. Poisson over-dispersion: Papworth's *u*-test[23], *D*-test[24] and *L*-test[25]; Zero-inflated Poisson (ZIP): *CR*-test[25]; *Z*-test[26], Bayesian test ZIP vs Poisson: Bayes factor[27-28] using a Shiny R Studio application, named GOF Poisson, based on R language[29-30]. This application is freely available at http://manu2h.shinyapps.io/gof_poisson/. Poisson assumption was considered rejected when *p*-values were lower than 0.05 for *u*, *D*, *L*, *Z*, and *CR*-tests. For Bayes factor (2 log BF), values 0-2, 2-6, 6-10, and > 10 give 'weak positive', 'positive', 'strong', and 'very strong' evidence respectively, in support of the ZIP model as compared with the Poisson model[28].

Robust *Z*-score was obtained between α coefficients of modified previously published DRC equations and our DRC equation using R. Any absolute *Z*-score values higher than 3 were outliers.

Results (Chapter 1)

Checking if Tr yield followed a Poisson distribution

The Tr yield data was first verified for Poisson distribution assumption before curve fitting[31]. As the distribution of observed Tr was not recorded in the previously published paper[10], tests for Poisson distribution compliance were performed on the Dic distribution of the same population, by assuming that the frequencies of Dic and Tr arising immediately after irradiation were the same[32].

Results from the dispersion (*u*-test, *D*-test, *L*-test), ZIP (*CR*-test, *Z*-test) and Bayesian tests (ZIP versus Poisson) are shown in Table 2. Overall, the dispersion index was 1 or close to 1 for most of the data, and their corresponding *u*-tests were within –1.96 to 1.96. Some data were over-dispersed ($u > 1.96$), which was expected when the Dic distribution of those analyzed samples were considered. Similar results were found using the additional over-dispersion (i.e. *D*, *L*) and ZIP (i.e. *CR, Z*) tests. The more rigorous Bayesian test gave mixed results. The strength of evidence that argued for the ZIP distribution and against the Poisson distribution was generally weakly positive at lower doses (0.02 to 0.5 Gy) but negative at the higher doses (> 0.5 to 1 Gy) (Table 1). Nevertheless, for the subsequent steps of curve fitting, Tr yields were assumed to be following a Poisson distribution, and the dispersion index was fixed constant at 1.

Constructing FISH-Tr DRC with R

FISH-Tr DRC construction was performed with the help of "readxl", which imported data sets from Microsoft Excel to RStudio. If a negative Tr yield was obtained after age-adjustment, age-adjusted Tr yield was zeroed for generalized linear modelling. Tr yield data was indexed in separate columns with the headings 'dose', 'cells_eq' and 'tr_zero'. After file importation, the entire code was copied into RStudio for execution. An annotation of the main steps for DRC construction is shown in Figure 1A. The results output include the DRC with data calibration points and its associated 95 % CL, the coefficient matrix (`bstat`) with DRC coefficients (`x0`: C, `x1`: α, `x2`: β), their standard errors (`Std. Error`) and significance of coefficients (`Pr>|z|`), the Pearson's chi-square goodness-of-fit values (`df, p, chisq`), the variance-covariance matrix (`vakoma`) and the correlation matrix (`corma`) (Figure 1B).

Table 1: Results of Poisson validation on Dic distribution of donors A to E, using over-dispersion tests (*u*, *D*, *L*), ZIP tests (*CR*, *Z*) and Bayesian test (ZIP versus Poisson).

Donor	Dose (Gy)	Disp. index	Over-dispersion tests				Significant and over-dispersed?	ZIP tests			Zero-inflated?	Bayesian tests	
			u-test	*u* (*p*-value)	*D* (*p*-value)	*L* (*p*-value)		CR (p-value)	Z index	Z (p-value)		Bayes factor (2 log BF)	Evidence strength
A	0	1.9980	34.8999	< 1e-4	< 1e-4	< 1e-4	Yes	< 1e-4	0.3327	< 1e-4	Yes	15.9584	VS; Su ZIP
	0.01	1.2829	9.7081	< 1e-4	0.0104	0.0104	Yes	0.0104	0.1416	< 1e-4	Yes	5.6589	VS; Su ZIP
	0.02	0.9990	-0.0224	0.4911	0.9995	1	No	0.9995	-5e-04	0.4874	No	1.2944	WP; Su ZIP
	0.05	0.9990	-0.0384	0.4847	0.9985	1	No	0.9985	-7e-04	0.4812	No	1.2394	WP; Su ZIP
	0.1	0.9975	-0.0864	0.4656	0.9926	1	No	0.9926	-0.0015	0.4623	No	1.0742	WP; Su ZIP
	0.2	0.9940	-0.1968	0.4220	0.9619	1	No	0.9619	-0.0032	0.4186	No	0.7064	WP; Su ZIP
	0.5	0.9833	-0.5413	0.2942	0.7449	1	No	0.7449	-0.0087	0.2899	No	-0.3292	NEG; Su POIS
	1	1.0141	0.4528	0.3254	0.4036	0.3998	No	0.3998	0.0075	0.3166	No	-0.4996	NEG; Su POIS
B	0	0.9985	-0.0547	0.4782	0.9970	1	No	0.9970	-0.0010	0.4748	No	1.1829	WP; Su ZIP
	0.01	0.9980	-0.0700	0.4721	0.9951	1	No	0.9951	-0.0012	0.4688	No	1.1305	WP; Su ZIP
	0.02	0.9980	-0.0706	0.4719	0.9950	1	No	0.9950	-0.0012	0.4685	No	1.1284	WP; Su ZIP
	0.05	0.9975	-0.0858	0.4658	0.9927	1	No	0.9927	-0.0015	0.4625	No	1.0762	WP; Su ZIP
	0.1	0.9980	-0.0704	0.4719	0.9951	1	No	0.9951	-0.0012	0.4686	No	1.1289	WP; Su ZIP
	0.2	0.9990	-0.0381	0.4848	0.9986	1	No	0.9986	-7e-04	0.4814	No	1.2407	WP; Su ZIP
	0.5	0.9890	-0.3555	0.3611	0.8809	1	No	0.8809	-0.0058	0.3574	No	0.2094	WP; Su ZIP
	1	0.9659	-1.1462	0.1258	0.2649	1	No	0.2649	-0.0177	0.1203	No	-1.8134	NEG; Su POIS
C	0	-	-	-	-	-	-	-	-	-	-	-	-
	0.01	0.9980	-0.0700	0.4721	0.9951	1	No	0.9951	-0.0012	0.4688	No	1.1305	WP; Su ZIP
	0.02	-	-	-	-	-	-	-	-	-	-	-	-
	0.05	0.9995	-0.0223	0.4911	0.9995	1	No	0.9995	-5e-04	0.4874	No	1.2948	WP; Su ZIP
	0.1	-	-	-	-	-	-	-	-	-	-	-	-
	0.2	0.9980	-0.0704	0.4719	0.9951	1	No	0.9951	-0.0012	0.4686	No	1.1289	WP; Su ZIP
	0.5	0.9920	-0.2607	0.3972	0.9341	1	No	0.9341	-0.0043	0.3937	No	0.5020	WP; Su ZIP
	1	1.0096	0.3075	0.3792	0.5243	0.5243	No	0.5243	0.0048	0.3808	No	-0.0639	NEG; Su POIS

Table 1 (continued)

D	0	-	-	-	-	-	-	-	-	-	-	-
	0.01	0.9990	-0.0387	0.4846	0.9985	1	No	0.9985	-8e-04	0.4811	No	1.2382	WP; Su ZIP
	0.02	0.9990	-0.0384	0.4847	0.9985	1	No	0.9985	-7e-04	0.4812	No	1.2394	WP; Su ZIP
	0.05	0.9991	-0.0375	0.4851	0.9986	1	No	0.9986	-7e-04	0.4817	No	1.2430	WP; Su ZIP
	0.1	0.9980	-0.0705	0.4719	0.9950	1	No	0.9950	-0.0012	0.4686	No	1.1288	WP; Su ZIP
	0.2	0.9965	-0.1180	0.4530	0.9862	1	No	0.9862	-0.0020	0.4497	No	0.9671	WP; Su ZIP
	0.5	1.0719	2.3271	0.0100	0.1289	0.1289	Yes	0.1289	0.0361	0.0111	Yes	2.4262	POS; Su ZIP
	1	1.0022	0.0706	0.4718	0.5666	0.5666	No	0.5666	0.0012	0.4692	No	-0.8891	NEG; Su POIS
E	0	0.9985	-0.0545	0.4783	0.9970	1	No	0.9970	-0.0010	0.4749	No	1.1839	WP; Su ZIP
	0.01	-	-	-	-	-	-	-	-	-	-	-	-
	0.02	0.9995	-0.0222	0.4911	0.9995	1	No	0.9995	-5e-04	0.4875	No	1.2951	WP; Su ZIP
	0.05	0.9975	-0.0859	0.4658	0.9926	1	No	0.9926	-0.0015	0.4625	No	1.0759	WP; Su ZIP
	0.1	0.9990	-0.0385	0.4846	0.9985	1	No	0.9985	-7e-04	0.4812	No	1.2391	WP; Su ZIP
	0.2	0.9970	-0.1021	0.4593	0.9896	1	No	0.9896	-0.0017	0.4560	No	1.0208	WP; Su ZIP
	0.5	0.9811	-0.6073	0.2718	0.6900	1	No	0.6900	-0.0098	0.2673	No	-0.5105	NEG; Su POIS
	1	0.9926	-0.2369	0.4063	0.6419	0.7225	No	0.6419	-0.0039	0.4033	No	-0.9667	NEG; Su POIS

Su = Supports, WP = Weak positive, POS = Positive, NEG = Negative, VS = Very strong, POIS = Poisson, ZIP = Zero-inflated Poisson. Validation of Poisson distribution was performed with GOF Poisson[29-30]. Data was significant and over-dispersed if $p < 0.05$ for u, D and L-test, and zero-inflated if $p < 0.05$ for CR and Z-test. Tests were only carried out for data sets with more than 2 Dic.

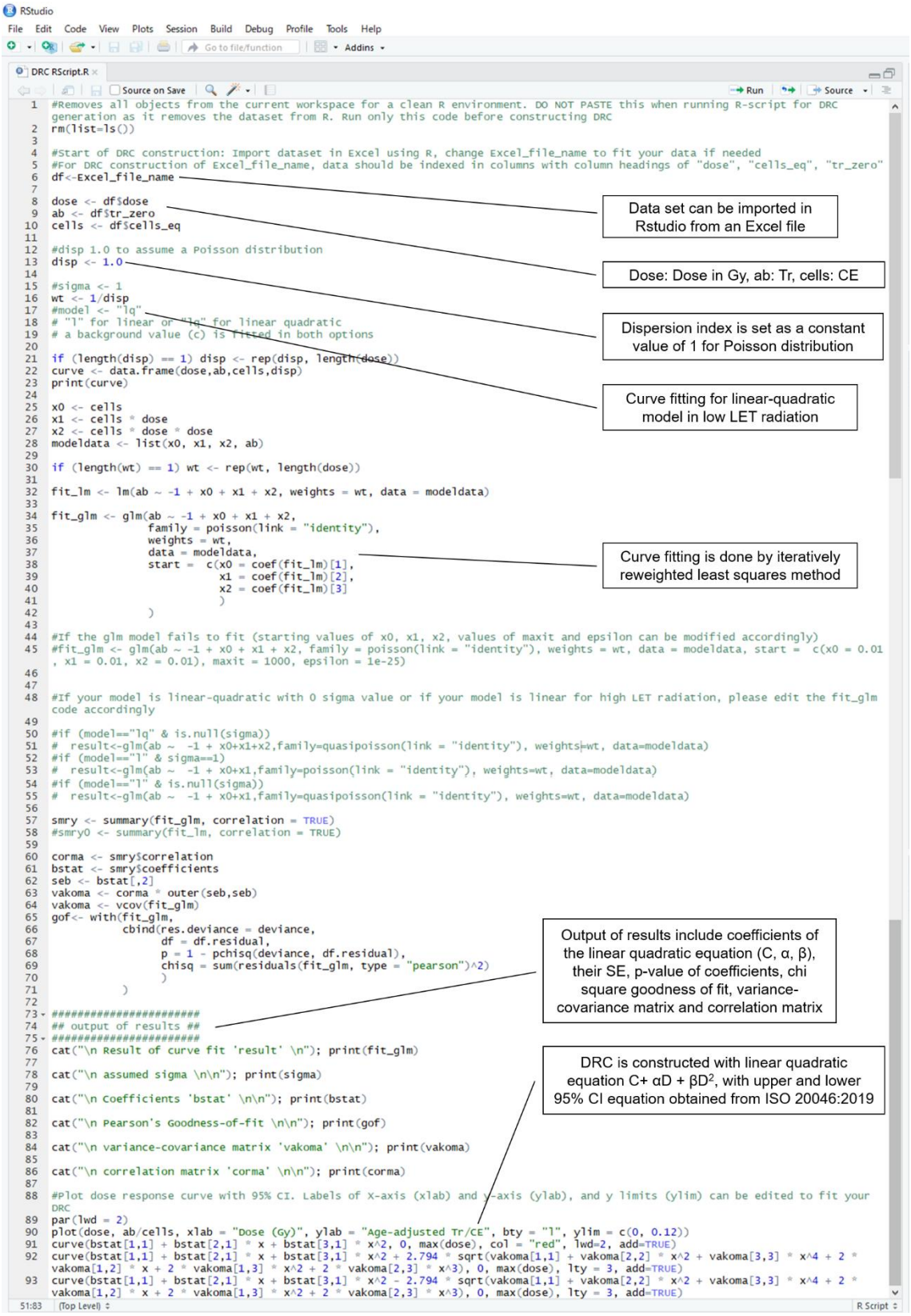

Figure 1A: Annotated R-Script for FISH-Tr DRC construction with age-adjusted Tr/CE.

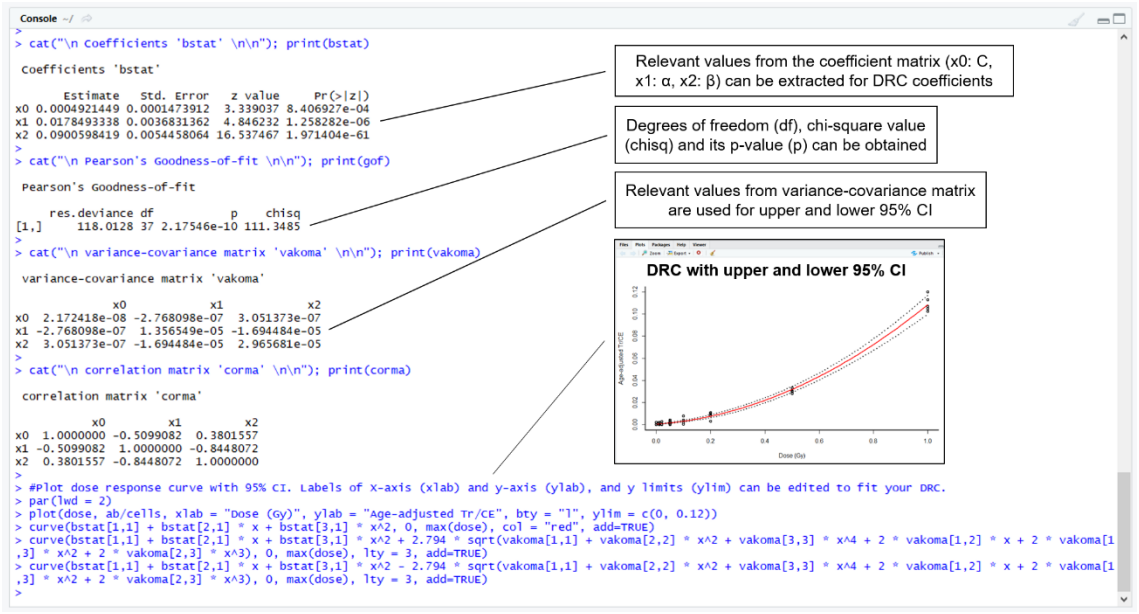

Figure 1B: Results output after successful execution of FISH-Tr DRC R-script. DRC was obtained by plotting age-adjusted Tr per cell equivalent (age-adjusted Tr/CE) against dose expressed as Gy, with pooled separated data from five donors.

Comparing DRC constructed from pooled separated, pooled and averaged age-adjusted Tr/CE

As the number of donor data sets recommended for FISH-Tr DRC construction was not stated in ISO 20046:2019, DRCs were constructed using individual (one data set from one donor), pooled separated (five data sets from five donors), pooled (one data set from five donors) and averaged (one data set averaged from five donors) age-adjusted Tr/CE to compare DRC coefficients obtained. Table 2 shows the Tr yield from individual donors A to E, pooled and averaged respectively.

Table 2: Individual (pooled separated), pooled and averaged Tr yield of donors A to E. Observed Tr and number of cells scored were previously published[10].

	Donor	Sex	Age	Dose (Gy)	Cells scored	CE	Observed Tr	Age-adjusted Tr	Age-adjusted Tr/CE
Pooled (separated)	A	M	44	0	6498	2565.34	3	0	0
				0.01	6003	2369.92	12	0	0
				0.02	5320	2100.28	10	0	0
				0.05	5555	2193.05	22	6.90	0.0032
				0.1	5625	2220.69	16	0.71	0.0003
				0.2	6043	2385.71	24	7.58	0.0032
				0.5	5120	2021.32	71	57.09	0.0282
				1	5120	2021.32	242	228.09	0.1128
	B	M	55	0	5333	2105.41	18	0	0
				0.01	5501	2171.73	16	0	0
				0.02	6516	2572.44	25	0.50	0.0002
				0.05	5357	2114.88	18	0	0
				0.1	5900	2329.25	32	9.81	0.0042
				0.2	6328	2498.22	50	26.21	0.01050
				0.5	6000	2368.73	101	78.44	0.0331
				1	5327	2103.04	272	251.97	0.1198
	C	M	35	0	5184	2046.59	8	0	0
				0.01	5479	2163.05	15	4.02	0.0019
				0.02	5628	2221.87	12	0.72	0.0003
				0.05	5965	2354.92	7	0	0
				0.1	5185	2046.98	15	4.61	0.0023
				0.2	5340	2108.17	34	23.30	0.0111
				0.5	5102	2014.21	70	59.77	0.0297
				1	5143	2030.40	218	207.69	0.1023
	D	M	23	0	5164	2038.69	4	0	0
				0.01	5337	2106.99	8	1.49	0.0007
				0.02	5141	2029.61	3	0	0
				0.05	5121	2021.71	8	1.75	0.0009
				0.1	5167	2039.87	7	0.70	0.0003
				0.2	7412	2926.17	37	27.96	0.0096
				0.5	5104	2015.00	68	61.77	0.0307
				1	5188	2048.16	225	218.67	0.1068
	E	F	33	0	5579	2173.35	15	4.75	0.0022
				0.1	5943	2315.15	16	5.09	0.0022
				0.02	5217	2032.33	15	5.42	0.0027
				0.05	5184	2019.48	18	8.48	0.0042
				0.1	5243	2042.46	26	16.37	0.0080
				0.2	5169	2013.63	26	16.51	0.0082
				0.5	7182	2797.82	97	83.81	0.0300
				1	5209	2029.22	222	212.43	0.1047

Table 2 (continued)

Pooled	0	27758	10929.37	48	4.75	0.0004
	0.1	28263	11126.84	67	10.60	0.0010
	0.02	27822	10956.53	65	6.64	0.0006
	0.05	27182	10704.04	73	17.14	0.0016
	0.1	27120	10679.26	96	32.21	0.0030
	0.2	30292	11931.91	171	101.55	0.0085
	0.5	28508	11217.08	407	340.88	0.0304
	1	25987	10232.14	1179	1118.85	0.1093
Averaged	0	5551.6	2185.87	9.6	0.95	0.0004
	0.1	5652.6	2225.37	13.4	2.12	0.0010
	0.02	5564.4	2191.31	13.0	1.33	0.0006
	0.05	5436.4	2140.81	14.6	3.43	0.0016
	0.1	5424.0	2135.85	19.2	6.44	0.0030
	0.2	6058.4	2386.38	34.2	20.31	0.0085
	0.5	5701.6	2243.42	81.4	68.18	0.0304
	1	5197.4	2046.43	235.8	223.77	0.1093

FISH-Tr DRCs (Figure 2) and their coefficients (C, α, β) (Table 3) were obtained from individual donors A to E, and from their pooled separated, pooled and averaged age-adjusted Tr/CE. DRCs constructed on individual donor data sets showed lower overall statistical significance in α and β as compared to DRCs constructed with pooled or averaged data sets from all five donors. In addition, generalized linear modelling was unsuccessful in donor D and no DRC coefficients were obtained. As a result, DRCs generated from individual donors were excluded from subsequent analyses in determining which data set would be the most suitable for retrospective dose estimation.

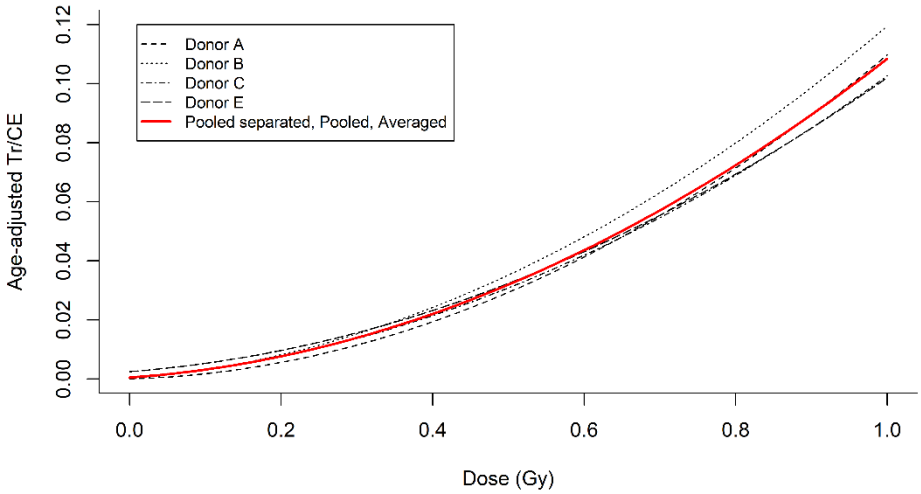

Figure 2: FISH-Tr DRCs obtained from donors A, B, C, E and their pooled/averaged age-adjusted Tr/CE. Generalized linear modelling was unsuccessful in donor D. DRC coefficients obtained from pooled separated, pooled and averaged values were identical and hence shown as a single curve.

Table 3: FISH-Tr DRC coefficients with goodness-of-fit (age-adjusted Tr/CE).

Data set	$C \pm SE_C$	**p*-value (C)	$\alpha \pm SE_\alpha$	**p*-value (α)	$\beta \pm SE_\beta$	**p*-value (β)	Goodness-of-fit		
							χ^2	df	*p*-value
Donor A	0.0000 ± 0.0000	0.100	0.0076 ± 0.0052	0.145	0.1021 ± 0.0097	4.04×10^{-26}	27.85	5	0.001
Donor B	0.0000 ± 0.0000	1.00	0.0213 ± 0.0067	0.0014	0.0982 ± 0.0110	5.00×10^{-19}	6.48	5	0.086
Donor C	0.0003 ± 0.0003	0.259	0.0197 ± 0.0082	0.0161	0.0826 ± 0.0120	5.04×10^{-12}	15.85	5	0.004
Donor D	NA	NA	NA	NA	NA	NA	NA	5	NA
Donor E	0.0025 ± 0.0006	9.81×10^{-5}	0.0199 ± 0.0104	0.0555	0.0796 ± 0.0140	1.43×10^{-8}	4.46	5	0.533
Pooled (separated)	0.0005 ± 0.0001	0.0008	0.0178 ± 0.0037	1.26×10^{-6}	0.0901 ± 0.0055	1.97×10^{-61}	111.35	37	2.2×10^{-10}
Pooled	0.0005 ± 0.0001	0.0008	0.0178 ± 0.0037	1.26×10^{-6}	0.0901 ± 0.0054	1.97×10^{-61}	4.38	5	0.501
Averaged	0.0005 ± 0.0003	0.135	0.0178 ± 0.0082	0.0302	0.0901 ± 0.0122	1.41×10^{-13}	0.88	5	0.972

Goodness-of-fit was determined using Pearson's chi-squared test.
NA: R was unable to fit a generalized linear model to the data.
**p*-values of coefficients were computed using F-test.

FISH-Tr DRC coefficients obtained with pooled separated, pooled and averaged age-adjusted Tr/CE were identical, but a difference in standard error (SE) was seen. Comparing the three options, DRC coefficients and their associated SE had a higher level of statistical significance if pooled age-adjusted Tr/CE was used. A narrower 95% CLwas seen if pooled age-adjusted Tr/CE was used instead of averaged age-adjusted Tr/CE (Figure 3), most likely caused by the smaller variance and covariance values (Table 4). There was no difference in 95% CL and in the significance of coefficients between pooled separated and pooled values. However, the high degrees of freedom (df) in the pooled separated DRC resulted in the rejection of the null hypothesis (a significant difference between observed and expected values) due to the high chi-square value. As a result, because of the invalid goodness-of-fit with pooled separated values, subsequent comparisons were performed on DRCs obtained with pooled and averaged age-adjusted Tr/CE.

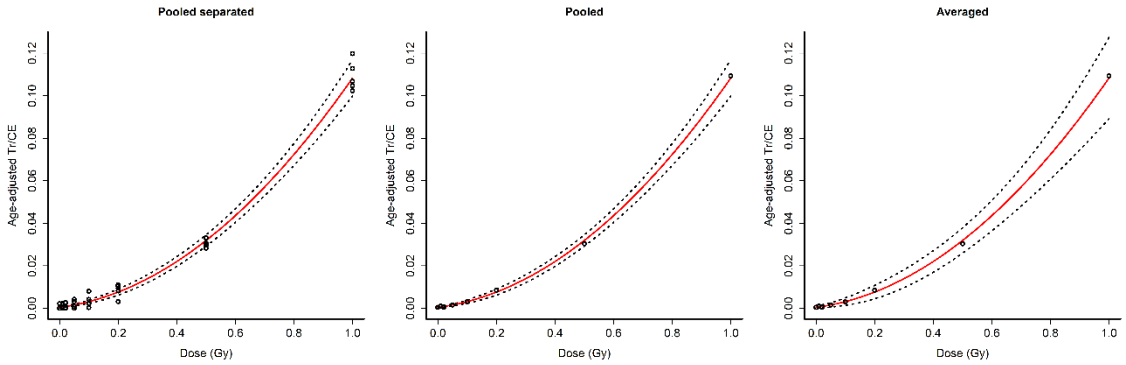

Figure 3: DRCs constructed with pooled separated, pooled and averaged age-adjusted Tr/CE from five donors (red solid line) with their 95% CL (dashed line). Each open circle represents the Tr yield.

Table 4: Variance-covariance matrix coefficients from DRCs constructed with pooled separated, pooled and averaged age-adjusted Tr/CE.

Data set	Var(C)	Var(α)	Var(β)	Covar(C)	Covar(α)	Covar(β)
Pooled (separated)	2.17×10^{-8}	1.36×10^{-5}	2.97×10^{-5}	-2.77×10^{-7}	3.05×10^{-7}	-1.69×10^{-5}
Pooled	2.17×10^{-8}	1.36×10^{-5}	2.97×10^{-5}	-2.77×10^{-7}	3.05×10^{-7}	-1.69×10^{-5}
Averaged	1.09×10^{-7}	6.78×10^{-5}	1.48×10^{-4}	-1.38×10^{-6}	1.53×10^{-6}	-8.47×10^{-5}

To translate the differences in 95% CL seen in pooled and averaged DRC to actual estimated doses, Merkle's approach of Method C was used to account for both the Poisson error of Tr yield and errors associated with DRC[2), 33)]. D_U and D_L were respectively obtained when Y_U crossed the lower 95% CL curve and when Y_L crossed the upper 95% CL curve. D_U and D_L averaged from five donors were calculated from 95% CL in pooled and averaged DRCs (Figure 4).

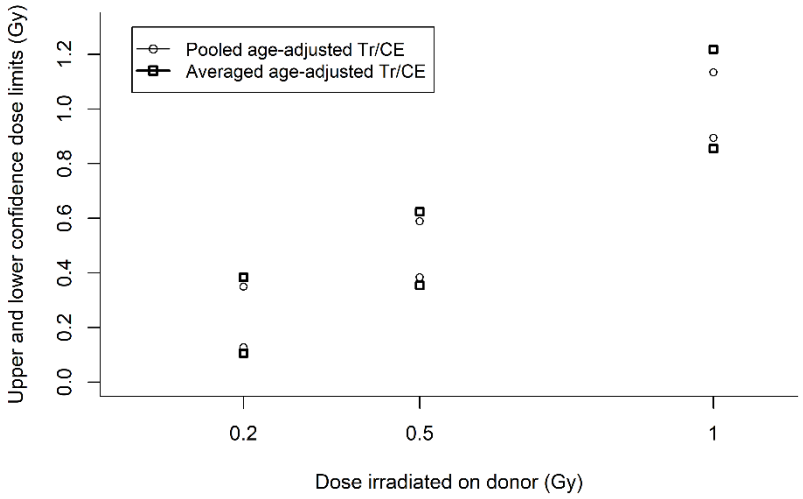

Figure 4: Upper and lower confidence dose limits (averaged among 5 donors) estimated from upper and lower Poisson Tr yields and 95% CL, obtained from FISH-Tr DRCs generated with pooled (open circle) or averaged (open square) age-adjusted Tr/CE. Dose estimated from donor A irradiated with 0.2 Gy was omitted as the observed Tr yield was lower than its detection limit.

D_U and D_L were not calculated from Tr scored in doses below 0.2 Gy as the detection limit was lower than its corresponding observed Tr yield, thus estimated D_U and D_L were not statistically reliable. Moreover, MDD with valid data sets was approximately 0.2 Gy. The estimated dose range ($D_U - D_L$ in Gy) was approximately 1.3 to 1.5 times larger if averaged age-adjusted Tr/CE was used, with a possibility of a wider dose range obtained in higher doses above 1 Gy.

Adjusting `glm()` function fitting conditions in R in the event that curve fitting with `glm()` fails

Despite satisfying ISO requirements for the age-adjusted Tr/CE data set in donor D, curve fitting with `glm()` function unexpectedly failed and no DRC equation was obtained. We investigated various reasons that could have contributed to the failure to converge and came up with a possible solution. Firstly, in order for `glm()` function to run in R, some starting values for C, α and β (`x0`, `x1` and `x2` in the code respectively) must be provided.

In the original R-script provided by H. Braselmann, no starting values were defined with `start=` in `glm()`. As a result, we modified the code by providing starting values obtained with `lm()`. Starting values derived from `lm()` were compared among the different Tr data sets, and it was possible that negative starting values in `x0` caused `glm()` fitting to fail in donor D (Table 5).

Table 5: Starting values for x0, x1 and x2 in `glm()` function obtained from `lm()` function.

Data set	glm converged?	Starting x0	Starting x1	Starting x2
Donor A	Success	0.0004	-0.0039	0.1166
Donor B	Success	0.0002	0.0196	0.0996
Donor C	Success	0.0002	0.0220	0.0798
Donor D	Failed	-0.0001	0.0222	0.0844
Donor E	Success	0.0030	0.0084	0.0930
Pooled (separated)	Success	0.0007	0.0138	0.0947
Pooled	Success	0.0007	0.0136	0.0948
Averaged	Success	0.0007	0.0136	0.0948

To confirm this, starting values of `x0`, `x1` and `x2` were fixed at 0.01 with alternating negative values on a successful modelling data set of pooled age-adjusted Tr/CE. Once again, negative starting values in `x0` resulted in failed `glm()` convergence. C, α and β values after `glm()` fitting were also very similar, despite having different starting `x0`, `x1` and `x2` values (Table 6).

Table 6: Values of C, α, β (`x0`, `x1`, `x2` in the R-script respectively) after `glm()` fitting with fixed starting values of `x0`, `x1` and `x2`, using the data set of pooled age-adjusted Tr/CE.

Starting `x0`	Starting `x1`	Starting `x2`	C	α	β	glm converged?
0.0007	0.0136	0.0948	0.0005	0.0178	0.0901	Yes
0.01	0.01	0.01	0.0005	0.0178	0.0901	Yes
-0.01	0.01	0.01	NA	NA	NA	No
0.01	-0.01	0.01	0.0005	0.0178	0.0901	Yes
0.01	0.01	-0.01	0.0005	0.0178	0.0901	Yes

Initial `x0`, `x1` and `x2` of 0.0007, 0.0136 and 0.0948 respectively were obtained from `lm()` function with pooled age-adjusted Tr/CE.
NA: R was unable to fit a generalized linear model to the data.

Next, as `glm()` fitting in R was performed with IRLS, the number of iterations and ε values (positive convergence tolerance ε; iterations converge when |deviance – old deviance|/(|deviance| + 0.1) < ε ("stats" package, ver 3.5.3[13]) were modified in the `glm()` argument to check for possible `glm()` fitting with donor D. Positive starting values of `x0`, `x1`, and `x2` from 0.001 to 0.500, with simultaneous 0.001 increments in all

3 variables, were tested with various combinations of maximum iteration and ε values (Table 7).

Table 7: Values of C, α and β (`x0`, `x1`, `x2` in the R-script respectively) after `glm()` fitting with starting values of `x0`, `x1` and `x2` fixed from 0.001 to 0.500 with simultaneous 0.001 increments in all three variables, while modifying maximum number of iterations and ε in donor D.

Max no. of iterations	ε	C	Difference between C	α	Difference between α	β	Difference between β	glm converged?
25	1e-8	8.24×10^{-6} - 3.02×10^{-5}	2.19×10^{-5}	0.0165 - 0.0170	5.19×10^{-4}	0.0906 - 0.0912	6.32×10^{-4}	Yes
1000	1e-8	3.00×10^{-5} - 3.01×10^{-5}	1.22×10^{-7}	0.0165	3.06×10^{-6}	0.0912	3.76×10^{-5}	Yes
1000	1e-10	3.00×10^{-5} - 3.01×10^{-5}	1.23×10^{-8}	0.0165	3.07×10^{-7}	0.0912	3.78×10^{-7}	Yes
1000	1e-25	3.00×10^{-5}	6.57×10^{-11}	0.0165	1.64×10^{-9}	0.0912	2.02×10^{-9}	Yes

The default setting of IRLS in R is a maximum of 25 iterations and ε of 1e-8.
Values of C, α and β are shown up to 4 decimal places, and up to 2 decimal places in scientific notation.

If `glm()` fitting is still required after a failed initial convergence, a maximum number of iterations of 1000 and an ε value of 1e-25 should be used to ensure the least amount of differences seen in C, α and β despite varying starting values of `x0`, `x1` and `x2`.

Comparing our FISH-Tr DRC coefficients with other published curves

Our derived coefficients for FISH-Tr DRC were further validated with other published DRCs[8-9), 34-37)] constructed with ^{60}Co gamma irradiation. To accurately compare DRC coefficients between different laboratories which utilized different chromosome FISH probes, their data sets were corrected to age-adjusted Tr/CE within the dose range of 0 to 1 Gy, except for the DRC equation published in ISO 20046:2019. Robust *Z*-score was obtained for α coefficients between different DRCs which fulfilled the goodness-of-fit test and showed reasonable DRCs constructed with 95 % CL. No outliers were detected as the absolute robust *Z*-score was within 3 (Table 8).

Table 8: Comparison of previously published FISH-Tr DRC coefficients using age-adjusted Tr/CE from 0 to 1 Gy.

Reference	Donor(s)/ Sex (Age)	Doses (Gy)	Dose rate (Gy/min)	CE	C ± SE_C	α ± $SE_α$	β ± $SE_β$	Goodness-of-fit			Absolute robust *Z*-score
								χ^2	df	*p*-value	
^{60}Co, reciprocal Tr, all cells scored											
34)[a]	1/M (43), 1/F (30)	0, 0.05, 0.1, 0.25, 0.75, 1	0.24	16,039 (averaged CE)	0.0016 ± 0.0005	0.0121 ± 0.0087	0.0367 ± 0.0140	0.72	4	0.950	
				16,433 (actual CE)	0.0014 ± 0.0005	**0.0119** ± 0.0083	0.0357 ± 0.0135	0.72	4	0.949	0.158
35)[b]	1/M (31)	0, 0.25, 0.5, 0.75, 1	0.5	2371	6.57×10^{-5} ± 0.0003	0.0595 ± 0.0201	-0.0213 ± 0.0255	0.2	2	0.906	
8)[a, b]	1/F (25) for radiation, 3/F (25, 26, 27) for 0 Gy	0, 0.1, 0.25, 0.5, 0.75, 1	0.294 − 0.3	5673	NA	NA	NA	NA	3	NA	
^{60}Co, total simple Tr, all cells scored											
34)[a]	1/M (43), 1/F (30)	0, 0.05, 0.1, 0.25, 0.75, 1	0.24	16,039 (averaged CE)	0.0044 ± 0.0008	-0.0076 ± 0.0110	0.0835 ± 0.0177	1.68	4	0.792	
				16,433 (actual CE)	0.0042 ± 0.0008	**-0.0074** ± 0.0107	0.0814 ± 0.0172	1.67	4	0.793	0.674
36)[a, b]	2/M (24)	0, 0.32, 0.62, 0.92	0.000111 − 0.000319	38,952	NA	NA	NA	NA	1	NA	
35)[a, b]	1/M (31)	0, 0.25, 0.5, 0.75, 1	0.5	2371	0.0065 ± 0.0031	0.0608 ± 0.0283	-0.0039 ± 0.0339	2.72	2	0.229	
8)[a]	1/F (25) for radiation, 3/F (25, 26, 27) for 0 Gy	0, 0.1, 0.25, 0.5, 0.75, 1	0.294 − 0.3	5673	0.0009 ± 0.0008	**0.0644** ± 0.0156	-0.0015 ± 0.0205	4.10	3	0.266	1.247
37)[a, b]	1/F (47)	0, 0.05, 0.1, 0.15, 0.2, 0.25, 0.3, 0.5, 0.75, 1	0.3	64,341	NA	NA	NA	NA	7	NA	
Our DRC	4/M (23, 35, 44, 45); 1/F (33)	0, 0.01, 0.02, 0.05, 0.1, 0.2, 0.5, 1	0.2626t + 0.0642 (t:min)	87,777 (pooled)	0.0005 ± 0.0001	**0.0178** ± 0.0037	0.0901 ± 0.0054	4.38	5	0.501	0
				17,555 (averaged)	0.0005 ± 0.0003	0.0178 ± 0.0082	0.0901 ± 0.0122	0.88	5	0.972	

Table 9 (continued)

^{60}Co, total Tr (including insertions and inversions), all cells scored											
8)[a]	1/F (25) for radiation, 3/F (25, 26, 27) for 0 Gy	0, 0.1, 0.25, 0.5, 0.75, 1	0.294 − 0.3	5673	0.0009 ± 0.0008	**0.0656** ± 0.0160	0.0047 ± 0.0212	2.68	3	0.474	1.279
^{60}Co, reciprocal Tr, stable cells scored											
35)[a, b]	1/M (31)	0, 0.25, 0.5, 0.75, 1	0.5	2290	NA	NA	NA	NA	2	NA	
8)[a, b]	1/F (25) for radiation, 3/F (25, 26, 27) for 0 Gy	0, 0.1, 0.25, 0.5, 0.75, 1	0.294 − 0.3	5523	NA	NA	NA	NA	3	NA	
^{60}Co, total simple Tr, stable cells scored											
35)[a, b]	1/M (31)	0, 0.25, 0.5, 0.75, 1	0.5	2290	0.0062 ± 0.0030	0.0223 ± 0.0254	0.0385 ± 0.0318	0.24	2	0.885	
8)[a]	1/F (25) for radiation, 3/F (25, 26, 27) for 0 Gy	0, 0.1, 0.25, 0.5, 0.75, 1	0.294 − 0.3	5523	0.0010 ± 0.0008	**0.0447** ± 0.0144	0.0142 ± 0.0195	2.36	3	0.521	0.800
9)	Based on RENEB's inter-comparison study[38]				0.0001 ± 0.0021	**0.0152** ± 0.0108	0.0809 ± 0.0061	-	-	-	0.070
^{60}Co, total Tr (including insertions and inversions), stable cells scored											
8)[a]	1/F (25) for radiation, 3/F (25, 26, 27) for 0 Gy	0, 0.1, 0.25, 0.5, 0.75, 1	0.294 − 0.3	5523	0.0010 ± 0.0008	0.0447 ± 0.0144	0.0142 ± 0.0195	2.36	3	0.521	

[a]: Original DRC coefficients were published with respect to observed Tr/Cell. The data had been converted to age-adjusted Tr/CE within the dose range of 0 to 1 Gy for inter-laboratory comparisons. DRC was computed using R and confirmed with Dose Estimate ver. 5.2.
[b]: Omitted from robust Z-score of α coefficients due to poor fit of DRC and its 95% CL.
Bold: Selected α coefficients used for robust Z-score.
NA: R was unable to fit a generalized linear model to the data.
Goodness-of-fit was determined using Pearson's chi-squared test.

Discussion (Chapter 1)

The FISH-Tr DRC constructed in this paper is the first to fulfil most of the requirements in ISO 20046:2019 for cytogenetic biodosimetry. This DRC was constructed with IRLS, using 8 dose points from 0 to 1 Gy and age-adjusted Tr in > 2000 CE scored per dose. As a Japanese population-specific background Tr frequency is not yet available, age-adjustment was perfromed with Sigurdson's equation. The equation was derived from a comprehensive meta-analysis of many individuals across different countries from ages 0 to over 80[20]. The DRC plot with its upper and lower 95% CL curves, the DRC coefficients (C, α, β) with their respective *p*-values, and goodness-of-fit were generated with R and reported. No distinction was made between stable and unstable Tr. As previously reported by Rodríguez *et al.*[8], the percentage of stable cells is 91.1 % after 1 Gy irradiation using a ^{60}Co source, although the stable cell proportion decreases to about 85 % when irradiated with ^{137}Cs[39-40]. The FISH-Tr DRC equation established in this paper, $Y = 0.0005 (\pm 0.0001) + 0.0178 (\pm 0.0037) * D + 0.0901 (\pm 0.0054) * D^2$, should still be valid for dose estimation with a stable cell population up to 1 Gy.

Over 20 attempts were previously published for FISH-Tr DRC construction for retrospective biodosimetry, mostly with *in vitro* ^{60}Co gamma irradiation. The accuracy of DRC conefficients obtained could be affected by several important factors that differed among the various attempts. The (1) use of cells scored or CE scored, (2) method and inclusion of age-adjustment, (3) types of Tr scored (reciprocal two-way, simple one and two-way, total Tr including inversions and insertions), (4) type of cells scored (stable or all cells) and (5) dose range used are all factors that should be considered and standardized for reliable FISH-Tr DRC construction. Despite the absence of outliers between α coefficients of previously published DRCs and our DRC as seen in Table 9, ISO 20046:2019 can help to further reduce variability between laboratories in future DRCs constructed.

For FISH-Tr DRC coefficients to be reliably compared for validation and/or for previously established DRC equations to be used in different laboratories for dose estimation, cells scored should be converted to CE as different laboratories stain different chromosomes with WCP-FISH. CE conversion performed by most laboratories used Lucas *et al.*'s formula[21] and sex-specific chromosome lengths derived by Morton[22],

except for Lindholm *et al.*[34] who used the averaged CE between males and females. The α coefficients obtained with sex-specific or averaged CE were very similar in our pooled age-adjusted Tr/CE data set (0.0178 vs. 0.0181, Figure 5). However, for consistency and accuracy, CE should be separately calculated for males and females.

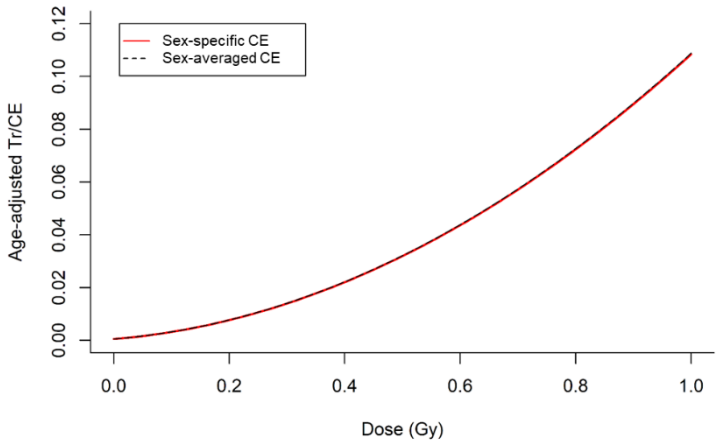

Figure 5: FISH-Tr DRCs constructed with our pooled age-adjusted Tr/CE data set shown in Table 3. CE conversion was performed separately for males and females (sex-specific CE) and averaged between males and females (sex-averaged CE). DRCs obtained with both methods were extremely similar.

One of the major issues of FISH-Tr DRC construction is the significant increase of background Tr with increasing age[41]. No such issue is seen with Dic DRCs as Dic is formed almost specifically with radiation exposure with no statistically significant age-dependency[42]. Age-adjustment of Tr frequency before DRC construction is therefore necessary to ensure that the increased Tr frequency observed is predominantly attributed to radiation exposure, and not due to other external factors such as age and smoking[43]. Age-adjustment is performed with equations derived from background Tr/CE of many individuals at 0 Gy. In most FISH-Tr DRCs, including ISO 20046:2019, Tr age-adjustment uses the Sigurdson's equation derived from a meta-analysis of 1933 individuals from 13 countries. Total simple Tr were counted in ≥ 100 CE scored in each individual[20]. Liu *et al.*[44], on the other hand, used the age-adjustment equation from Lucas *et al.*[45], which was derived from total simple Tr scored in > 300 CE in each of the 29 individuals from North America (assumed age 0 had 0 Tr, Tr scored from ages 23 to 98). Sigurdson's background Tr/CE with increasing age was an exponential relationship (background Tr/CE = exp(–7.925) + exp(–9.284) * (age * exp(0.01062 * age)), while Lucas's was a linear-quadratic relationship (background Tr/CE = 7e-4 + 6.9e-6 * age +

1.35e-6 * age^2). When Tr age-adjustment using Sigurdson's or Lucas' equation was compared, DRC α coefficients in the pooled age-adjusted Tr/CE data set differed slightly (0.0178 vs. 0.0245, Figure 6).

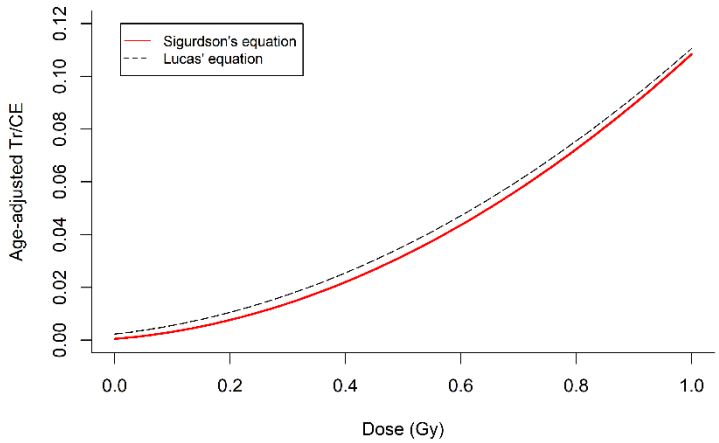

Figure 6: FISH-Tr DRCs constructed with our pooled age-adjusted Tr/CE data set shown in Table 3. Age-adjustment was performed with both Sigurdon's and Lucas' equations. DRCs obtained with both equations differed slightly.

Comparing the two equations, Sigurdson's equation is evidently more statistically reliable than the Lucas equation, due to the larger sample size of individuals from multiple age groups. Surprisingly, in most retrospective biodosimetry, no Tr age-adjustment with Sigurdson's equation was performed for dose estimation. Instead, the age-dependent increase of Tr was accounted for by comparing between spontaneous Tr between age-matched irradiated and control populations[23), 46-49)], such that doses were only estimated in irradiated individuals above the Tr baseline frequency. In that particular scenario, the background Tr yield obtained from the age, sex and lifestyle-matched control population will be more accurate than the background Tr compiled from Sigurdson's data set. Age-adjustment should hence be preferably done based on the matched control population.

The reliability of retrospective dose estimation using Tr is also heavily dependent on Tr half-life, as biodosimetry is performed long after the initial radiation exposure. Irradiated victims from the Estonian radiological accident showed that total simple Tr scored in all stable and unstable cells had a sharp initial decrease to 70 % and 60 % of its initial value after chronic 1 Gy and chronic 3 Gy exposure after 2 years respectively, and continued to remain stable after 6.2 years. No initial decline of Tr was seen if stable cells were only scored[5)]. Similarly seen in Cho *et al.*'s study, total simple Tr in stable cells in radiological workers exposed to > 500 mGy persisted up to 1.64 years, with an estimated

half-life longer than an average human's lifespan[6]. However, more complicated forms of irradiation such as partial-body exposure could decrease Tr stability. Reciprocal Tr in both stable and unstable cells of a 13 year old victim in the Estonian accident, who was non-uniformly irradiated with high and low dose rates for 4 weeks, showed a half-life of 4.31 ± 1.06 years[50]. Similarly, total simple Tr in all partially-irradiated lymphocyte cells decreased with prolonged culture as compared to uniformly-irradiated cells[51]. The decrease in Tr could also be accelerated by the presence of unstable cells. Cells with unstable aberrations such as Dic showed a much shorter half-life than cells with Tr[6, 50, 52].Thus, for retrospective biodosimetry, Tr in stable cells should only be scored for FISH-Tr DRCs as Tr shows strong persistence with little variation up to 10 to 13 years[53-54].

There were also several disagreements about (1) which chromosomes should be stained that could capture the most Tr information, (2) which aberration scoring method should be used, and (3) which type of highly persistent Tr should be scored for retrospective biodosimetry. Some studies initially reported some chromosomes were more sensitive than others after radiation, particularly in chromosome 4[55-56], which might lead to an uneven detection of Tr among differently painted chromosomes in different laboratories. This was not seen in other studies[57-59], and it is now generally agreed that Tr yield is independent of which chromosomes are painted[60]. Tr can also be scored with either the traditional system of classification or the PAINT system[61]. Both are essentially the same, except that the PAINT system treats reciprocal Tr as two separate events, possibly increasing and overestimating Tr frequency. Matsumoto *et al.*[62] compared Tr scored with the two methods, and traditionally scored Tr followed a Poisson distribution, similar to the Dic induced in the same population. However, it is now accepted in most laboratories to score one reciprocal Tr as one Tr event, and one non-reciprocal Tr as one Tr event[17], which we also used for our DRC construction. The types of Tr scored in previously constructed FISH-Tr DRCs were also mainly divided between reciprocal Tr or total simple Tr, although some laboratories also used total Tr which included insertions and inversions[8, 63-64]. Notably, reciprocal Tr was argued to be the most stable as no significant decrease was seen when they were scored in all or stable cells[65-66]. An attempt of Tr frequency correction to account for unstable non-transmissible pseudosimples and other hidden complexes was also made to reduce dose estimation error[7-8]. Several European laboratories, however, came to a consensus that all simple Tr in stable cells

should be recorded, as the omission of unstable cells would eliminate the main source of Tr instability, without the need for additional corrections[31]. Even though insertions and inversions are stable over time, the proportion is significantly much lower than reciprocal or one-way Tr after low LET radiation[67], hence they can be ignored for scoring.

In ISO 20046:2019, emphasis was instead placed on the consistency in the types of Tr scored for DRC generation and for dose estimation. Scoring of all types of Tr was also allowed. However, in our attempts of Tr age-adjustment with previously published FISH-DRC data sets, many data sets, especially those who only scored reciprocal Tr, failed to properly fit into a Poisson regression model. Age-adjustment using Sigurdson's equation removed background simple (reciprocal and one-way) Tr. As a result, to apply Sigurdson's equation accurately, and to increase the possibility of successful Poisson regression modelling, total simple Tr in stable cells should be scored.

Interestingly, the use of multiple donors was emphasized and required for DRC construction with cytokinesis-block micronucleus (CBMN) assay[68], but not with Dic[69]. The increase in number of donors for CBMN accounts for the significant age and sex-dependent effects on micronucleus frequency[70-71], which was not seen in Dic[42]. For FISH-Tr DRC, background Tr were removed with age-adjustment, which could explain why the number of donors was not explicitly stated in ISO 20046:2019. Nevertheless, the possibility of successful Poisson regression modelling could be significantly increased with multiple donors as it is very risky to construct the DRC based on one donor, as seen from the failure of convergence after age-correction in donor D. If DRC failed to converge initially for any statistically robust data set, convergence can be forced by modifying starting `x0`, `x1` and `x2` values to 0.01, increasing maximum number of iterations to 1000 and reducing ε to 1e-25. Number of iterations in IRLS changes depending on the data set, maximum number of iterations and ε value, hence the modification of IRLS conditions in `glm()` function should be exercised with caution (Figure 7).

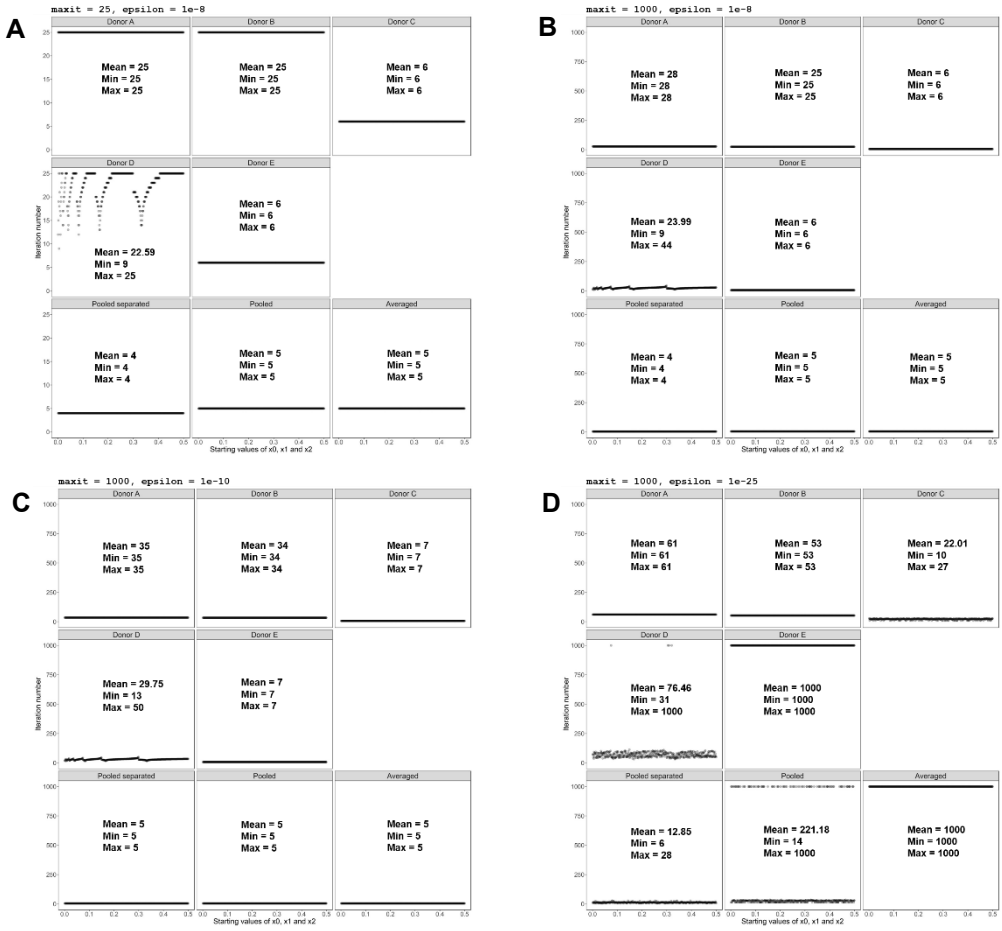

Figure 7: Number of iterations in IRLS with varying starting values of `x0`, `x1` and `x2` from 0.001 to 0.500 with simultaneous 0.001 increments, varying maximum values of iterations (maxit) and ε values, for individual donors A to E, pooled separated, pooled and averaged DRCs. Mean, minimum and maximum number of iterations are included in each figure. (A) maxit = 25, ε = 1e-8, (B) maxit = 1000, ε = 1e-8, (C) maxit = 1000, ε = 1e-10, (D) maxit = 1000, ε = 1e-25.

FISH-Tr DRCs constructed also differed greatly between donors B and C, even though there was sufficient dose points and a high number of CE scored per dose point. It is possible that DRC variability between donors B and C could be caused by their difference in age. Especially in the lower doses below 0.1 Gy and in older donors, the use of multiple donors can ensure that age-adjusted Tr/CE have positive non-zero values for successful modelling. In contrast, the number of donors is not as critical in Dic DRCs as Dic frequency is always above 0 with increasing dose. Furthermore, increasing the number of donors could account for inter-individual variability for both FISH-Tr and Dic DRCs.

Comparing between FISH-Tr DRCs constructed with averaged and pooled age-adjusted Tr/CE from 5 donors, DRC coefficient values remained the same while the range

of the 95 % CL was higher in averaged than pooled data sets. In other words, the dose estimated will be identical in both conditions, but the dose range obtained from the interval between D_U and D_L will differ by ~1.3 to 1.5 times up to 1 Gy. The difference in dose range might also increase in higher doses above 1 Gy. Thus, the decision behind the use of averaged or pooled age-adjusted Tr/CE should be justified by each cytogenetic laboratory. If individual data points of age-adjusted Tr/CE in multiple donors are required to be shown, pooled separated Tr/CE can be used for DRC generation. However, due to poor goodness-of-fit, the DRC equation derived from pooled Tr/CE should be used instead for dose estimation.

Finally, the MDD of our FISH-Tr DRC was approximately 0.2 Gy. The MDD published in EPR-Biodosimetry[2)] and the TMT Handbook[1)] ranged from 0.25 to 0.4 Gy. Consistent to other published data, the MDD can range from 0.08 to 0.5 Gy[60), 72)] as MDD depends on the individual's age, number of cells scored and type of radiation exposure. Moreover, a linear increase in MDD was seen with increasing age, for individuals aged 20 to 69[73)]. In applications of retrospective biodosimetry to estimate accumulated doses in chronic low dose exposures in occupational work exposure, MDD from FISH-Tr DRCs should be much lower as the annual threshold of 20 mSv is recommended by the International Committee of Radiation Protection[74)]. There is a need to improve the accuracy of dose estimation by increasing number of cells scored during dose estimation to lower MDD. It is also important to emphasize that dose estimated with FISH-Tr DRC is the cumulative radiation dose over a lifetime. In individuals with previous radiation exposures caused by X-rays, CT scans or radiotherapy, the dose will be significantly higher than expected, and thus should be noted when reporting dose estimates. Lastly, Tr clones were not identified in our study as clones are more likely to appear after chronic or long periods after radiation[75)]. It is hence important to exclude clones during retrospective dose estimation.

In conclusion, the R-Script provided in this paper serves as another user-friendly tool for FISH-Tr DRC construction, in addition to other available software such as Dose Estimate[11)] and CABAS[12)], for cytogeneticists with some basic knowledge of R. The R-script, which was modified from H. Braselmann's original code published in EPR-Biodosimetry, outputs all relevant statistical values needed for DRC and dose estimation

reports in accordance to ISO standards. Multiple donors (> 3) should be used for DRC construction to ensure a proper linear-quadratic fit with Poisson regression after age-adjustment. Furthermore, the decision of choosing averaged or pooled data values for DRC construction (wider or narrower 95% CL respectively) heavily depends on the use of dose estimates. Medical professionals often utilize the upper limit of dose estimates for medical treatment after acute radiation. In retrospective biodosimetry (prior radiation exposure long before blood collection or chronic low dose exposure), however, a more accurate dose estimate with a narrower dose range is recommended. Thus, for retrospective biodosimetry using FISH-Tr DRC, we suggest scoring age-adjusted pooled simple Tr in stable cells (>2000 CE in each dose) from multiple donors for up to 1 Gy, preferably within the same age group as specified by Sigurdson *et al*.

References (Chapter 1)

1. Rojas-Palma C, Liland A, Jerstad AN, Etherington G, del Rosarlo Pérez M, Rahola T, Smith K: TMT handbook, triage, monitoring and treatment of people exposed to ionizing radiation following a malevolent act. Norwegian Radiation Protection Authority, Norway, 2009.
2. International Atomic Energy Agency. Cytogenetic dosimetry: applications in preparedness for and response to radiation emergencies. EPR-Biodosimetry. IAEA, Vienna, Austria, 2011.
3. Kanda R, Minamihisamatsu M, Hayata I: Dynamic analysis of chromosome aberrations in three victims of the Tokai-mura criticality accident. Int J Radiat Biol, 78(9):857–862, 2002.
4. Lloyd DC, Purrott RJ, Reeder EJ: The incidence of unstable chromosome aberrations in peripheral blood lymphocytes from unirradiated and occupationally exposed people. Mutat Res, 72(3):523–532, 1980.
5. Lindholm C, Edwards A: Long-term persistence of translocations in stable lymphocytes from victims of a radiological accident. Int J Radiat Biol, 80(8):559–566, 2004.
6. Cho MS, Lee JK, Bae KS, Han EA, Jang SJ, Ha WH, Lee SS, Barquinero JF, Kim WT: Retrospective biodosimetry using translocation frequency in a stable cell of occupationally exposed to ionizing radiation. J Radiat Res, 56(4):709–716, 2015.

7. Savage JRK, Papworth DG, Bauchinger M, Natarajan AT, Pantelias GE, Griffin CS, Figgitt M, Knehr S, Braselmann H, Darroudi F: Constructing a 2B calibration curve for retrospective dose reconstruction. Radiat Prot Dosim, 88(1):69–76, 2000.
8. Rodríguez P, Montoro A, Barquinero JF, Caballín MR, Villaescusa I, Barrios L: Analysis of translocations in stable cells and their implications in retrospective biological dosimetry. Radiat Res, 162(1):31–38, 2004.
9. ISO 20046: Radiological protection – Performance criteria for laboratories using Fluorescence In Situ Hybridization (FISH) translocation assay for assessment of exposure to ionizing radiation, 2019.
10. Abe Y, Yoshida MA, Fujioka K, Kurosu Y, Ujiie R, Yanagi A, Tsuyama N, Miura T, Inaba T, Kamiya K, et al.: Dose-response curves for analyzing of dicentric chromosomes and chromosome translocations following doses of 1000 mGy or less, based on irradiated peripheral blood samples from five healthy individuals. J Radiat Res, 59(1):35–42, 2018.
11. Ainsbury EA, Lloyd DC: Dose estimation software for radiation biodosimetry. Health Phys: 98(2):290–295, 2010.
12. Deperas J, Szluinska M, Deperas-Kaminska M, Edwards A, Lloyd D, Lindholm C, Romm H, Roy L, Moss R, Morand J, et al.: CABAS: a freely available PC program for fitting calibration curves in chromosome aberration dosimetry. Radiat Prot Dosim, 124(2):115–123, 2017.
13. R Core Team: R: A language and environment for statistical computing. R Foundation for Statistical Computing, Vienna, Austria, 2019.
14. Abe Y, Miura T, Yoshida MA, Ujiie R, Kurosu Y, Kato N, Katafuchi A, Tsuyama N, Ohba T, Inamasu T: Increase in dicentric chromosome formation after a single CT scan in adults. Sci Rep, 5:13882, 2015.
15. Abe Y, Yoshida MA, Fujioka K, Kurosu Y, Ujiie R, Yanagi A, Tsuyama N, Miura T, Inaba T, Kamiya K, et al.: Dose-response curves for analyzing of dicentric chromosomes and chromosome translocations following doses of 1000 mGy or less, based on irradiated peripheral blood samples from five healthy individuals. J Radiat Res, 59(1):35–42, 2018.
16. Fomina J, Darroudi F, Boei JJ, Natarajan AT: Discrimination between complete and incomplete chromosome exchanges in X-irradiated human lymphocytes using FISH

with pan-centromeric and chromosome specific DNA probes in combination with telomeric PNA probe. Int J Radiat Biol, 76(6):807–813, 2000.

17. Nakano M, Kodama Y, Ohtaki K, Itoh M, Delongchamp R, Awa AA, Nakamura N: Detection of stable chromosome aberrations by FISH in A-bomb survivors: comparison with previous solid Giemsa staining data on the same 230 individuals. Int J Radiat Biol, 77(9):971–977, 2001.
18. RStudio Team: RStudio: Integrated development for R. Boston, MA: RStudio, Inc, 2016.
19. Wickham H, Bryan J: readxl: Read excel files. R package version 1.3.1, 2019.
20. Sigurdson AJ, Ha M, Hauptmann M, Bhatti P, Sram RJ, Beskid O, Tawn EJ, Whitehouse CA, Lindholm C, Nakano M, et al.: International study of factors affecting human chromosome translocations. Mutat Res, 652(2):112–121, 2008.
21. Lucas JN, Awa A, Straume T, Poggensee M, Kodama Y, Nakano M, Ohtaki K, Weier HU, Pinkel D, Gray J: Rapid translocation frequency analysis in humans decades after exposure to ionizing radiation. Int J Radiat Biol, 62(1):53–63, 1992.
22. Morton NE: Parameters of the human genome. Proc Natl Acad Sci USA. 88(17):7474–7476, 1991.
23. Merkle W: Poisson goodness-of-fit tests for radiation-induced chromosome aberrations. Int J Radiat Biol Relat Stud Phys Chem Med, 40(6):685–692, 1981.
24. Fisher RA: The significance of deviations from expectation in a Poisson series. Biometrics, 6(1):17–24, 1950.
25. Rao CR, Chakravarti IM: Some small sample tests of significance for a Poisson distribution. Biometric, 12(3):264–282, 1956.
26. van den Broek J: A score test for zero inflation in a Poisson distribution. Biometrics, 51(2):738–743, 1995.
27. Bayarri MJ, Berger JO, Datta GS: Objective Bayes testing of poisson versus inflated poisson models. Inst Math Stat Collect, 3:105–121, 2008.
28. Higueras M, Puig P, Ainsbury EA, Vinnikov VA, Rothkamm K: A new Bayesian model applied to cytogenetic partial body irradiation estimation. Radiat Prot Dosim, 168(3):330–336, 2016.

29. Fernández-Fontelo A, Puig P, Ainsbury EA, Higueras M: An exact goodness-of-fit test based on the occupancy problems to study zero-inflation and zero-deflation in biological dosimetry data. Radiat Prot Dosim, 179(4):317–326, 2018.
30. Higueras M, González JE, Di Giorgio M, Barquinero JF. 2018. A note on Poisson goodness-of-fit tests for ionizing radiation induced chromosomal aberration samples. Int J Radiat Biol, 94(7):656–663, 2018.
31. Edwards AA, Lindholm C, Darroudi F, Stephan G, Romm H, Barquinero J, Barrios L, Caballin MR, Roy L, Whitehouse CA, et al.: Review of translocations detected by FISH for retrospective biological dosimetry applications. Radiat Prot Dosim, 113(4):396–402, 2005.
32. Tucker JD, Ramsey MJ, Lee DA, Minkler JL: Validation of chromosome painting as a biodosimeter in human peripheral lymphocytes following acute exposure to ionizing radiation in vitro. Int J Radiat Biol, 64(1):27–37, 1993.
33. Merkle W: Statistical methods in regression and calibration analysis of chromosome aberration data. Radiat Environ Biophys, 21:217–233, 1983.
34. Lindholm C, Luomahaara S, Koivistoinen A, Ilus T, Edwards AA, Salomaa S: Comparison of dose-response curves for chromosomal aberrations established by chromosome painting and conventional analysis. Int J Radiat Biol, 74(1):27–34, 1998.
35. Finnon P, Moquet JE, Edwards AA, Lloyd DC: The 60Co gamma ray dose-response for chromosomal aberrations in human lymphocytes analysed by FISH; applicability to biological dosimetry. Int J Radiat Biol, 75(10):1215–1222, 1999.
36. Hsieh WA, Deng W, Chang WP, Galvan N, Owens CL, Morrison DP, Gale KL, Lucas JN: Alpha coefficient of dose-response for chromosome translocations measured by FISH in human lymphocytes exposed to chronic 60Co gamma rays at body temperature. Int J Radiat Biol, 75(4):435–439, 1999.
37. Suto Y, Akiyama M, Noda T, Hirai M: Construction of a cytogenetic dose-response curve for low-dose range gamma-irradiation in human peripheral blood lymphocytes using three-color FISH. Mutat Res Genet Toxicol Environ Mutagen, 794:32–38, 2015.

38. Barquinero JF, Beinke C, Borràs M, Buraczewska I, Darroudi F, Grégoire E, Hristova R, Kulka U, Lindholm C, Moreno M, et al.: RENEB biodosimetry intercomparison analyzing translocations by FISH. Int J Radiat Biol, 93(1):30–35, 2017.
39. Bauchinger M, Schmid E, Zitzelsberger H, Braselmann H, Nahrstedt U: Radiation-induced chromosome aberrations analysed by two-colour fluorescence in situ hybridization with composite whole chromosome-specific DNA probes and a pancentromeric DNA probe. Int J Radiat Biol, 64(2):179–184, 1993.
40. Romm H, Stephan G: Dose dependency of FISH-detected translocations in stable and unstable cells after Cs gamma irradiation of human lymphocytes in vitro. Cytogenet Genome Res, 104(1–4):162–167, 2004.
41. Whitehouse CA, Edwards AA, Tawn EJ, Stephan G, Oestreicher U, Moquet JE, Lloyd DC, Roy L, Voisin P, Lindholm C, et al.: Translocation yields in peripheral blood lymphocytes from control populations. Int J Radiat Biol. 81(2):139–145, 2005.
42. Hoffmann W, Schmitz-Feuerhake I: How radiation-specific is the dicentric assay? J Expo Anal Environ Epidemiol, 9(2):113–133, 1999.
43. Tucker JD: Evaluation of chromosome translocations by FISH for radiation biodosimetry: a view from one laboratory. Radiat Prot Dosim, 88(1):87–92, 2000.
44. Liu QJ, Lu X, Zhao XT, Feng JB, L€u YM, Jiang EH, Zhang SL, Chen DQ, Jia TZ, Liang L: Assessment of retrospective dose estimation, with fluorescence in situ hybridization (FISH), of six victims previously exposed to accidental ionizing radiation. Mutat Res Genet Toxicol Environ Mutagen, 759:1–8, 2014.
45. Lucas JN, Deng W, Moore D, Hill F, Wade M, Lewis A, Sailes F, Kramer C, Hsieh A, Galvan N: Background ionizing radiation plays a minor role in the production of chromosome translocations in a control population. Int J Radiat Biol, 75(7):819–827, 1999.
46. Hayata I, Wang C, Zhang W, Chen D, Minamihisamatsu M, Morishima H, Yuan Y, Wei L, Sugahara T: Chromosome translocation in residents of the high background radiation areas in southern China. J Radiat Res, 41(Suppl):69–74, 2000.
47. Lindholm C: Stable and unstable chromosomal aberrations among Finnish nuclear power plant workers. Radiat Prot Dosim, 93(2):143–150, 2001.
48. Tawn EJ, Whitehouse CA, Riddell AE: FISH chromosome analysis of plutonium workers from the Sellafield nuclear facility. Radiat Res, 165(5):592–597, 2006.

49. Grégoire E, Roy L, Buard V, Delbos M, Durand V, Martin-Bodiot C, Voisin P, Sorokine-Durm I, Vaurijoux A, Voisin P, Baldeyron C, Barquinero JF: Twenty years of FISH-based translocation analysis for retrospective ionizing radiation biodosimetry. Int J Radiat Biol, 94(3):248–258, 2018.
50. Bauchinger M, Schmid E, Braselmann H: Time-course of translocation and dicentric frequencies in a radiation accident case. Int J Radiat Biol, 77(5):553–557, 2001.
51. Guerrero-Carbajal YC, Moquet JE, Edwards AA, Lloyd DC: The persistence of FISH translocations for retrospective biological dosimetry after simulated whole or partial body irradiation. Radiat Prot Dosim, 76(3):159–168, 1998.
52. Fucić A, Zeljezić D, Kasuba V, Kopjar N, Rozgaj R, Lasan R, Mijić A, Hitrec V, Lucas JN: Stable and unstable chromosome aberrations measured after occupational exposure to ionizing radiation and ultrasound. Croat Med J, 48(3):371–377, 2007.
53. Sevan'kaev A, Khvostunov I, Lloyd D, Voisin P, Golub E, Nadejina N, Nugis V, Sidorov O, Skvortsov V: The suitability of FISH chromosome painting and ESR-spectroscopy of tooth enamel assays for retrospective dose reconstruction. J Radiat Res, 47(Suppl A):A75–80, 2006.
54. Sakamoto-Hojo ET: Lessons from the accident with 137Cesium in Goiania, Brazil: Contributions to biological dosimetry in case of human exposure to ionizing radiation. Mutat Res Genet Toxicol Environ Mutagen, 836(Pt A):72–77, 2018.
55. Boei JJ, Vermeulen S, Natarajan AT: Differential involvement of chromosomes 1 and 4 in the formation of chromosomal aberrations in human lymphocytes after X-irradiation. Int J Radiat Biol, 72(2):139–145, 1997.
56. Braselmann H, Kulka U, Huber R, Figel HM, Zitzelsberger H: Distribution of radiation-induced exchange aberrations in all human chromosomes. Int J Radiat Biol, 79(6):393–403, 2003.
57. Barquinero JF, Knehr S, Braselmann H, Figel M, Bauchinger M: DNA-proportional distribution of radiation induced chromosome aberrations analysed by fluorescence in situ hybridization (FISH)-painting of all chromosomes of a human female karyotype. Int J Radiat Biol, 74(3):315–323, 1998.
58. Cigarran S, Barrios L, Barquinero JF, Caballín MR, Ribas M, Egozcue J: Relationship between the DNA content of human chromosomes and their

involvement in radiation-induced structural aberrations, analysed by painting. Int J Radiat Biol, 74(4):449–455, 1998.

59. Bothwell AM, Whitehouse CA, Tawn EJ, The application of FISH for chromosome aberration analysis in relation to radiation exposure. Radiat Prot Dosim, 88(1):7–14, 2000.
60. Pressl S, Romm H, Ganguly BB, Stephan G: Experience with FISH-detected translocations as an indicator in retrospective dose reconstructions. Radiat Prot Dosim, 88(1):45–49, 2000.
61. Tucker JD, Morgan WF, Awa AA, Bauchinger M, Blakey D, Cornforth MN, Littlefield LG, Natarajan AT, Shasserre C: A proposed system for scoring structural aberrations detected by chromosome painting. Cytogenet Cell Genet, 68(3–4):211–221, 1995.
62. Matsumoto K, Ramsey MJ, Nelson DO, Tucker JD: Persistence of radiation-induced translocations in human peripheral blood determined by chromosome painting. Radiat Res, 149(6):602–613, 1998.
63. Schmid E, Zitzelsberger H, Braselmann H, Gray JW, Bauchinger M. 1992. Radiation-induced chromosome aberrations analysed by fluorescence in situ hybridization with a triple combination of composite whole chromosome-specific DNA probes. Int J Radiat Biol. 62(6):673–678.
64. McKenna MJ, Robinson E, Taylor L, Tompkins C, Cornforth MN, Simon SL, Bailey SM: Chromosome translocations, inversions and telomere length for retrospective biodosimetry on exposed U.S. atomic veterans. Radiat Res, 191(4):311–322, 2019.
65. Nakano M, Nakashima E, Pawel DJ, Kodama Y, Awa A: Frequency of reciprocal translocations and dicentrics induced in human blood lymphocytes by X-irradiation as determined by fluorescence in situ hybridization. Int J Radiat Biol, 64(5):565–569, 1993.
66. Moquet JE, Edwards AA, Lloyd DC, Hone P: The use of FISH chromosome painting for assessment of old doses of ionising radiation. Radiat Prot Dosim, 88(1):27–33, 2000.
67. Tucker JD, Cofield J, Matsumoto K, Ramsey MJ, Freeman DC: Persistence of chromosome aberrations following acute radiation: I, PAINT translocations,

dicentrics, rings, fragments, and insertions. Environ Mol Mutagen, 45(2–3):229–248, 2005.

68. International Organization for Standardization: Radiological protection – Performance criteria for laboratories using the cytokinesis block micronucleus (CBMN) assay in peripheral blood lymphocytes for biological dosimetry. ISO 17099, 2014.
69. International Organization for Standardization: Radiological protection – Performance criteria for service laboratories performing biological dosimetry by cytogenetics. ISO 19238, 2014.
70. Thierens H, Vral A, De Ridder L: A cytogenetic study of radiological workers: effect of age, smoking and radiation burden on the micronucleus frequency. Mutat Res, 360(2):75–82, 1996.
71. Wojda A, Zietkiewicz E, Witt M: Effects of age and gender on micronucleus and chromosome nondisjunction frequencies in centenarians and younger subjects. Mutagenesis, 22(3):195–200, 2007.
72. Darroudi F, Natarajan AT: Application of FISH chromosome painting assay for dose reconstruction: state of art and current views. Radiat Prot Dosim, 88(1):51–58, 2000.
73. Tucker JD, Luckinbill LS: Estimating the lowest detectable dose of ionizing radiation by FISH whole-chromosome painting. Radiat Res, 175(5):631–637, 2011.
74. International Committee of Radiation Protection: Protecting people against radiation exposure in the event of a radiological attack. ICRP Publication 96, 2005.
75. Tucker JD: Low-dose ionizing radiation and chromosome translocations: a review of the major considerations for human biological dosimetry. Mutat Res, 659(3):211–220, 2008.

Chapter 2:

「Improved harvest methodology for cytokinesis-block micronucleus assay with isolated human peripheral blood mononuclear cell culture」

「細胞質分裂阻害微小核法における分離ヒト末梢血単核細胞培養における細胞固定法の改善」

弘前大学大学院保健学研究科保健学専攻

提出者氏名：Valerie Goh Swee Ting

所　　属：　生体検査科学領域

指導教員：　三浦富智

List of Abbreviations (Chapter 2)

BNC: binucleated cell(s)

CBMN: cytokinesis-block micronucleus

CBPI: cytokinesis-block proliferation index

CM: complete medium

CRG: Chromosome Research Group

Cyt-B: cytochalasin B

DAPI: 4′,6-diamidino-2-phenylindole

Dic: dicentric chromosome(s)

DRC: dose-response calibration curve

FA: formaldehyde

FMU: Fukushima Medical University

HU: Hirosaki University

HUMN: HUman Micronucleus Project

HUS: Hokkaido Pharmaceutical University

IAEA: International Atomic Energy Agency

ISO: International Organization for Standardization

LET: linear energy threshold

MN: micronucleus/micronuclei

NATO: North-Atlantic Treaty Organization

NDI: nuclear division index

PBMC(s): peripheral blood mononuclear cells

PHA: phytohemagglutinin

RENEB: Realizing the European Network in Biodosimetry

SNRSI: Singapore Nuclear Research and Safety Initiative

WB: whole blood

Introduction (Chapter 2)

The cytokinesis-block micronucleus (CBMN) assay uses cytochalasin B (Cyt-B) to arrest cells during cytokinesis, allowing micronuclei (MN) to be detected in binucleated cells (BNC). MN can indicate the presence of acentric fragments from chromosome breakage, chromosome aberrations (i.e. dicentric chromosomes [Dic]) or chromosome loss[1)]. In cytogenetic biodosimetry, CBMN assay is performed with human peripheral blood for dose estimation in individuals after suspected or accidental radiation exposures[2-4)]. Peripheral blood lymphocytes are either cultured from whole blood (WB) or peripheral blood mononuclear cells (PMBCs) isolated with density centrifugation[1-2, 5-6)]. MN frequency in 1000 BNC (MN/1000 BNC) and nuclear division index (NDI), an indicator of cell-cycle progression[7)], are commonly reported.

Traditionally, microscope slides of hypotonic- treated and fixed cells are prepared by dropping cells on slides. Cell spreading is facilitated by the low viscosity and fast evaporating mixture of methanol and acetic acid in the fixative. On the other hand, a cytocentrifuge can also be used to spread fresh cells on slides with *g* force, and these cells are then post-fixed in methanol or acetone[1)]. Cells are stained with Giemsa and manually scored with light microscopy. In recent years, improvements to conventional imaging and scoring were made to prepare for triage and mass-casualty radiological accidents. Slide-based semi-automated and automated scoring were developed for Giemsa-stained cells using the PathFinder™ platform by IMSTAR[8)], DAPI-stained cells using MNScore™ by Metasystems[9)] and DAPI/Fast Green-stained cells using laser scanning cytometry[10)]. Non-slide based imaging flow cytometry coupled with Rapid Automated Biodosimetry Technology was also developed to handle multiple low volume blood samples for high throughput CBMN imaging analysis[11)]. Even though CBMN scoring is advancing toward high throughput and automated scoring, routine biodosimetry methods are still important as they are commonly used as teaching materials and should be well established as a baseline in cytogenetic laboratories. Therefore, in our study, we focused on routine biodosimetry with Giemsa-stained cells and manual scoring with light microscopy.

Recommended culture, harvest, and fixation protocols for CBMN assay were published for WB cultures by the International Atomic Energy Agency (IAEA) in Annex IV of Technical Reports No. 405 in 2001[5)] and EPR-Biodosimetry in 2011[12)]. Surprisingly,

both harvest protocols differed greatly in centrifuge time, centrifuge speed, use of formaldehyde (FA) and fixative composition. As there was no explanation in the manuals behind the change in protocols, it could cause additional confusion to users when deciding on the protocol for cell harvest and fixation. In addition, in large-scale inter-comparison exercises conducted by the HUman MicroNucleus (HUMN) Project[13], the North Atlantic Treaty Organization (NATO)[14] and the European Network of biological and physical-retrospective dosimetry RENEB[15], there was no consensus in the protocols used in multiple laboratories. For WB cultures in general, hypotonic treatment with potassium or sodium chloride is used to remove erythrocytes, and a mixture of methanol and acetic acid is used for cell fixation. However, in isolated PBMC cultures, cytocentrifugation of fresh lymphocytes is recommended to overcome the high incidence of ruptured lymphocytes caused by harvest and fixation protocols commonly used in cytogenetic assays[1, 6, 12].

In the MN scoring criteria established by the HUMN project, a large proportion of unruptured scorable BNCwith clear and distinguishable cytoplasmic boundaries after fixation is essential[1), 12-13]. Conventional MN analysis requires a minimum of 1000 scorable BNC based on the estimated detection limit of 0.3 Gy for CBMN assay after low-LET radiation[16]. However, 200 BNC can be scored for triage when identifying individuals with more than 1 Gy exposure[17]. As most CBMN scoring is still performed manually with light microscopy, the decreased incidence of ruptured lymphocytes can considerably reduce scoring time. Furthermore, to the best of our knowledge, the influence of humidity during cell spreading on the quality of BNC used in MN scoring have not yet been analyzed in detail, though it was stated as a variable in ISO 17099[6]. It is widely accepted that humidity and temperature play huge roles during metaphase spreading[18-19] in slide-based routine biodosimetry for Dic and translocation analysis. Similar to chromosome spreads, we hypothesized that humidity could also affect BNC rupture and possibly NDI and MN frequency analyzed in CBMN assay. The increased rupture of BNC could cause MN to escape when cell suspensions are dropped on slides and affect MN frequency scored in nuclear-stained BNC.

In this study, we present a viable alternative to cytocentrifugation, by optimizing the CBMN harvest and fixation protocol of isolated PBMC cultures to greatly increase

the number of scorable BNC in multiple donors. Routine biodosimetry methods were used instead of specialized equipment and reagents used in cytocentrifugation, allowing cells to be fixed for long-term storage in a cell suspension. This protocol was developed by the Chromosome Research Group (CRG) in Hirosaki University. The effects of humidity during cell spreading were also explored. Endpoints of cytoplasm status, NDI and MN frequency were compared in both scorable cells and all cells with and without intact cytoplasm. In addition, PBMCs harvested with the CRG protocol were compared to WB cultures harvested with protocols in Technical Reports No. 405 and EPR-Biodosimetry by IAEA in 2001 and 2011, respectively. The CRG protocol was also validated for multiple stains and in multiple laboratories.

Materials & Methods (Chapter 2)

Blood collection and irradiation conditions

Peripheral blood from four healthy males (24, 34, 41, 51 y.o.) and four healthy females (26, 37, 44, 56 y.o.) was collected in lithium-heparin tubes (BD, Franklin Lakes, NJ) with their informed consent. The informed consent form was approved by the Committee of Medical Ethics in Hirosaki University Graduate School of Health Sciences (Approval number: 2012-278). Donors D and F were smokers.

Dose-rate was initially calibrated with reference lithium-heparin tubes containing water placed in an angled tube rack. Blood in lithium-heparin tubes was then directly irradiated with 2 Gy X-ray at 1 Gy/min (150 kVp, 20 mA, 0.5 mm Al + 0.3mm Cu filter; MBR-1520R-3, Hitachi Power Solutions, Tokyo, Japan). For 0 Gy blood, tubes were placed in the X-ray generator without irradiation. The cumulative radiation dose and dose-rate were monitored in real-time with a thimble ionization chamber (TN31013, PTW, Freiburg, Germany) connected to a dosimeter (MZ-BD-3 (Type 153), Hitachi Medical Corporation, Tokyo, Japan). The X-ray generator automatically stops once the radiation dose has reached its desired value. The detector and dosimeter are annually calibrated by the Japan Quality Assurance Organization, satisfying national standard traceability and ISO/IEC 17025 requirements. To simulate DNA repair, blood was incubated in a 37 °C water bath for 2 h.

WB culture for CBMN assay

0.6 ml of WB was added to 5.4 ml of complete medium (CM) (RPMI 1640 [Thermo

Fisher Scientific, Waltham, MA], 20 % heat-inactivated fetal bovine serum (FBS) [Sigma-Aldrich, St. Louis, MO] and 1 × kanamycin sulfate [Thermo Fisher Scientific]). A final concentration of 180 μg/ml phytohemagglutinin (PHA) HA-15 (Remel Europe, Dartford, UK) was added for mitogenic stimulation of T lymphocytes. 15 ml polypropylene conical centrifuge tubes (Falcon, Corning Inc., Corning, NY) containing cells were placed in a slanted tube rack and cultured in a humidified incubator at 37 °C, 5 % CO_2. Cyt-B (Sigma-Aldrich) was added to a final concentration of 6 μg/ml[12], 44 h after the start of culture for cytokinesis block.

Isolated PBMC culture for CBMN assay

PBMCs were isolated with Histopaque 1077 according to manufacturer's instructions (Sigma-Aldrich) by layering a 1:1 dilution of 3 ml blood and 3 ml washing medium (RPMI 1640, 2 % FBS, 1 × kanamycin sulfate) on 3 ml Histopaque. PBMCs were washed twice in washing medium, then suspended in 3 ml CM. 1.2 ml of suspended PBMCs (cell-equivalent to 0.6 ml whole blood) was then added to 4.8 ml of CM. Twice the volume of PBMCs than WB was used to account for incomplete retrieval of buffy coat. A final concentration of 180 μg/ml PHA HA-15 was added in 15 ml tubes and cultured in a humidified chamber. Cyt-B was added to a final concentration of 4.5 μg/ml[1], 44 h after the start of culture for cytokinesis block.

Cell harvest, fixation, spreading, staining, and image capturing

Cells were harvested after a total culture time of 72 h, using the protocols in IAEA 2001[5], IAEA 2011[12] with and without FA (Sigma-Aldrich), or with our new protocol (CRG) detailed in Supplemental Materials. FA was added with the fixative consisting of Ringer's solution, methanol and acetic acid in Step 8 of IAEA 2011 protocol. WB cultures were harvested with the IAEA protocols while PBMC cultures were harvested with the CRG protocol. Briefly for the CRG protocol, hypotonic treatment of cells was performed with 125 mM KCl on ice for 6 min. 1 % FA (i.e. 50 μl of 37 wt. % in H_2O FA in 5 ml cell suspension) was added and centrifuged immediately. Cells were fixed with cold fresh fixative I (13:12:6 0.9 % NaCl: methanol: acetic acid), then fixed with three rounds of cold fresh fixative II (4:1 methanol: acetic acid). Each round of centrifugation was modified to 800 *g*, 25 s (35 s in total with no brake), using Compact Tabletop Centrifuge Model 2420 (Kubota Co., Tokyo, Japan).

Fixed cells were spread on a clean glass slide in a humidified HANABI chamber (ADSTEC, Chiba, Japan) at a dry index of 7.9 (high humidity) or 8.2 (low humidity). Dry index can be controlled with HANABI by varying the degree of dryness in the chamber. After the slides were completely dry in a heated oven at 60 °C, cells were stained with 5 % Giemsa (Merck Millipore, Burlington, MA) in pH 6.8 Gurr buffer (Thermo Fisher Scientific) for 12 min and mounted with malinol (Muto Pure Chemicals, Tokyo, Japan). Duplicate slides with two spots were prepared from a single culture for each donor and condition. Cell spreading at other high humidity conditions was also done on a moist Kimwipe™ (Kimberly-Clark Worldwide, Inc., Irving, TX) and on a tube rack in a 63 °C water bath. Cells were left to spread on the slide for 2 min before removing to dry in the oven.

DAPI staining was also performed by directly mounting cells with VECTASHIELD HardSet™ Antifade Mounting Medium with 4',6-diamidino-2-phenylindole (DAPI) (Vector Laboratories, Burlingame, CA). Acridine orange (Life Technologies Co., Carlsbad, CA) staining was performed by initially mounting diluted stock solution (0.04 mg/ml in PBS) on slides and staining for 1 min. Coverslips were then carefully removed and slides were washed in distilled water (7 dips for WB cultures, 10 dips for PBMC cultures). Excess water was removed with a hand-held dryer. Slides were mounted in PBS and imaged immediately. Giemsa, DAPI, and acridine orange-stained BNC were captured with auto-exposure at a total magnification of 400 × using Zeiss Axio Imager M2 (Carl Zeiss AG, Oberkochen, Germany). Acridine orange images were captured with a single filter cube FITC-LP01-Clinical-ZHE (Semrock Inc., Rochester, NY).

Cell analysis (cytoplasm status, NDI, MN frequency) by light microscopy

Cells were counted by a single experienced scorer with a light microscope, Olympus CX31, (Olympus Co., Tokyo, Japan) at a total of 400 × magnification. 250 BNC of each spot on each slide (1000 BNC in total) were evaluated for cytoplasm status ("Loss", "Ruptured", "Scorable") and MN frequency (MN/1000 BNC). MN frequency was also evaluated in ≥ 1000 scorable BNC with intact cytoplasm only. Induced MN frequency was calculated using the difference between MN frequency at 2 Gy and background MN frequency at 0 Gy. BNC identification and MN scoring were performed according to the

standard criteria established by the HUMN project[1, 12-13]. A minimum of 125 cells with and without intact cytoplasm of each spot on each slide (≥ 500 cells in total) were evaluated for NDI using the formula below. Additional care was taken to count only stimulated cells with enlarged nuclei in WB cultures. M_1, M_2, M_3, and M_4 indicate the number of cells with one, two, three or four daughter nuclei respectively, and N is the total number of cells analyzed[7].

$$NDI = \frac{M_1 + 2M_2 + 3M_3 + 4M_4}{N}$$

Validation of CRG protocol in multiple laboratories

0 Gy peripheral blood from one donor (M, 51 y.o.) was sent to Fukushima Medical University (FMU) and Hokkaido Pharmaceutical University (HUS) via domestic mail. PBMCs were isolated and cultured within 24 h after delivery. 0 Gy peripheral blood from one donor (F, 32 y.o.) was used in Singapore Nuclear Research and Safety Initiative (SNRSI). PBMCs were cultured within 3 h after blood collection. The CRG protocol was provided to the participating laboratories as a reference. Each laboratory used their own equipment and reagents for PBMC isolation and culture, cell harvest, Giemsa staining, and slide preparation.

Prepared slides from FMU and HUS were mailed back to Hirosaki University (HU) for slide imaging at a total magnification of 200 × with Zeiss Axio Imager M2. Slides from SNRSI were imaged at a total magnification of 200 × with Leica DMi8 (Leica Camera AG, Wetzlar, Germany).

Statistical tests

Graphical representation and statistical analyses were carried out with R ver 4.0.2[20], RStudio ver 1.3.1056[21], "car"[22] and "tidyverse"[23] package. Data were represented as Mean ± SD where applicable. Normality assumption was verified with Q-Q plot and Shapiro-Wilk test. Equality of variances was verified with Levene's test. Welch's *t*-test was used to evaluate differences between means of two independent samples. Type III 2-way ANOVA was used for both balanced and unbalanced data sets. Linear regression analysis was performed using the linear model y = A + Bx. *p*-values < 0.05 were significant.

Results (Chapter 2)

Choice of harvest protocols for cell analysis

An initial evaluation was performed to determine which harvest protocols were suitable for cell analysis. For WB cultures, IAEA 2001, IAEA 2011, and IAEA 2011 + FA harvest protocols were used. For isolated PBMC cultures, CRG + FA after hypotonic treatment and CRG + FA during first fixation were used. FA was added in two different steps in the CRG protocol as FA was always added in the first fixation step in the IAEA protocols.

For WB cultures, cells harvested with IAEA 2001 protocol showed a much smaller cell pellet than IAEA 2011 ± FA protocols. Donor variance in cell pellet size was observed IAEA 2011 ± FA and CRG ± FA protocols, with the former showing a much obvious donor variance (Figure 1A). Most of the donors harvested with IAEA 2011 ± FA protocols also showed a yellowish substance above the actual cell pellet (Figure 1B), which was also present in the form of a larger pellet after hypotonic treatment (Figure 1C). Erythrocyte hemolysis was seen only with WB cultures after the first fixation step (Figure 1D). In addition, cell debris was only seen in cell suspensions of IAEA 2011 ± FA protocols (IAEA 2011 + FA not shown) but not in CRG protocols (CRG + FA during first fixation not shown) (Figure 1E).

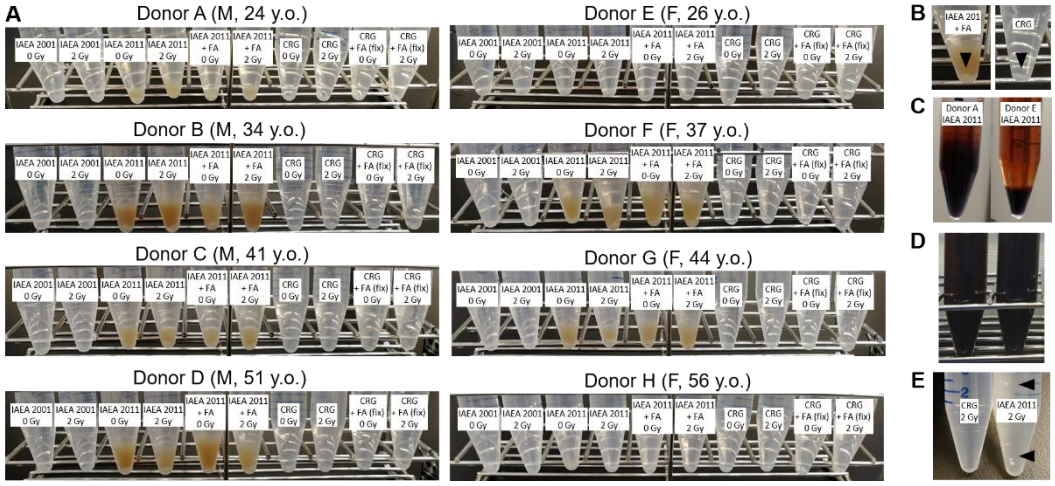

Figure 1: Effects of different donors and harvest protocols on cell pellets during harvest. WB cultures were harvested with IAEA protocols. Isolated PBMC cultures were harvested with CRG protocols. (A) Different sized cell pellets were observed in different donors after three rounds of fixation. IAEA 2011 ± FA cell pellets were smaller after 2 Gy irradiation. (B) The "true" cell pellet (black arrows) obtained after harvesting in IAEA 2011 ± FA and CRG protocols. (C) A larger cell pellet was seen in Donor A than Donor E after hypotonic treatment in IAEA 2011 protocol. (D) Erythrocyte hemolysis in WB cultures after fixative addition during first fixation. (E) Cell debris was observed (black arrows) after cell pellet suspension in IAEA 2011 protocol. No cell debris was seen in CRG protocol.

Both IAEA 2001 and CRG + FA during fixation showed low cell count, high background noise and many cells with ruptured or loss of cytoplasm in both low (dry index 8.2) and high (dry index 7.9) humidity spreading (Figure 2). They were hence excluded from further analysis. The key differences between the chosen protocols for cell analysis (IAEA 2011, IAEA 2011 + FA, CRG + FA during hypotonic treatment [referred to as CRG henceforth]) are listed in Table 1.

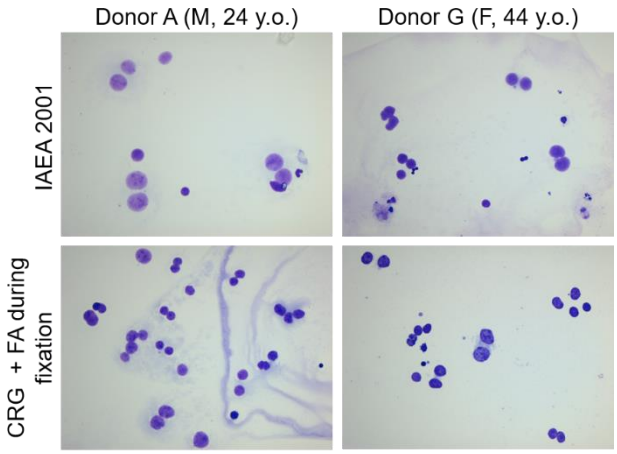

Figure 2: Representative images of Giemsa-stained cells at 400 × magnification harvested with IAEA 2001 and CRG + FA during fixation protocols. High background noise, low cell number and a high percentage of ruptured cells were observed.

Table 1: Key differences between types of cell cultured, Cyt-B concentration, harvest and fixation conditions of different protocols used.

	CRG	IAEA 2001[d]	IAEA 2011[e]	IAEA 2011[e] + FA
Type of cells cultured	Isolated PBMCs	Whole blood	Whole blood	Whole blood
Cyt-B concentration	4.5 µg/ml	6 µg/ml	6 µg/ml	6 µg/ml
Centrifuge conditions	800 *g*, 25 s (35 s w/o brake)[a]	800 rpm, 5 min 800 rpm, 8 min 600 rpm, 8 min	180 *g*, 10 min	180 *g*, 10 min
Hypotonic treatment	Cold 125 mM KCl[b]	Cold 75 mM KCl	Cold 75 mM KCl	Cold 75 mM KCl
Length of hypotonic treatment	6 min* on ice	8 min	10 min	10 min
When formaldehyde[c] (FA) is added	After hypotonic treatment	During first fixation	No FA treatment	During first fixation
Length of FA[c] treatment	< 1 min	8 min	No FA treatment	10 min
Cold fixative I	13:12:6 0.9 % NaCl: methanol: acetic acid[b]	3:1 methanol: acetic acid and FA	1:1 of Ringer's solution (NaCl, KCl, $CaCl_2$) and 10:1 methanol: acetic acid	1:1 of Ringer's solution (NaCl, KCl, $CaCl_2$) and 10:1 methanol: acetic acid, and FA
Cold fixative II	4:1 methanol: acetic acid*	3:1 methanol: acetic acid	10:1 methanol: acetic acid	10:1 methanol: acetic acid
Time taken to harvest one sample	< 25 min	< 50 min	< 1 h	< 1 h

[a] Period of centrifuge is dependent on the model of centrifuge. For reference, the centrifuge used in this paper is Kubota 2420.
[b] Concentrations of KCl and fixatives, and length of KCl treatment were referenced from Senthamizhchelvan *et al.*[24].
[c] 1 % FA concentration was used (i.e. 50 µl of 37 % w/w FA in 5 ml cell suspension).
[d] Protocol from Annex IV of Technical Reports No. 405[5].
[e] Protocol from Annex IV of EPR-Biodosimetry[12].

Effect of humidity during cell spreading on cells stained with Giemsa, DAPI, and acridine orange

For the remaining protocols (IAEA 2011, IAEA 2011 + FA, CRG), fixed cells were spread at different humidity conditions (low: HANABI dry index 8.2; high: HANABI dry index 7.9, moist Kimwipe™, 63 °C water bath) (Figure 3). Cell spreading with Kimwipe™ and 63 °C water bath were included as viable alternatives for high humidity spreading for laboratories without HANABI.

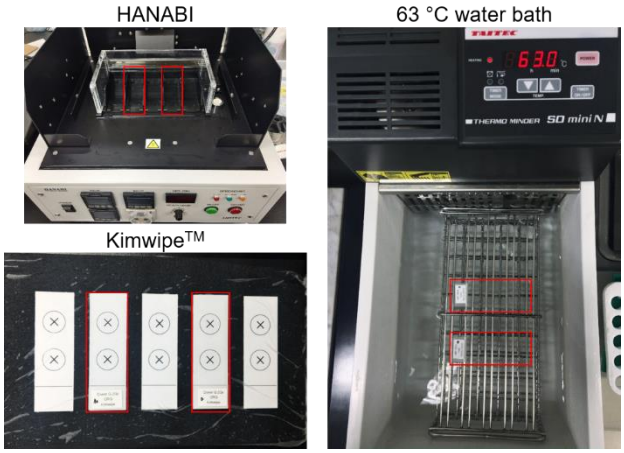

Figure 3: Different methods to modify humidity during cell spreading. Humidity can be modified by changing the dry index on HANABI, where lower values increase humidity. If high humidity for cell spreading is needed without the use of HANABI, a moistened Kimwipe™ with distilled water can be placed above a two-spot slide guide, or slides can be placed on a tube rack above a heated water bath. Red boxes show possible slide placements during spreading.

Donor A was chosen to represent cells that were easy to spread while Donor G was chosen to represent cells that were resistant to spreading. In addition to Giemsa, DAPI and acridine orange were included as they are commonly used fluorescent stains for automated CBMN scoring.

Cells harvested with the three protocols were able to be stained successfully in all three stains, showing clear contrast between daughter nuclei and cytoplasm, and clear distinction with neighboring cells. In particular, WB cultures showed high amount of background noise from dead and/or unstimulated cells and cell debris, while PBMC cultures had low or no background noise. Bright autofluorescence from background noise reduced the staining intensity of BNCwhen fluorescent images of DAPI and acridine orange were captured with auto-exposure. Cells harvested with IAEA 2011 protocol showed a higher frequency of cell rupture in high humidity in Giemsa and acridine

orange-stained cells. The addition of FA in IAEA 2011 + FA and CRG protocols helped the cells retain their cytoplasm in high humidity (Figure 4).

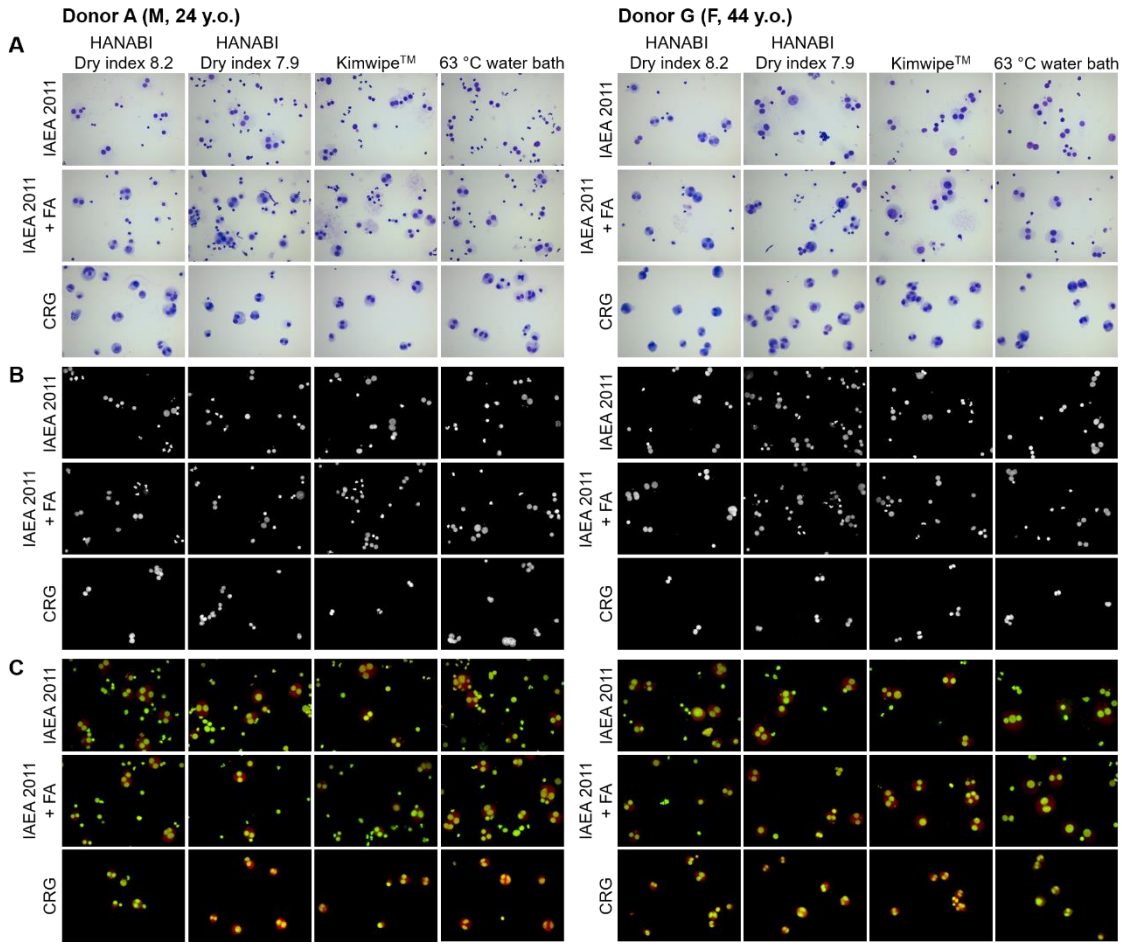

Figure 4: Representative images of 2 Gy cells at 400 × magnification with different harvest protocols, humidity during spreading and staining. Donor A was selected to represent cells which spread easily, while Donor G was selected to represent cells resistant to spreading. Cells were harvested with IAEA 2011, IAEA 2011 + FA and CRG protocols and spread on slides at low (HANABI dry index 8.2) and high humidity (HANABI dry index 7.9, moist KimwipeTM and 63 °C water bath). (A) Giemsa-stained cells. (B) DAPI-stained cells (converted to grayscale). (C) Acridine orange-stained cells. Whole blood cultures showed high background noise of dead/unstimulated cells and cell debris, while isolated PBMCs had low or no background noise in all three stains. Spreading at high humidity improved the Giemsa contrast between nuclei and cytoplasm. The addition of FA reduced cell rupture and loss of cytoplasm, even at high humidity. All harvest protocols showed good staining for Giemsa, DAPI and acridine orange, with clear distinction of daughter nuclei, cytoplasm and neighboring cells.

Validation of CRG protocol in multiple laboratories

The replicability of CRG protocol in multiple laboratories was also assessed in various methods of high humidity spreading. Participating laboratories (FMU, HUS, SNRSI) were only provided with the CRG protocol. Giemsa-stained slides were prepared with their own reagents and equipment. A high frequency of cells retained their cytoplasm in all three laboratories, although Giemsa staining was inconsistent between laboratories (Figure 5).

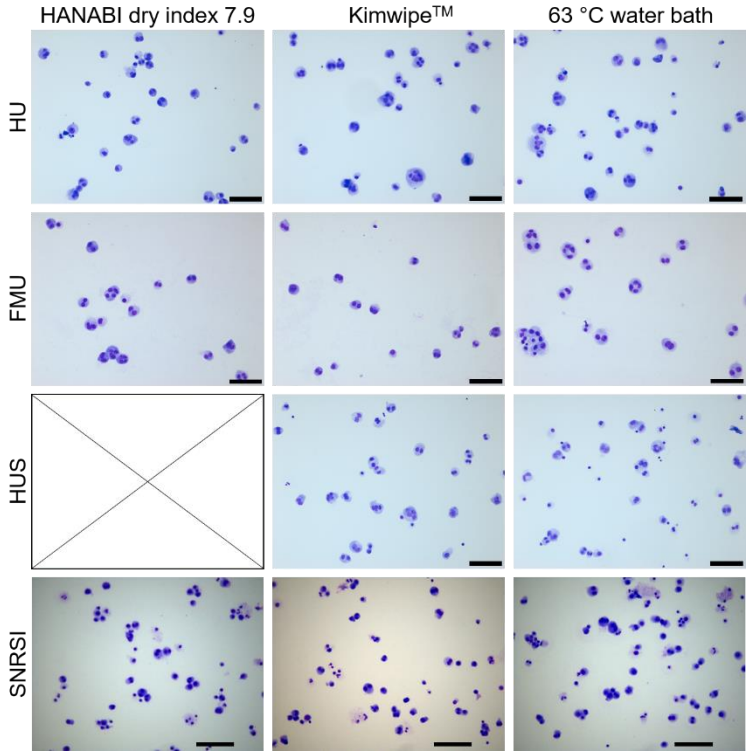

Figure 5: Representative images of 0 Gy Giemsa-stained cells at 200 × magnification harvested with CRG protocol in multiple laboratories. PBMC isolation, culture, harvest and Giemsa stain were performed in each laboratory (HU: Hirosaki University; FMU: Fukushima Medical University; HUS: Hokkaido Pharmaceutical University; SNRSI: Singapore Nuclear Science and Safety Initiative) with their own equipment and reagents. The CRG protocol was provided as a reference. HANABI was not available in HUS. As different microscopes were used for image capture, scale bars of 100 µm were provided. All laboratories showed a high frequency of cells with intact cytoplasm in all three cell spreading methods.

Cytoplasm status in 1000 BNC

To quantify the effect of harvest protocols and humidity on cytoplasm status of BNC, cytoplasm status of 1000 Giemsa-stained BNC were manually scored with light microscopy. Cytoplasm status was categorized into 3 groups: “loss”, “ruptured”, and “scorable”. BNC with two similarly sized and stained daughter nuclei with lack of cytoplasm staining were considered as “loss”. BNC with some cytoplasm staining were

considered as “ruptured”. BNC with daughter nuclei surrounded by a distinct cytoplasm membrane with mostly clear cytoplasm staining were considered as “scorable” (Figure 6A). To reduce variation in humidity during cell spreading, parameters were only evaluated on cells spread with HANABI (low humidity: dry index 8.2; high humidity: dry index 7.9).

In cells harvested with IAEA 2011 ± FA protocols, the percentage of scorable BNC varied between donors and humidity. FA addition and low humidity during cell spreading reduced cell rupture overall. Male and female donors in their 20s and 50s also showed higher susceptibility for cell rupture than those in their 30s and 40s. On the other hand, high scorable BNC percentage of $> 94\%$ was consistently seen in cells harvested with CRG protocol in all donors regardless of age and humidity. Irradiation dose of 2 Gy did not induce cell rupture overall (Figure 6B).

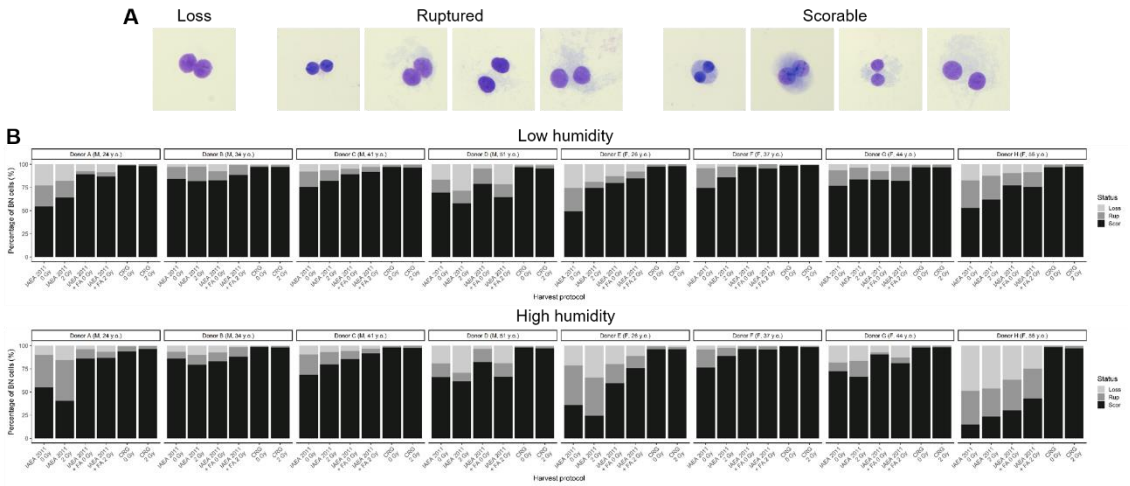

Figure 6: Cytoplasm status of 1000 BNC harvested with different protocols and humidity during cell spreading. (A) Representative images of Giemsa-stained cells with different cytoplasm status of “loss”, “ruptured”, and “scorable”. Cells were considered scorable if the cytoplasmic boundary was clear and surrounded the daughter nuclei. (B) Scorable BNC proportion was shown as black bars. Percentage of BNC with different cytoplasm status of donors A to H and at low (dry index 8.2) and high (dry index 7.9) humidity spreading conditions. Cells harvested with CRG protocol consistently showed high scorable percentage above 94 % across donors and humidity levels. Higher humidity induced higher cell rupture in IAEA 2011 and IAEA 2011 + FA protocols. Male and female donors in their 20s and 50s showed higher susceptibility to cell rupture. Scorable cells increased when harvested with IAEA 2011 + FA than IAEA 2011 protocol. 2 Gy irradiation did not induce cell rupture.

NDI in ≥ 500 cells irradiated with 0 and 2 Gy

Next, NDI was evaluated in ≥ 500 cells with intact cytoplasm only (scorable cells) and cells with and without intact cytoplasm (all cells). In Figure 7A, humidity during cell spreading did not affect NDI in scorable cells as there were no significant differences (*p*

= 0.264 – 0.531; Welch's *t*-test) when comparing each humidity condition per protocol and dose (e.g. low IAEA 2011 0 Gy versus high IAEA 2011 0 Gy). When NDI was compared between 0 and 2 Gy, NDI was lower after 2 Gy irradiation in each humidity condition per protocol (e.g. low IAEA 2011 0 Gy versus low IAEA 2011 2 Gy). However, a significantly lower NDI was only seen in WB cultures (p = 0.026 – 0.040). In NDI evaluated in all cells, humidity did not significantly affect NDI (p = 0.271 – 0.984). However, NDI in WB cultures was significantly lower when evaluated in cells regardless of cytoplasm status than in scorable cells (p = 1.22e-05 – 0.012). NDI was unaffected in PBMC cultures (p = 0.177 – 0.670) (Figure 7B).

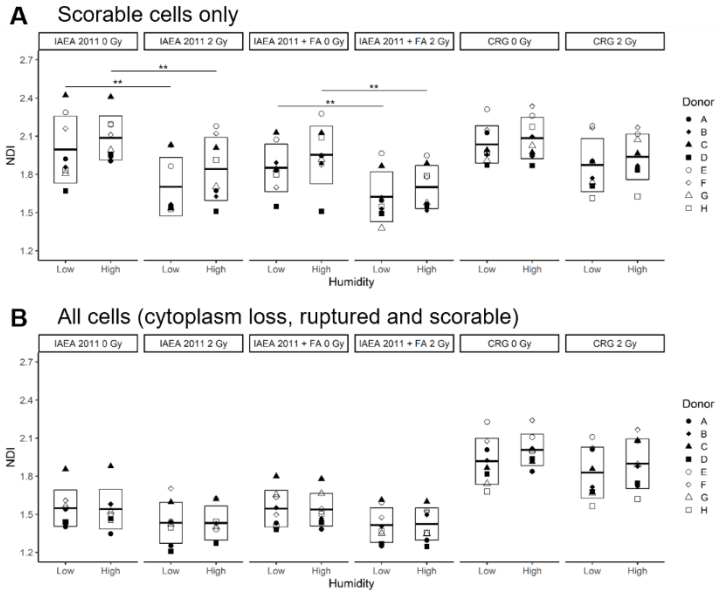

Figure 7: NDI in ≥ 500 cells analyzed in various harvest protocols and humidity conditions during cell spreading. Crossbars represent Mean ± SD. (A) Humidity did not significantly affect NDI in scorable cells as Welch's *t*-tests comparing each humidity condition per protocol and dose were not significant. Although NDI after 2 Gy irradiation was lower, significant differences were only seen in WB cultures (**: p = 0.026 – 0.040). (B) Humidity did not also affect NDI evaluation in all cells. NDI in WB cultures was significantly lower when evaluated in cells regardless of cytoplasm status than in scorable cells only (p = 1.22e-05 – 0.012). NDI was unaffected for isolated PBMC cultures.

Induced MN frequency (MN/1000 BNC) in 2 Gy irradiated cells

To further reduce donor variance for analysis, induced MN frequency (MN frequency at 2Gy – background MN frequency at 0 Gy) was compared. Type III 2-way ANOVA was performed in each harvest protocol to examine the effect of type of cells scored (scorable BNC with intact cytoplasm or all BNC regardless of cytoplasm status) and humidity during cell spreading. Significant differences were only observed between humidity conditions of WB cultures (IAEA 2011: p = 0.011, IAEA 2011 + FA: p = 0.027, CRG: p

= 0.227). Induced MN frequency was significantly higher (p = 0.016 – 0.033, Welch's t-test) only in WB cultures at high humidity for each condition (e.g. low versus high 2011 2 Gy scorable cells). Induced MN frequency in PBMC cultures were significantly lower (p = 9.57e-07 – 0.008, Welch's t-test) than WB cultures after 2 Gy irradiation (Figure 8).

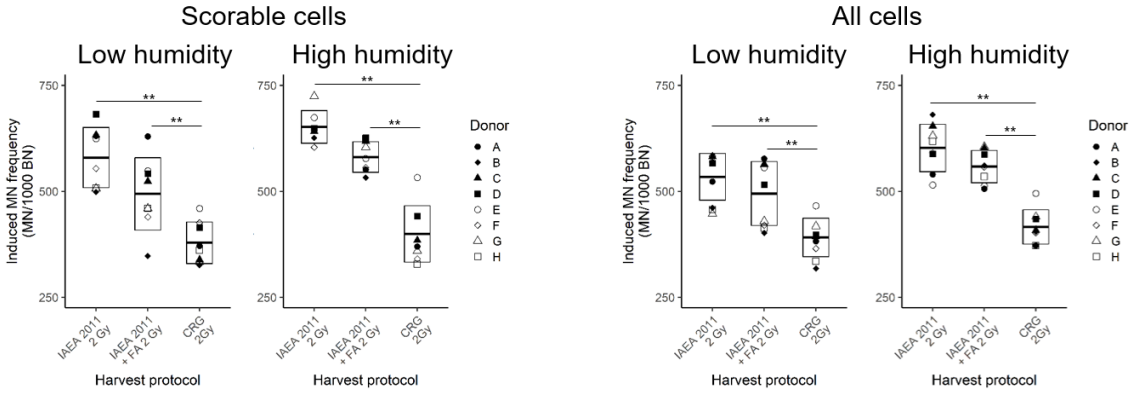

Figure 8: Induced MN frequency in 1000 BNC analyzed in various harvest protocols and humidity conditions during cell spreading. Induced MN frequency in scorable cells was omitted for Donor H IAEA 2011 at high humidity due to high incidence of cell rupture. Crossbars represent Mean ± SD. Higher humidity significantly increased induced MN frequency at each condition only for WB cultures (p = 0.016 – 0.033). Induced MN frequency in PBMC cultures were significantly lower than WB cultures after 2 Gy irradiation (**: p = 9.57e-07 – 0.007). MN frequency in each type of cell culture was similar in when evaluated in scorable and all cells.

Age-dependent increase in background MN frequency compared between WB and PBMC cultures

Age-dependent increase in background MN frequency in males and females was analyzed separately in WB and PBMC cultures with linear regression (Figure 9). Background MN frequency in all conditions (dry index 7.9 and 8.2, all and scorable cells, and all harvest protocols) was used to increase sample size while data from scorable cells (dry index 7.9, CRG and IAEA 2011 + FA) were included as reference only. Our results showed an increase of 0.603 MN/year (M) and 0.991 MN/year (F) for WB, and 0.472 MN/year (M) and 0.797 MN/year (F) for isolated PBMC cultures.

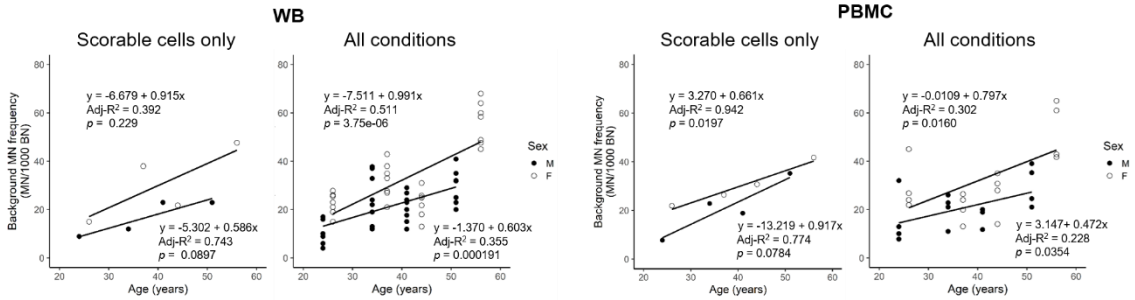

Figure 9: Age-dependent increase of background MN frequency in 1000 BNC separated in sex and type of cell culture. MN frequency in scorable cells were omitted for Donor H IAEA 2011 at high humidity due to high incidence of cell rupture. MN frequency scored in scorable cells from dry index 7.9 CRG and IAEA 2011 + FA protocols were only included in "Scorable cells only". Data from dry index 7.9 and 8.2, all and scorable cells, and all harvest protocols were included in "All conditions". Linear regression results of "Scorable cells only" were included as reference only. Background MN frequency increased 0.603 MN/year (M) and 0.991 MN/year (F) for whole blood, and 0.472 MN/year (M) and 0.797 MN/year (F) for isolated PBMC cultures. Age-dependent background MN frequency increase was higher in females than males, and higher in WB than PBMC cultures.

Discussion (Chapter 2)

CBMN assay is a commonly used cytogenetic biodosimetry tool for radiation dose estimation with MN frequency in BN human peripheral lymphocytes. Recommended harvest protocols with hypotonic treatment and fixation for WB cultures are provided in Technical Reports No. 405[5)] and EPR-Biodosimetry[12)] by IAEA, although many laboratories have their own optimized protocols[13-15)]. On the other hand, the current recommended cell harvest after isolated PBMC cultures is performed with cytocentrifugation of fresh cells to ensure a high number of scorable BNC with intact cytoplasm[1, 12-13)]. However, cytocentrifugation requires specialized equipment such as cytocentrifuges and cytology funnels, and these equipment are not commonly found in laboratories performing dose assessment by cytogenetic analysis. It also does not allow laboratories to store cells long-term in fixed cell suspensions for future MN scoring or perform downstream experiments such as fluorescence *in situ* hybridization with pan-centromeric probes[25-26)]. The remaining unfixed cell suspensions could be stored in -20 °C in freezing medium. However, the effect of freezing medium on hypotonic-treated peripheral blood lymphocyte cytoplasm status, NDI and MN frequency have not yet been evaluated. As a result, many still prefer to use WB cultures for CBMN assay to obtain fixed cells with routine harvest and fixation methods. However, in the process of removing erythrocytes, lymphocytes are exposed to longer periods of hypotonic treatment and cell fixation, which could compromise the number of scorable BNC.

In this paper, we developed an improved harvest and fixation protocol for isolated PBMC cultures for laboratories preferring to use reagents typically used in routine cytogenetic biodosimetry. This method of cell harvest provided an opportunity to compare CBMN results from WB and PBMC cultures of the same donor, and to compare the same harvest methodology in donors of varying age and sex. Different humidity conditions during cell spreading were also evaluated.

Some differences between WB and PBMC cultures were observed during harvest and cell imaging, and these could affect the choice of cell culture type to use for CBMN assay. For WB cultures, supernatant removal after the first fixation was inconvenient as the distinction between the supernatant and cell pellet was unclear due to erythrocyte hemolysis seen in Figure 1D. Cells harvested from PBMCs did not have this issue as erythrocytes were removed with density centrifugation before culture. The presence of cell debris, together with dead and/or unstimulated cells in WB cultures, also contributed to high background noise on stained slides with Giemsa, DAPI and acridine orange. The high-intensity autofluorescence of cell debris affected the staining intensity of viable cells when auto-exposure was used in fluorescence image capture, especially in the cytoplasm staining of acridine orange. For laboratories intending to use automated scoring with acridine orange, PBMCs could be a better option than WB cultures.

Furthermore, cells harvested with IAEA 2001 protocol was not ideal for our donors due to the surprisingly small cell pellets obtained, which were much smaller than those harvested with IAEA 2011 ± FA protocols even though they were cultured in the same conditions. The stronger fixative (3:1 methanol: acetic acid) used in the first fixation in IAEA 2001 protocol most likely caused many cells to rupture as 3:1 fixative is typically used in the Dic assay[12, 27)] to obtain clear metaphase spreads without any cytoplasm. Thus, fixative proportions should be optimized to ensure no loss of cytoplasm in BNC for CBMN assay, such as the 10:1 methanol: acetic acid used in the updated IAEA 2011 protocol.

Our CRG protocol also showed good staining for Giemsa, DAPI and acridine orange in high humidity conditions achieved with HANABI, moist Kimwipe™ and 63 °C water bath. It was also replicable in different laboratories with many cells showing intact cytoplasm. However, Giemsa staining was inconsistent between laboratories, which

could be due to the brand of Giemsa used. Laboratories are, hence, recommended to optimize the concentration and length of Giemsa stain.

In 1000 Giemsa-stained BNC analyzed with light microscopy, there was a high percentage of scorable BNC with intact cytoplasm in all donors harvested with CRG protocol, regardless of age, sex and humidity during cell spreading, even after 2 Gy irradiation. In contrast, scorable cell frequency varied among individuals and was affected by high humidity in cells harvested with IAEA 2011 ± FA protocols, though cells harvested with IAEA 2011 + FA fared better. The inclusion of FA in both the CRG and the modified IAEA 2011 + FA protocols helped to reduce cell rupture even at high humidity by increasing cytoplasmic protein crosslinks. Scorable cell frequency was also affected by age in IAEA 2011 ± FA protocols, as both males and females in their 20s and 50s showed a lower frequency of scorable cells than those in their 30s and 40s. Donor variability in scorable BNC frequency could be attributed to differences in cytoplasmic membrane fluidity. Membrane fluidity could be affected by age[28-29)], blood cholesterol level[30)] and inflammatory diseases such as rheumatoid arthritis[31)], which could affect cell rupture after hypotonic treatment and fixation. Moreover, it was not surprising that irradiation of 2 Gy did not increase the cells' susceptibility to rupture as increased radio-resistance and decreased cell death[32-33)] had been observed in PHA-stimulated lymphocytes after radiation. It is hence important to optimize the CBMN harvest protocol for multiple donors of varying ages as some donors were more susceptible to cell rupturing than others within the same age group. NDI and MN frequency scoring will also be more efficient if slides with many BNC showing intact cytoplasm can be prepared.

Another endpoint in the CBMN assay is NDI scored in viable cells with cytoplasm, which indicates lymphocyte cell-cycle progression after mitogen stimulation. It can also possibly identify irradiated samples based on their lower NDI values[12)]. Humidity during cell spreading did not affect NDI and a lower NDI was seen in 2 Gy samples. In particular, similar NDI was observed in both WB and PBMCs at 0 Gy (WB: 1.97 ± 0.22; PBMCs: 2.06 ± 0.15), while a significantly higher NDI was seen in 2 Gy PBMCs (WB: 1.72 ± 0.22; PBMCs: 1.91 ± 0.19) in our study. In Miszczyk and Rawojc's study, similar NDI in 0 Gy samples was also seen (1.90 ± 0.25) in both WB and PBMCs. A higher NDI was instead observed in 2 Gy X-ray irradiated WB (1.72 ± 0.25) than PBMCs (1.50 ±

0.25)[34].The difference in Cyt-B concentration (1.2 μg/ml versus 4.5–6 μg/ml in our study) most likely attributed to the different NDI obtained. The higher NDI values seen in our study was likely due to a higher Cyt-B concentration used, which was also seen in multiple studies[35-36]. In addition, even though the same Cyt-B concentration was used, cell-cycle progression was inconsistent as both higher[37] and lower[35] BNC percentage were seen in PBMC than WB cultures. As NDI is significantly affected by Cyt-B, its concentration should be standardized in each type of cell culture to allow a fair comparison across future studies. 4.5 and 6 μg/ml of Cyt-B for isolated PBMCs and WB cultures respectively were shown to obtain an optimal number of BNC[1].

NDI was also evaluated by comparing values obtained in scorable cells and in cells with and without intact cytoplasm. A significantly lower NDI was only seen in WB cultures when all cells were counted, as lymphocyte nuclei could not be easily differentiated from other cells with Giemsa staining. NDI should hence be scored only in viable cells with intact cytoplasm as recommended by Eastmond and Tucker[7], especially in WB cultures. For laboratories intending to only use Metafer for MN scoring in DAPI-stained cells for WB, it is very likely that NDI will be severely underestimated as only nuclei are counted. To overcome this problem, both cytoplasm and nuclear staining with DAPI and propidium iodide had been developed by Metasystems to automatically evaluate cytokinesis-block proliferation index (CBPI) with Metacyte function for toxicology assessment[38]. CBPI is similar to NDI, but multi-nucleated cells are evaluated together in CBPI while cells with 3 or 4 nuclei are separately evaluated in NDI. As Metafer only automatically counts mono- and multi-nucleated BNC for cell-cycle proliferation indication, NDI evaluation is still manually performed if Metafer is used. In addition, as cytoplasm status is also important for NDI evaluation, harvest protocols and humidity during cell spreading should be optimized to ensure many cells with intact cytoplasm for fast and accurate scoring.

As for MN frequency, a significantly higher induced MN frequency was scored in cells spread in high humidity condition regardless of the type of cells scored (intact cytoplasm or cells with and without cytoplasm) only in WB cultures. At this stage, it is unclear why a higher MN frequency was observed at high humidity with high cell rupture, even though the same cell suspension was used for cell spreading. Despite the observation, this still shows that even if a cell ruptures upon contact with the glass slide after cell

spreading, it is highly likely MN will remain close to the main daughter nuclei. Nonetheless, cytoplasm status for MN scoring was not a key factor in influencing MN frequency in our study. Instead, the method of MN scoring could play a greater role in influencing MN frequency.

In RENEB's inter-comparison study, considerable differences in MN frequency were observed among laboratories irrespective of the scoring method. The highest MN frequency for 0 and 0.85 Gy cells was seen with automated DAPI scoring, while in 2.7 Gy cells, manual scoring with Giemsa showed higher MN frequency than semi-automated and automated DAPI scoring[15]. This was also similarly seen in NATO's CBMN dose-response calibration curve (DRC) study, where manual and automated scoring had similar MN frequency at the lower doses, but MN frequency was significantly higher with manual scoring at higher doses of 1–4 Gy[14]. A higher percentage of MN was also falsely identified at higher doses DAPI-stained cells using MNScore[9, 39], although its accuracy could be improved by manually checking the images captured[40]. From these studies, even though MN frequency was comparable irrespective of cytoplasm status, the method of scoring should be kept consistent for samples used in dose estimation and DRCs, especially for reliable dose estimation. In the case of triage and identification of potential victims exposed to doses above 1 Gy, automated scoring may be more useful due to faster processing times. Similar to NDI, humidity during spreading should also be optimized depending on the harvest protocol. MN frequency in scorable BNC was unable to be evaluated in Donor H with two slides made due to a high percentage of cell rupture at high humidity. If high scorable BNC percentage can be obtained, manual MN scoring of 1000 BNC will be quickly completed.

It is well-known that MN frequency can be influenced by multiple factors, such as age, sex, obesity, smoking and cancer risk[41-42]. As a result, a high variance can be expected and was observed among multiple donors in both background and radiation-induced MN frequency, even with repeated measurements of the same donor in our study. Females also show higher background MN frequency due to X chromosomes lost as MN[43]. Our results also showed higher age-dependent increase of background MN frequency in females than males, and higher in WB than PBMC cultures (WB male: 0.603 MN/year; WB female: 0.991 MN/year; PBMC male: 0.472 MN/year, PBMC female: 0.797 MN/year). This was also seen in previous studies of WB (Male: 0.35 - 0.44

MN/year; female: 0.58 MN/year [44-46] and PMBC cultures (Female: 0.52 MN/year[47]). As such, it is recommended to estimate doses with MN frequency in DRCs in specific age groups and sex[6], and according to type of cell culture (WB or PBMCs) as seen in our study.

Our results also indicated a significantly higher MN frequency in 2 Gy WB (induced: 558.6 ± 77.7; actual: 585.3 ± 76.2) than PBMCs (induced: 392.5 ± 51.1, actual: 419.1 ± 52.8), in both cells with intact cytoplasm and cells with and without cytoplasm. This was also similarly seen in Sioen *et al.*'s study for 1 and 2 Gy samples[48]. Conversely, a significantly lower MN frequency was seen in 2 Gy X-ray WB (20) than PBMCs (45) in Miszczyk and Rawojc's study[34]. It is unclear why their MN frequency obtained was much lower as compared to other studies of the same irradiated dose[1, 14-15]. One reason could be Cyt-B concentration as it has been shown to affect radiation-induced MN frequency. Low Cyt-B concentration of 3 μg/ml overestimated MN frequency in WB after genotoxic exposure[36]. In another study, decreasing Cyt-B from 2 to 0.5 μg/ml increased, decreased or had no effect on radiation-induced MN frequency depending on the cell line used[49]. On the contrary, no substantial difference was seen in MN frequency when the effect of 3 or 6 μg/ml of Cyt-B was examined in the HUMN project. A higher MN frequency was instead seen in laboratories which used isolated PBMC instead of WB cultures. PBMCs were examined on slides prepared with cytocentrifugation while WB was prepared with hypotonic treatment and fixation. The paper attributed the observation to differences in lab protocol, blood storage before cell culture, genetic makeup, and lifestyle[13]. In our study, donors were kept constant and cells were harvested with routine biodosimetry methods, and yet a significantly lower MN frequency was seen in isolated PBMC cultures for all donors. Additional studies will be required to confirm if the presence of other cells and/or factors in WB could affect MN frequency, as cytokine presence could affect DNA repair and induce higher DNA damage[50-51].

In the guidelines published by IAEA[6, 12] and ISO[12, 27], results from WB and isolated PBMCs are commonly assumed to be similar as the target cells analyzed in cytogenetic biodosimetry assays are PHA-stimulated peripheral blood T lymphocytes. However, in limited studies comparing DNA damage in WB and PBMCs, some differences could arise and affect the accuracy of DNA damage evaluated. As seen in comet assays directly measuring DNA strand breaks in cells, control WB and PBMCs

showed statistically similar DNA damage[52], in contrast to the observations made by the ComNet project[53]. 2 Gy WB showed statistically higher DNA damage than PBMCs[52], but the opposite was seen in leukocytes irradiated in WB as compared to irradiated isolated lymphocytes for up to 0.5 Gy[54]. On the other hand, chromosome-type damage (Dic and deletions) was statistically similar between WB and PBMC-irradiated cultures up to 4 Gy[55]. As mentioned previously, MN frequency was lower in PBMC than WB cultures for 2 Gy-irradiated donors in our and Sioen *et al.*'s studies, while the opposite was seen in Miszczyk and Rawojc's study and the HUMN project. The difference between WB and PBMC cultures could be influenced by the presence of chemical factors and/or other cells in WB, difference in cell populations studied[56] and the type of DNA damage induced[52]. The process of PBMC isolation could also affect DNA damage. Increased oxidative damage was seen in isolated PBMCs possibly from direct exposure to oxygen[53] while decreased oxidative damage due to the hypoxic environment in pelleted PBMCs[55] was also seen. On the other hand, WB was found to protect cells from DNA damage caused by free radicals[54]. Interestingly, there was no difference in Dic frequency in irradiated WB and vigorously suspended PBMCs[55]. The differences in chromosome aberrations found after irradiation in WB and PBMC cultures could be enhanced in MN as MN are known to be affected by age, sex and lifestyle factors[42] but not in radiation-specific Dic[57].

In conclusion, the CRG protocol for isolated PBMC cultures is a viable alternative to cytocentrifugation for laboratories interested to store fixed cell suspensions with typically used equipment and reagents in cytogenetic biodosimetry. More than 94 % scorable BNC was obtained regardless of age, sex and humidity during cell spreading. The protocol was also shown to be replicable in multiple laboratories and multiple stains. For WB cultures, the IAEA 2011 protocol should be modified to include FA in first fixation step to increase scorable cell frequency. Our results also showed the importance of optimizing the CBMN harvest protocol for multiple donors as susceptibility to cell rupture is highly donor-dependent. Humidity during cell spreading should also be optimized depending on how strong the cells are fixed. Even though NDI and MN frequency were largely unaffected by different humidity conditions, NDI should be scored only in viable cells with cytoplasm, especially for WB cultures. MN frequency can be scored in cells with and without cytoplasm. Finally, NDI, MN frequency, DRC

construction and dose estimation should also be separately performed for WB and isolated PBMC cultures. Even though the target cells analyzed in both cultures are PHA-stimulated peripheral blood T lymphocytes, some factors present in WB could affect the frequency of DNA damage markers in the same donor after the same irradiation dose. Further study is thus required to confirm if the same phenomenon is seen in other cytogenetic biodosimetry markers.

References (Chapter 2)

1. Fenech M: Cytokinesis-block micronucleus cytome assay. Nat Protoc. 2(5):1084–1104, 2007.
2. International Atomic Energy Agency: The radiological accident in Istanbul. IAEA, Vienna, Austria, 2000.
3. Thierens H, De Ruyck K, Vral A, de Gelder V, Whitehouse CA, Tawn EJ, Boesman I: Cytogenetic biodosimetry of an accidental exposure of a radiological worker using multiple assays. Radiat Prot Dosimetry, 113(4):408–414, 2005.
4. Yao B, Li Y, Liu G, Guo M, Bai J, Man Q, Qiu L, Ai H: Estimation of the biological dose received by five victims of a radiation accident using three different cytogenetic tools. Mutat Res, 751(1):66–72, 2013.
5. International Atomic Energy Agency: Cytogenetic analysis for radiation dose assessment: a manual. Technical reports series no. 405. IAEA, Vienna, Austria, 2001.
6. International Organization for Standardization: Radiological protection–performance criteria for laboratories using the cytokinesis block micronucleus (CBMN) assay in peripheral blood lymphocytes for biological dosimetry. ISO 17099. Geneva: ISO, 2014.
7. Eastmond DA, Tucker JD: Identification of aneuploidy-inducing agents using cytokinesis-blocked human lymphocytes and an antikinetochore antibody. Environ Mol Mutagen, 13(1):34–43, 1989.
8. Decordier I, Papine A, Plas G, Roesems S, Vande Loock K, Moreno- Palomo J, Cemeli E, Anderson D, Fucic A, Marcos R, et al.: Automated image analysis of cytokinesis-blocked micronuclei: an adapted protocol and a validated scoring procedure for biomonitoring. Mutagenesis, 24(1):85–93, 2008.

9. Varga D, Johannes T, Jainta S, Schuster S, Schwarz-Boeger U, Kiechle M, Patino Garcia B, Vogel W: An automated scoring procedure for the micronucleus test by image analysis. Mutagenesis, 19(5):391–397, 2004.
10. François M, Hochstenbach K, Leifert W, Fenech MF: Automation of the cytokinesis-block micronucleus cytome assay by laser scanning cytometry and its potential application in radiation biodosimetry. Biotechniques, 57(6):309–312, 2014.
11. Wang Q, Rodrigues MA, Repin M, Pampou S, Beaton-Green LA, Perrier J, Garty G, Brenner DJ, Turner HC, Wilkins RC: Automated triage radiation biodosimetry: Integrating imaging flow cytometry with high-throughput robotics to perform the cytokinesis-block micronucleus assay. Radiat Res. 191(4):342–351, 2019.
12. International Atomic Energy Agency: Cytogenetic dosimetry: applications in preparedness for and response to radiation emergencies. EPR-Biodosimetry. IAEA, Vienna, Austria, 2011.
13. Bonassi S, Fenech M, Lando C, Lin YP, Ceppi M, Chang WP, Holland N, Kirsch-Volders M, Zeiger E, Ban S, et al.: HUman MicroNucleus project: international database comparison for results with the cytokinesis-block micronucleus assay in human lymphocytes: I. Effect of laboratory protocol, scoring criteria, and host factors on the frequency of micronuclei. Environ Mol Mutagen, 37(1):31–45, 2001.
14. Romm H, Barnard S, Boulay-Greene H, De Amicis A, Sanctis SD, Franco M, Herodin F, Jones A, Kulka U, Lista F, et al.: Laboratory intercomparison of the cytokinesis-block micronucleus assay. Radiat Res, 180(2):120–128, 2013.
15. Depuydt J, Baeyens A, Barnard S, Beinke C, Benedek A, Beukes P, Buraczewska I, Darroudi F, De Sanctis S, Dominguez I, et al.: RENEB intercomparison exercises analyzing micronuclei (Cytokinesis-block Micronucleus Assay). Int J Radiat Biol, 93(1):36–47, 2017.
16. Paillole N, Voisin P: Is micronuclei yield variability a problem for overexposure dose assessment to ionizing radiation? Mutat Res, 413(1):47–56, 1998.
17. McNamee JP, Flegal FN, Greene HB, Marro L, Wilkins RC: Validation of the cytokinesis-block micronucleus (CBMN) assay for use as a triage biological dosimetry tool. Radiat Prot Dosimetry, 135(4):232–242, 2009.
18. Spurbeck JL, Zinsmeister AR, Meyer KJ, Jalal SM: Dynamics of chromosome spreading. Am J Med Genet, 61(4):387–393, 1996.

19. Deng W, Tsao SW, Lucas JN, Leung CS, Cheung AL: A new method for improving metaphase chromosome spreading. Cytometry A, 51(1):46–51, 2003.
20. R Core Team: R: a language and environment for statistical computing. R Foundation for Statistical Computing, Vienna, Austria, 2020.
21. RStudio Team: RStudio: integrated development for R. RStudio Inc., Boston (MA), 2020.
22. Fox J, Weisberg S: An {R} companion to applied regression. 3rd ed. Sage, Thousand Oaks (CA), 2019.
23. Wickham H, Averick M, Bryan J, Chang W, McGowan L, François R, Grolemund G, Hayes A, Henry L, Hester J, et al.: Welcome to the Tidyverse. JOSS, 4(43):1686, 2019.
24. Senthamizhchelvan S, Pant GS, Rath GK, Julka PK, Nair O: Biodosimetry using micronucleus assay in acute partial body therapeutic irradiation. Phys Med, 25(2):82–87, 2009.
25. Vral A, Thierens H, De Ridder L: In vitro micronucleus-centromere assay to detect radiation-damage induced by low doses in human lymphocytes. Int J Radiat Biol, 71(1):61–68, 1997.
26. Wojcik A, Kowalska M, Bouzyk E, Buraczewska I, Kobialko G, Jarocewicz N, Szumiel I: Validation of the micronucleus centromere assay for biological dosimetry. Genet Mol Biol, 23(4):1083–1085, 2000.
27. International Organization for Standardization: Radiological protection — Performance criteria for service laboratories performing biological dosimetry by cytogenetics. ISO 19238. Geneva: ISO, 2014.
28. Huber LA, Xu QB, Jürgens G, Böck G, Bühler E, Gey KF, Schönitzer D, Traill KN, Wick G: Correlation of lymphocyte lipid composition membrane microviscosity and mitogen response in the aged. Eur J Immunol, 21(11):2761–2765, 1991.
29. Noble JM, Thomas TH, Ford GA: Effect of age on plasma membrane asymmetry and membrane fluidity in human leukocytes and platelets. J Gerontol A Biol Sci Med Sci, 54(12):M601–M606, 1999.
30. Rivnay B, Bergman S, Shinitzky M, Globerson A: Correlations between membrane viscosity, serum cholesterol, lymphocyte activation and aging in man. Mech Ageing Dev, 12(2):119–126, 1980.

31. Beccerica E, Piergiacomi G, Curatola G, Ferretti G: Changes of lymphocyte membrane fluidity in rheumatoid arthritis: a fluorescence polarisation study. Ann Rheum Dis, 47(6):472–477, 1988.
32. Stewart CC, Stevenson AP, Habbersett RC: The effect of low-dose irradiation on unstimulated and PHA-stimulated human lymphocyte subsets. Int J Radiat Biol Relat Stud Phys Chem Med, 53(1):77–87, 1988.
33. Meijer AE, Saeidi AB, Zelenskaya A, Czene S, Granath F, Harms-Ringdahl M: Influence of dose-rate, post-irradiation incubation time and growth factors on interphase cell death by apoptosis and clonogenic survival of human peripheral lymphocytes. Int J Radiat Biol, 75(10):1265–1273, 1999.
34. Miszczyk J, Rawojć K. Effects of culturing technique on human peripheral blood lymphocytes response to proton and X-ray radiation. Int J Radiat Biol, 96(4):424–433, 2020.
35. Ellard S, Parry EM. A modified protocol for the cytochalasin B in vitro micronucleus assay using whole human blood or separated lymphocyte cultures. Mutagenesis, 8(4):317–320, 1993.
36. Surrallés J, Antoccia A, Creus A, Degrassi F, Peris F, Tanzarella C, Xamena N, Marcos R. The effect of cytochalasin-B concentration on the frequency of micronuclei induced by four standard mutagens. Results from two laboratories. Mutagenesis, 9(4):347–353, 1994.
37. Elhajouji A, Santos AP, Van Hummelen P, Kirsch-Volders M. Metabolic differences between whole blood and isolated lymphocyte cultures for micronucleus (MN) induction by cyclophosphamide and benzo[a]pyrene. Mutagenesis, 9(4):307–313, 1994.
38. MetaSystems. MetaSystems White Paper: Obtaining CBPI in micronucleus tests, 2011. [accessed 2020 Nov 21]. https://metasystems-international.com/en/support/downloads/white-papers-and-applications/wpc-cbpi-2011-11-01-x.pdf.
39. Willems P, August L, Slabbert J, Romm H, Oestreicher U, Thierens H, Vral A. 2010. Automated micronucleus (MN) scoring for population triage in case of large scale radiation events. Int J Radiat Biol, 86(1):2–11, 2010.

40. Thierens H, De Ruyck K, Vral A, de Gelder V, Whitehouse CA, Tawn EJ, Boesman I. Cytogenetic biodosimetry of an accidental exposure of a radiological worker using multiple assays. Radiat Prot Dosimetry, 113(4):408–414, 2005.
41. Bonassi S, El-Zein R, Bolognesi C, Fenech M. Micronuclei frequency in peripheral blood lymphocytes and cancer risk: evidence from human studies. Mutagenesis, 26(1):93–100, 2011.
42. Fenech M, Bonassi S. The effect of age, gender, diet and lifestyle on DNA damage measured using micronucleus frequency in human peripheral blood lymphocytes. Mutagenesis, 26(1):43–49, 2011.
43. Tucker JD, Nath J, Hando JC. Activation status of the X chromosome in human micronucleated lymphocytes. Hum Genet, 97(4):471–475, 1996.
44. Thierens H, Vral A, De Ridder L. A cytogenetic study of radiological workers: effect of age, smoking and radiation burden on the micronucleus frequency. Mutat Res, 360(2):75–82, 1996.
45. Thierens H, Vral A, Barbé M, Aousalah B, De Ridder L. A cytogenetic study of nuclear power plant workers using the micronucleus-centromere assay. Mutat Res, 445(1):105–111, 1999.
46. Thierens H, Vral A, Morthier R, Aousalah B, De Ridder L. Cytogenetic monitoring of hospital workers occupationally exposed to ionizing radiation using the micronucleus centromere assay. Mutagenesis, 15(3):245–249, 2000.
47. Fenech M. The cytokinesis-block micronucleus technique: a detailed description of the method and its application to genotoxicity studies in human populations. Mutat Res, 285(1):35–44, 1993.
48. Sioen S, Cloet K, Vral A, Baeyens A. The cytokinesis-block micronucleus assay on human isolated fresh and cryopreserved peripheral blood mononuclear cells. JPM, 10(3):125, 2020.
49. Champion AR, Hanson JA, Court JB, Venables SE. The micronucleus assay: an evaluation of its use in determining radiosensitivity in vitro. Mutagenesis, 10(3):203–208, 1995.
50. Jaiswal M, LaRusso NF, Burgart LJ, Gores GJ. Inflammatory cytokines induce DNA damage and inhibit DNA repair in cholangiocarcinoma cells by a nitric oxide-dependent mechanism. Cancer Res, 60(1):184–190, 2000.

51. Centurione L, Aiello FB. DNA repair and cytokines: TGF-β, IL-6, and thrombopoietin as different biomarkers of radioresistance. Front Oncol, 6:175, 2016.
52. Bausinger J, Speit G. The impact of lymphocyte isolation on induced DNA damage in human blood samples measured by the comet assay. Mutagenesis,s 31(5):567–572, 2016.
53. Collins A, Koppen G, Valdiglesias V, Dusinska M, Kruszewski M, Møller P, Rojas E, Dhawan A, Benzie I, Coskun E, et al.; ComNet Project. The comet assay as a tool for human biomonitoring studies: the ComNet project. Mutat Res Rev Mutat Res, 759:27–39, 2014.
54. Vijayalaxmi Strauss GH, Tice RR. 1993. An analysis of gamma-ray induced DNA damage in human blood leukocytes, lymphocytes and granulocytes. Mutat Res. 292(2):123–128.
55. Kligerman AD, Halperin EC, Erexson GL, Honoré G, Westbrook-Collins B, Allen JW. 1988. A cytogenetic comparison of the responses of mouse and human peripheral blood lymphocytes to 60Co gamma radiation. Radiat Res, 115(2):334–346.
56. Morillas MJ, Guillamet E, Surrallés J, Creus A, Marcos R. Spontaneous and induced genetic damage in T lymphocyte subsets evaluated by the Comet assay. Mutat Res, 514(1–2):39–48, 2002.
57. Rozgaj R, Kasuba V, Simić D. The frequency of dicentrics and acentrics and the incidence of rogue cells in radiation workers. Mutagenesis, 17(2):135–139, 2002.

Chapter 3:

「Cytokinesis-block micronucleus assay performed in 0 and 2 Gy whole blood and isolated PBMCs in a 6-well transwell co-culture system」

「トランスウェル共培養システムを用いた細胞質分裂阻害微小核法における全血培養と分離単核球画分培養の比較」

弘前大学大学院保健学研究科保健学専攻

提出者氏名：Valerie Goh Swee Ting

所　　属：　生体検査科学領域

指導教員：　三浦富智

List of Abbreviations (Chapter 3)

BNC: binucleated cell(s)

CBMN: cytokinesis-block micronucleus

CM: complete medium

CRG: Chromosome Research Group

Cyt-B: cytochalasin B

DCA: dicentric chromosome assay

IAEA: International Atomic Energy Agency

ISO: International Organization for Standardization

MN: micronucleus/micronuclei

NDI: nuclear division index

PBMC(s): peripheral blood mononuclear cells

PHA: phytohemagglutinin

RIBE: radiation-induced bystander effect(s)

WB: whole blood

Introduction (Chapter 3)

The cytokinesis-block micronucleus (CBMN) assay can detect DNA damage in the form of micronuclei (MN) in binucleated cells (BNC) arrested at cytokinesis. MN has been found to contain chromosome aberrations, acentric fragments and whole chromosomes caused by mis-segregation[1]. In cytogenetic biodosimetry, MN frequency from CBMN assay is used to estimate whole-body ionizing radiation dose exposed in suspected individuals from 0.3 to 4 Gy[2-3], as seen from previously reported radiation incidents in Istanbul, Turkey[4] and Henan Province, China[5]. Nuclear division index (NDI), a cell proliferation indicator[6], is also often reported.

To assess DNA damage caused by radiation exposure in humans, peripheral blood is used due to their easy access, good approximation of dose to soft tissue using dose to lymphocytes for photons and neutrons, and estimation of whole-body dose[2]. According to the guidelines established by IAEA and International Organization for Standardization (ISO) 17099, both whole blood (WB) and peripheral mononuclear cells (PBMCs) isolated from WB with density centrifugation can be used for CBMN assay[2, 7]. Both NDI and MN frequency are assumed to be analyzed predominantly in dividing T lymphocytes in both types of cell cultures, due to the specific external mitogen stimulation with phytohemagglutinin (PHA)[8-9]. However, the presence of cytokines in blood plasma and other cells such as erythrocytes, platelets and granulocytes in WB cultures could influence cell-cycle progression[10], DNA damage induction and repair[11-13] and cell survival[14] in PBMCs. Furthermore, the action of PBMC isolation could also increase[15] or decrease[16] DNA damage.

In our previous CBMN study of 4 males and 4 females in their 20s to 50s in Chapter 2, single cultures of WB and PBMCs in 15 ml polypropylene conical centrifuge tubes were compared. A higher NDI and lower MN frequency were observed in 2 Gy PBMC than WB cultures in almost all donors[17]. We thus hypothesized that differences in NDI and MN frequency could be due to other soluble components present in WB but absent in PBMCs. Hence, in this study, 6-well transwell co-cultures with various combinations of unirradiated and 2 Gy irradiated WB and PBMCs were compared with mono-cultures of the same condition. Co-cultures were separated by a 0.4 μm transwell membrane insert to allow soluble factors to pass through, but not cells. To the best of our

knowledge, the use of a transwell co-culture system for WB and PBMC cultures in CBMN assay has not yet been performed. NDI and MN/1000 BNC from 2 male and 2 female donors were manually analyzed by 3 scorers in Giemsa-stained cells.

Materials & Methods (Chapter 3)

Peripheral blood collection, irradiation and PBMC isolation

Peripheral blood from two healthy males (25, 51 y.o.) and two healthy females (23, 26 y.o.) was collected in lithium-heparin tubes (BD, Franklin Lakes, NJ) with their informed consent. The informed consent form was approved by the Committee of Medical Ethics in Hirosaki University Graduate School of Health Sciences (Approval number: 2012-278). The 51 y.o. male donor is a smoker.

X-ray dose-rate was first calibrated with lithium-heparin tubes containing water in an angled tube rack. Blood in lithium-heparin tubes was then directly irradiated with 2 Gy X-ray at 1 Gy/min (150 kVp, 20 mA, 0.5 mm Al + 0.3 mm Cu filter; MBR-1520R-3, Hitachi Power Solutions, Tokyo, Japan). For 0 Gy blood, tubes were placed in the X-ray generator without irradiation. The cumulative radiation dose and dose-rate were monitored in real-time with a thimble ionization chamber (TN31013, PTW, Freiburg, Germany) connected to a dosimeter (MZ-BD-3 (Type 153), Hitachi Medical Corporation, Tokyo, Japan). The X-ray generator automatically stops once the radiation dose has reached its desired value. The detector and dosimeter are annually calibrated by the Japan Quality Assurance Organization, satisfying national standard traceability and ISO/IEC 17025 requirements.

To simulate DNA repair, blood was incubated in a 37 °C water bath for 2 h. PBMCs were isolated with Histopaque 1077 according to manufacturer's instructions (Sigma-Aldrich, St. Louis, MO), by layering a 1:1 dilution of 3 ml blood and 3 ml washing medium (RPMI 1640 [Thermo Fisher Scientific, Waltham, MA], 2 % heat-inactivated fetal bovine serum (FBS) [Sigma-Aldrich], 1 × kanamycin sulfate [Thermo Fisher Scientific]) on 3 ml Histopaque. After washing twice with washing medium, PBMCs were suspended in 3 ml complete medium (CM) (RPMI 1640, 20 % heat-inactivated FBS, 1 × kanamycin sulfate).

CBMN assay in WB and PBMC 6-well transwell co-culture

Co-cultures and mono-cultures for WB, WB-IR, PBMC and PBMC-IR were prepared according to the conditions shown in Figure 1. A total volume of 2.5 ml and 3.0 ml were used for upper and lower wells, respectively. Corning Costar polystyrene 6-well plates with transwell cell-inserts of 0.4 µm polycarbonate membrane (Sigma-Aldrich) were used. A ratio of 1:10 WB:CM was used, while a ratio of 1:5 PBMC:CM was used to account for incomplete retrieval of buffy coat during PBMC isolation. A final concentration of 180 µg/ml PHA HA-15 (Remel Europe, Dartford, UK) was added to stimulate T lymphocyte division. Cells in 6 well-plates were cultured in a humidified incubator 37 °C, 5 % CO_2. At 44 h, a final concentration of 4.5 or 6 µg/ml cytochalasin B (Cyt-B) (Sigma-Aldrich) was added to PBMC and WB cultures respectively, separately in each well. The different Cyt-B concentration used was shown to obtain an optimal frequency of BNC in each type of cell culture[1)]. Cyt-B was added to wells with and without cells.

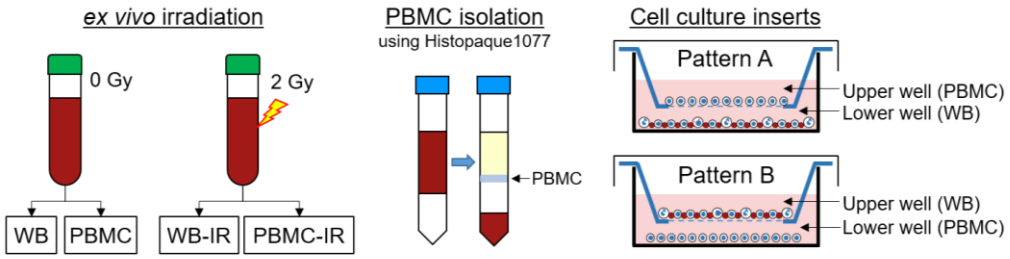

Co-culture pattern A

	1	2	3	4	5	6	7	8
Upper well	PBMC	PBMC-IR	PBMC	PBMC-IR	-	-	PBMC	PBMC-IR
Lower well	WB	WB	WB-IR	WB-IR	WB	WB-IR	-	-

Co-culture pattern B

	1	2	3	4	5	6	7	8
Upper well	WB	WB	WB-IR	WB-IR	WB	WB-IR	-	-
Lower well	PBMC	PBMC-IR	PBMC	PBMC-IR	-	-	PBMC	PBMC-IR

Figure 1: Experimental set-up for transwell co-culture system. Peripheral blood was first irradiated with 0 and 2 Gy X-rays before PBMC isolation. Different combinations of WB, PBMC, WB-IR and PBMC-IR were set up for mono- and co-cultures, as seen in co-culture patterns A and B.

WB and PBMC cell harvest, cell spreading and Giemsa stain

Cells were harvested after 72 h of cell culture. Cell suspensions in each well were transferred separately in individual 15 ml snap conical centrifuge tubes (SPL Life Sciences Co., Ltd., Pocheon-si, Korea) for ease of cell harvest. For lower wells, cells were pipetted thoroughly to dislodge cells at the bottom of each well before transferring to 15

ml tubes. For upper transwell cell inserts, cells were first carefully mixed well then transferred to 15 ml tubes. 2 ml washing medium was used to wash the remaining cells before transferring to 15 ml tubes. For the 26 y.o. female donor, the transwell insert membrane was unfortunately punctured during cell retrieval. Thus, well A-2 L was omitted from analysis.

Detailed protocols of cell harvest for WB and PBMC cultures were previously described in Chapter 2[17]. Annex IV in EPR-Biodosimetry (IAEA 2011) with 1 % formaldehyde (Sigma-Aldrich) added during the first fixation was used for WB harvest. The CRG protocol was used for PBMC harvest. Cell spreading was performed with HANABI (ADSTEC, Chiba, Japan) at a dry index 7.9 for PBMCs, while a dry index of 8.5 was used for WB. Slides were stained with 5 % Giemsa (Merck Millipore, Burlington, MA) in pH 6.8 Gurr Buffer (Thermo Fisher Scientific) for 12 min and mounted with malinol (Muto Pure Chemicals, Tokyo, Japan).

NDI and MN scoring on Giemsa-stained slides with light microscopy

Duplicate two-spot slides were prepared for each condition in each well, and the area of analysis was defined at each spot with a permanent marker. Three experienced scorers analyzed the slides for NDI and MN frequency at total of 400 × magnification with Olympus CX31 (Olympus Co., Tokyo, Japan). ≥ 125 viable cells with cytoplasm and ≥ 250 BNC were analyzed per spot for NDI and MN frequency, for total of 500 cells and 1000 BNC respectively. BNC identification and MN scoring were performed according to the guidelines established by the HUman MicroNucleus project[1-2, 18]. NDI was calculated with the formula established by Eastmond and Tucker[6].

Statistical tests

Graphical representation and statistical analyses were carried out with R ver 4.0.3[19], RStudio ver 1.3.1093[20], and "tidyverse" package[21]. As the coefficient of variation (CV) was within 20 % in the MN frequency for 2 Gy samples[7], MN frequency was averaged from 3 scorers. Likewise, NDI and MN frequency at 0 Gy were averaged from 3 scorers and used in the figures. Normality assumption was verified using Shapiro-Wilk test. Levene's test in "car"[22] package was used to check for equal variances. Welch's *t*-test and Kruskal-Wallis rank sum test (pairwise comparison with Dunn test in "FSA"[23] package if significant differences seen, with *p*-values adjusted with Benjamini-Hochberg

method) were used to evaluate differences between independent samples. p-values < 0.05 were significant.

Results (Chapter 3)

Differences in NDI and MN frequency seen between upper and lower wells of the same culture condition

Firstly, NDI and MN frequency were compared in bi-directional co-culture configurations, as seen in co-culture patterns A and B in Figure 1. In other words, parameters were assessed if differences between upper and lower wells were seen in cells cultured in the same conditions. For example, co-cultures of WB (w/ PBMC) in wells B-1 U and A-1 L were compared. NDI was compared between upper and lower wells of the same culture condition for mono-cultures (Figure 2A) and co-cultures (Figure 2B). Most of the conditions showed a higher, though not significant, NDI in the upper than the lower wells in both 0 and 2 Gy WB and PBMCs.

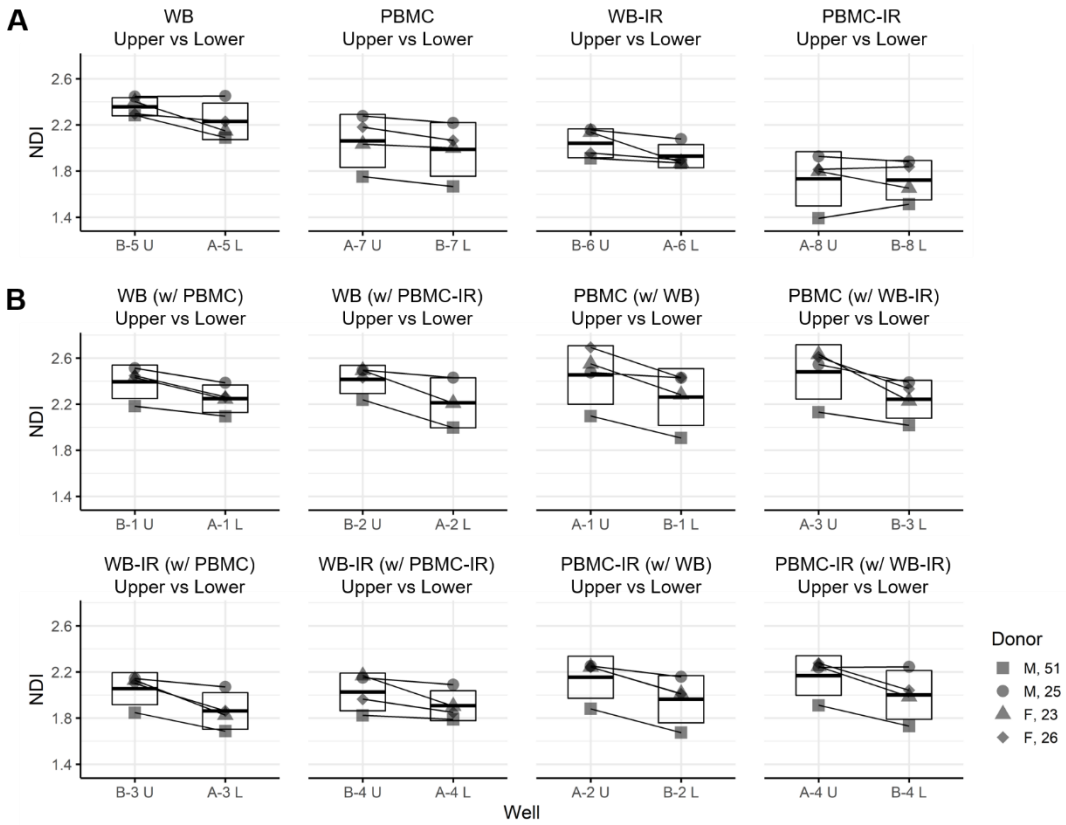

Figure 2: NDI compared in upper and lower wells of the same conditions in (A) mono- and (B) co-cultures. Crossbars represent Mean ± SD. Most of the conditions and donors showed higher NDI in the upper wells than the lower wells in WB, WB-IR, PBMC and PBMC-IR. No significant differences were seen with Welch's t-test ($p > 0.118$).

MN frequency was also compared between upper and lower wells of the same culture condition for mono-cultures (Figure 3A) and co-cultures (Figure 3B). Similar or lower MN frequency, though not significant, was largely seen between upper and lower wells of mono- and co-cultures in both 0 and 2 Gy WB and PBMCs.

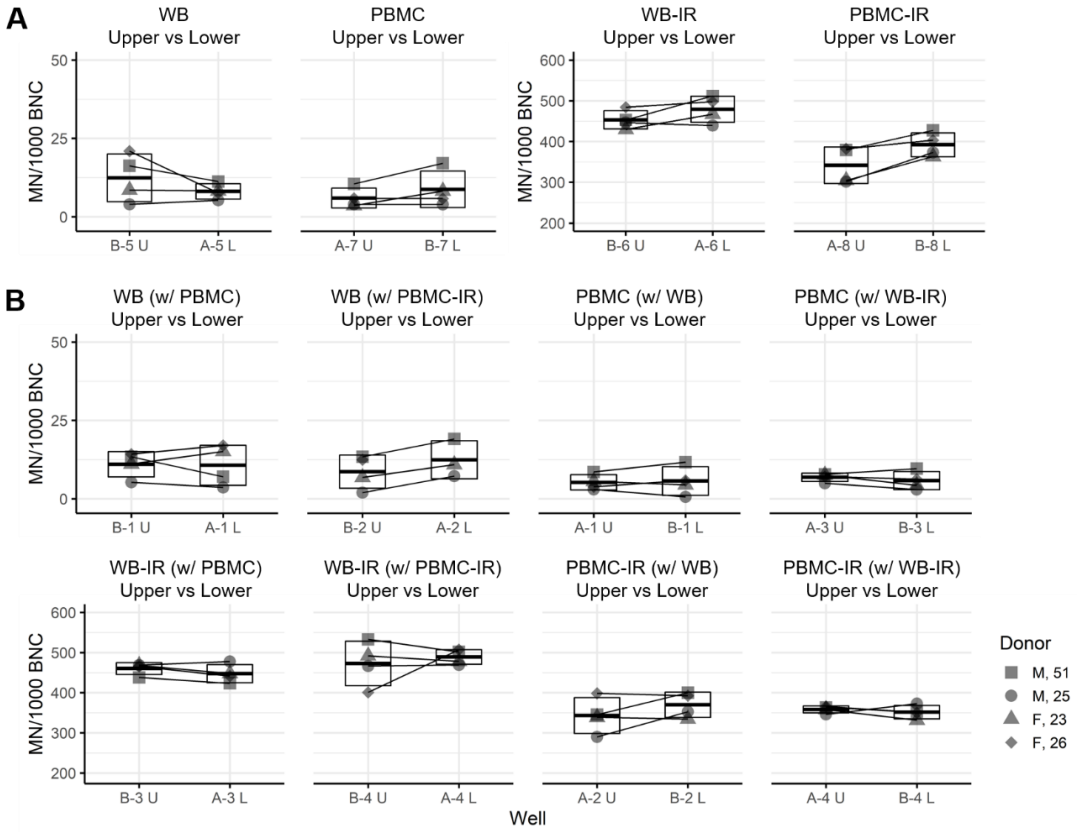

Figure 3: MN frequency compared in upper and lower wells of the same conditions in (A) mono- and (B) co-cultures. Crossbars represent Mean ± SD. MN frequency was largely either similar or lower in upper than lower wells in WB, WB-IR, PBMC and PBMC-IR. No significant differences were seen with Welch's *t*-test ($p > 0.119$).

Due to donor-specific differences seen between upper and lower wells of the same condition for WB, WB-IR, PBMC and PBMC-IR, wells of the same level were compared henceforth. For example, WB of lower wells A-1 L and A-5 L were compared.

Higher NDI seen only in PBMC and PBMC-IR co-cultured with WB or WB-IR as compared to mono-cultures

NDI was compared in wells of the same level in Figure 4. In both unirradiated and irradiated conditions of PBMCs, a higher, but not significant, NDI was seen in co-cultures with WB or WB-IR as compared to mono-cultures. No such trend was seen in WB and WB-IR cultures as NDI was similar in mono- and co-cultures with PBMC or PBMC-IR.

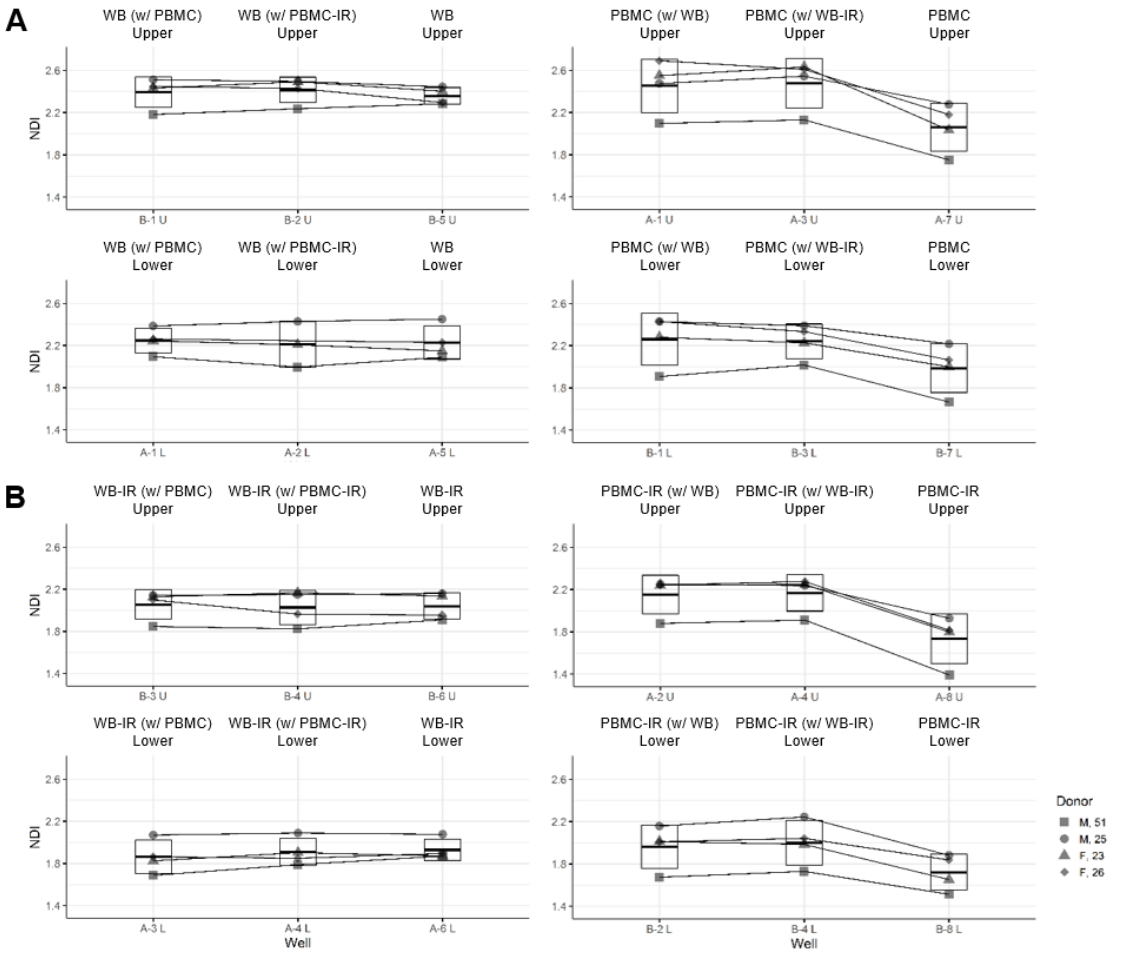

Figure 4: NDI compared in wells of the same level in (A) unirradiated (0 Gy) and (B) irradiated (2 Gy) cells. Crossbars represent Mean ± SD. A higher NDI in co-cultures with WB and WB-IR than mono-cultures was only seen in both PBMC and PBMC-IR. No significant differences were seen with Kruskal-Wallis rank sum test ($p > 0.058$)

No clear difference in MN frequency in co-cultures and mono-cultures of WB, WB-IR, PBMC and PBMC-IR

MN frequency was compared in wells of the same level in Figure 5. In both unirradiated and irradiated conditions, WB and PBMCs in both mono- and co-cultures showed similar MN frequency.

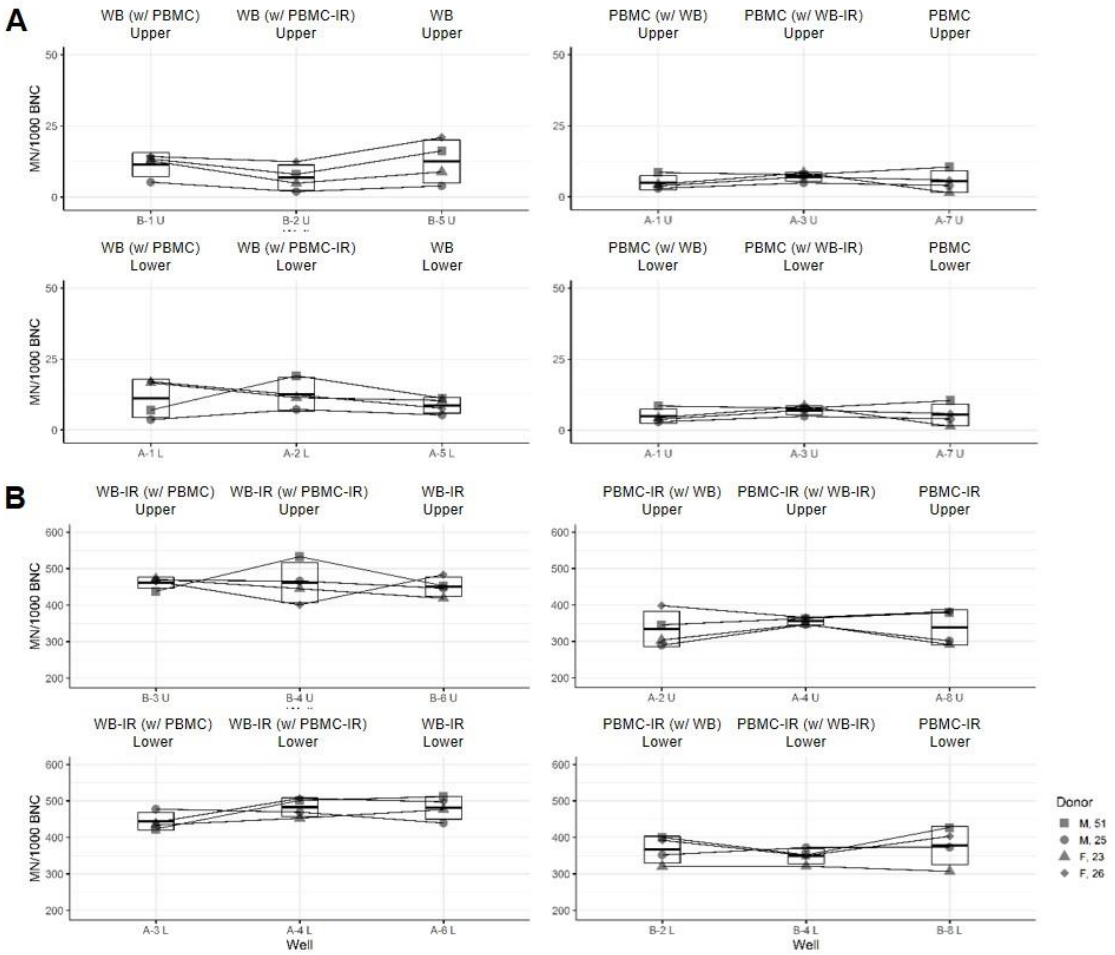

Figure 5: MN frequency compared in wells of the same level in (A) unirradiated and (B) irradiated cells. Crossbars represent Mean ± SD. A similar MN frequency was seen in both co- and mono-cultures of WB, WB-IR, PBMC and PBMC-IR. No significant differences were seen with Kruskal-Wallis rank sum test ($p > 0.098$)

Possible effect on NDI and MN frequency of WB, WB-IR, PBMC and PBMC-IR cultured in different vessels

To analyze if NDI and MN frequency in 0 and 2 Gy WB and PBMC cultures could be affected by different culture vessels, the parameters were compared in mono-cultures in 6-well polystyrene plates analyzed in this Chapter and single cultures of 15 ml polypropylene tubes previously analyzed in Chapter 2 (Figure 6). To ensure that a similar donor population was compared, males in their 20s and 50s and females in their 20s were included in the data set.

Some differences in NDI were seen between mono-cultures and single cultures of WB, WB-IR and PBMC-IR. MN frequency in both 2 Gy WB and PBMCs was higher in 15 ml cultures than mono-cultures. A significant difference was only seen in WB-IR MN frequency with Kruskal-Wallis rank sum test (p = 0.035). Pairwise comparison of only Upper versus 15 ml was significant (p = 0.031).

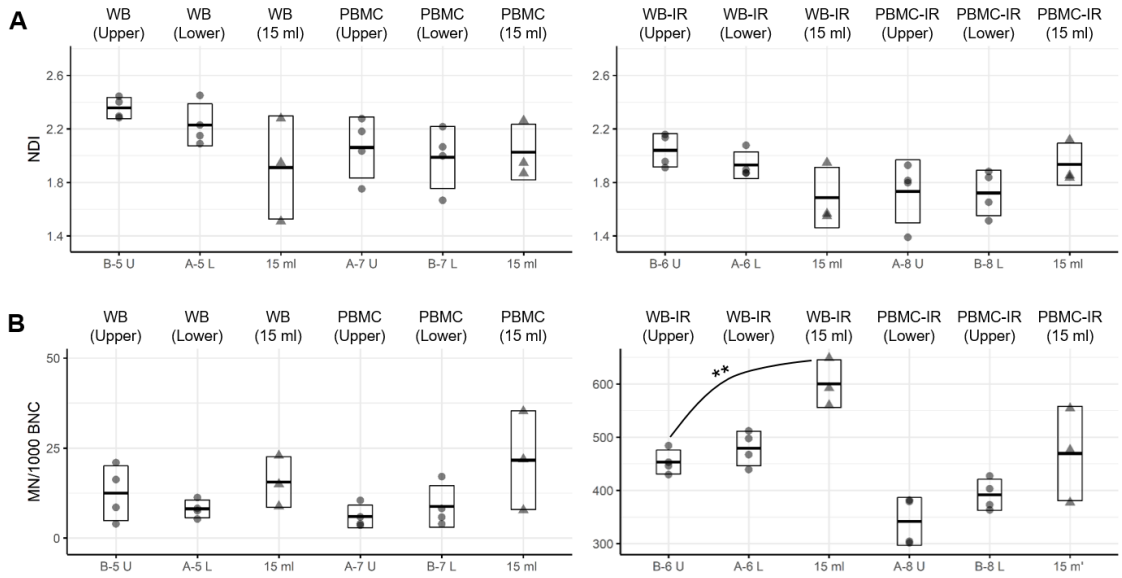

Figure 6: (A) NDI and (B) MN frequency of WB, WB-IR, PBMC and PBMC-IR compared in mono-cultures in 6-well plates (circle) and single cultures in 15 ml tubes (triangle). Crossbars represent Mean ± SD. Some differences in NDI were seen between mono-cultures and single cultures of WB, WB-IR and PBMC-IR. MN frequency in WB-IR and PBMC-IR was higher in single cultures than mono-cultures. A significant difference was only seen in WB-IR MN frequency between Upper and 15 ml cultures (**: p = 0.031).

Discussion (Chapter 3)

As previously shown in Chapter 2, CBMN assay performed in single cultures of 15 ml polypropylene tubes showed a similar NDI between 0 Gy WB and PBMCs. Furthermore, a higher NDI and a lower MN frequency was seen in 2 Gy PBMCs than WB. Assuming that the target cells analyzed in CBMN assays were PHA-stimulated T lymphocytes, we hypothesized that soluble components present in WB but absent in PBMCs could have influenced cell-cycle progression and DNA damage. In this chapter, CBMN assay was performed in a transwell co-culture system of 0 and 2 Gy WB and PBMCs of various combinations. The 0.4 μm transwell membrane insert allowed soluble factors to pass through, but not cells. According to our hypothesis and other previous experiments[10-17], NDI and MN frequency could be affected in PBMC and PBMC-IR co-cultured with WB or WB-IR, as compared to mono-cultures of PBMC and PBMC-IR. Likewise, trends in NDI and MN frequency observed in mono-cultures of WB, WB-IR, PBMC and PBMC-IR should be comparable to single 15 ml cultures performed in Chapter 2.

When PBMC or PBMC-IR was co-cultured with WB or WB-IR, a higher NDI was seen as compared to mono-cultures of the same conditions. No such trend was seen in mono- and co-cultures of WB and WB-IR. As for MN frequency, 2 Gy WB still consistently showed higher MN frequency than 2 Gy PBMCs in both mono- and co-cultures. Unexpectedly, PBMC-IR co-cultured with WB or WB-IR did not show an increase in MN frequency, in contrast to our hypothesis. In this experimental set-up, cell cycle progression could have been more influenced by soluble factors in WB as compared to DNA damage. Porto *et al.*[10] previously showed that the presence of erythrocytes increased mitotic index and ^{3}H-thymidine uptake of PHA-stimulated $CD8^{+}$ T cells, by possibly reducing reactive oxygen species production and upregulating cytoprotective proteins to inhibit T cell apoptosis[24-25]. Similarly, the addition of anti-human CD3 monoclonal antibody and recombinant human IL-2 increased PBMC proliferation in the absence of PHA stimulation, showing that cytokines could also influence PBMC cell cycle progression[26]. The different results seen in our two studies could also be attributed to the different experimental set-ups, as our previous study analyzed the effects with direct cell contact while this study analyzed the effects caused by soluble factors in the absence of cell contact. In a future study, the effects of individual blood components of plasma,

erythrocytes, platelets and neutrophils cultured together with PBMCs will be compared using CBMN assay endpoints. In addition, the same transwell co-culture set-up could also be extended to the highly radiation-sensitive dicentric chromosome assay (DCA)[27], where mitotic index (cell cycle progression indicator) and dicentric chromosome frequency (DNA damage marker) are evaluated. Cell cycle progression could also be further analyzed with premature chromosome condensation index (PCC index)[28] and cell-cycle progression index (CPI)[29] by prematurely condensing the chromosomes with calyculin A.

In mono-cultures of the same well level, NDI was lower in both 0 and 2 Gy PBMCs than WB in both upper and lower wells, which was contradictory to the results seen in Chapter 2. Moreover, differences in NDI and MN frequency were seen between mono-cultures and 15 ml single cultures. In particular, 2 Gy WB and PBMCs cultured in 15 ml tubes showed a higher MN frequency than mono-cultures of upper and lower wells. It was possible that the type and material of culture vessels could have affected NDI and MN frequency in both WB and PBMCs. In ISO 17099[7], the choice of culture vessels (cell culture microplates, tissue culture flasks, centrifuge tubes) was not standardized. The type of culture vessel was also not included as an important factor affecting MN frequency in multiple inter-comparison exercises of the CBMN assay[18, 30-31], in comparison to other factors such as scoring methodology, culture time, Cyt-B concentration and the length of Cyt-B treatment. However, in another study comparing 2 ml WB (20 ml culture in 25 cm^3 culture flask) and 200 µl WB (2 ml culture in 24-well plate), a similar MN frequency was seen in cells automatically scored with imaging flow cytometry[32]. Nevertheless, to ensure consistency in CBMN analysis and reliability in cytogenetic biodosimetry, culture protocols should be identical for dose-response calibration curve construction and dose estimation. It would also be interesting to compare the influence of different culture vessels on radiation-specific DCA.

A transwell co-culture system is also often used to analyze radiation-induced bystander effects (RIBE), where DNA damage could be indirectly induced in unirradiated cells due to cellular communication between irradiated and unirradiated cells. In our study, RIBE was not observed in X-ray irradiated cells as no clear differences in NDI and MN frequency were seen when unirradiated WB or PBMCs were co-cultured with PBMC-IR

or WB-IR respectively in both upper and lower wells. Interestingly, RIBE could be influenced by radiation quality and linear energy transfer (LET), as shown in other co-culture assays using cell lines. In Yin *et al.*'s study, MN was induced in unirradiated WS1 fibroblasts when co-cultured with HaCaT keratinocytes irradiated with α-particles but not X-rays[33]. Likewise, Shao *et al.* showed an enhanced nitric oxide-mediated MN increase in unirradiated human salivary gland HSG neoplastic cells co-cultured with HSG cells irradiated with higher LET carbon ion beams[34]. Anzenberg *et al.* also showed MN increase in both prostate carcinoma DU-145 cells and AG01522 fibroblasts co-cultured with DU-145 irradiated with X-rays or α-particles[35]. In contrast, Kaźmierczak *et al.*'s study showed no RIBE as similar cell survival was observed in unirradiated CHO-K1 cells co-cultured with irradiated CHO-K1 of ^{12}C or X-ray, and unirradiated cells[36]. As a follow-up, CBMN assay endpoints in WB and PBMCs in the same transwell co-culture set-up could be compared after different LET irradiation for RIBE investigation in the future.

In our set-up using co-culture patterns A and B, NDI was higher in upper than lower wells, while MN frequency remained largely similar. Cell cycle progression could have been affected by the surface area of the culture media exposed to carbon dioxide in the cell culture incubator, which was higher in upper wells than lower wells. Furthermore, in most transwell co-culture experiments, cells in the transwell insert (upper well) and the cells in the lower well tend to be in a unidirectional fixed configuration[33-39]. However, our results showed that the choice of cells in the upper and lower wells could affect the biological endpoint analyzed. Future experiments involving transwell co-culture systems should aim to evaluate sensitive biological endpoints in bidirectional configurations whenever possible.

In conclusion, co-cultures of 0 and 2 Gy WB and PBMCs showed that that some soluble factor(s) in WB in the absence of direct cell contact greatly increased NDI but not MN frequency in PBMCs, which was different from our initial hypothesis where we expected an increase in MN frequency. The type and material of culture vessel showed a possible influence in CBMN assay as higher MN frequency was seen in 15 ml polypropylene tubes than mono-cultures of 6-well polystyrene plates in both WB-IR and PBMC-IR. RIBE of cell-cycle progression and DNA damage were also not observed in

unirradiated WB and PBMCs co-cultured with PBMC-IR and WB-IR respectively. In all configurations, MN frequency in 2 Gy WB was still higher than 2 Gy PBMCs, which further supports the need to analyze MN frequency separately in each type of cell culture even though the target cells analyzed are assumed to be PHA-stimulated T lymphocytes.

References (Chapter 3)

1. Fenech M: Cytokinesis-block micronucleus cytome assay. Nat Protoc, 2(5):1084–1104, 2007.
2. International Atomic Energy Agency: Cytogenetic dosimetry: applications in preparedness for and response to radiation emergencies. EPR-Biodosimetry. IAEA, Vienna, Austria, 2011.
3. Rojas-Palma C, Liland A, Jerstad AN, Etherington G, del Rosarlo Pérez M, Rahola T, Smith K: TMT handbook, triage, monitoring and treatment of people exposed to ionizing radiation following a malevolent act. Norwegian Radiation Protection Authority, Norway, 2009.
4. International Atomic Energy Agency: The radiological accident in Istanbul. IAEA, Vienna, Austria, 2000.
5. Cao J, Zhang J, Wang Y, Du LQ, Xu C, Wang Q, Liu JX, Su X, Fan FY, Liu Q, Fan SJ: Cytogenetic abnormalities in lymphocytes from victims exposed to cobalt-60 radiation. Int J Mol Sci, 14(9):17525–17535, 2013.
6. Eastmond DA, Tucker JD: Identification of aneuploidy-inducing agents using cytokinesis-blocked human lymphocytes and an antikinetochore antibody. Environ Mol Mutagen, 13(1):34–43, 1989.
7. International Organization for Standardization: Radiological protection – Performance criteria for laboratories using the cytokinesis block micronucleus (CBMN) assay in peripheral blood lymphocytes for biological dosimetry. ISO 17099, 2014.
8. Knuutila S, Kovanen PE: Relative proportions of mitotic T and B cells in PHA-stimulated lymphocyte cultures. Cancer Genet Cytogenet, 29(1):151–154, 1987.
9. O'Donovan MR, Johns S, Wilcox P: The effect of PHA stimulation on lymphocyte sub-populations in whole-blood cultures. Mutagenesis, 10(4):371–374, 1995.
10. Porto B, Fonseca AM, Godinho I, Arosa FA, Porto G: Human red blood cells have

an enhancing effect on the relative expansion of CD8+ T lymphocytes in vitro. Cell Prolif, 34(6):359–367, 2001.

11. Vijayalaxmi, Strauss GHS, Tice RR: An analysis of gamma-ray induced DNA damage in human blood leukocytes, lymphocytes and granulocytes. Mutat Res, 292(2):123–128, 1993.
12. Bausinger J, Speit G: The impact of lymphocyte isolation on induced DNA damage in human blood samples measured by the comet assay. Mutagenesis, 31(5):567–572, 2016.
13. Centurione L, Aiello FB: DNA repair and cytokines: TGF-β, IL-6, and thrombopoietin as different biomarkers of radioresistance. Front Oncol, 6:175, 2016.
14. Sahu RK, Salman A, Mordechai S, Manor E: Study of plasma-induced peripheral blood mononuclear cells survival using Fourier transform infrared microspectroscopy. J Biomed Opt, 18(11):115004, 2013.
15. Collins A, Koppen G, Valdiglesias V, Dusinska M, Kruszewski M, Møller P, Rojas E, Dhawan A, Benzie I, Coskun E, et al.:ComNet Project. The comet assay as a tool for human biomonitoring studies: the ComNet project. Mutat Res Rev Mutat Res, 759:27–39, 2014.
16. Kligerman AD, Halperin EC, Erexson GL, Honoré G, Westbrook-Collins B, Allen JW: A cytogenetic comparison of the responses of mouse and human peripheral blood lymphocytes to 60Co gamma radiation. Radiat Res, 115(2):334–346, 1988.
17. Goh VST, Nakayama R, Blakely WF, Abe Y, Chua CEL, Chew ZH, Nakata A, Fujishima Y, Yoshida MA, Kasai K, Ariyoshi K, Miura T. Improved harvest and fixation methodology for isolated human peripheral blood mononuclear cells in cytokinesis-block micronucleus assay. Int J Radiat Biol, 97(2):194–207, 2021.
18. Bonassi S, Fenech M, Lando C, Lin YP, Ceppi M, Chang WP, Holland N, Kirsch-Volders M, Zeiger E, Ban S, et al.: HUman MicroNucleus project: international database comparison for results with the cytokinesis-block micronucleus assay in human lymphocytes: I. Effect of laboratory protocol, scoring criteria, and host factors on the frequency of micronuclei. Environ Mol Mutagen, 37(1):31–45, 2001.
19. R Core Team: R: a language and environment for statistical computing. R Foundation for Statistical Computing, Vienna, Austria, 2020.
20. RStudio Team: RStudio: integrated development for R. RStudio, Inc., Boston, MA,

USA, 2020.

21. Wickham H, Averick M, Bryan J, Chang W, McGowan L, François R, Grolemund G, Hayes A, Henry L, Hester J, et al. Welcome to the Tidyverse. JOSS, 4(43):1686, 2019.
22. Fox J, Weisberg S: An {R} companion to applied regression, 3rd ed. Sage Publications, Thousand Oaks, CA, 2019.
23. Ogle DH, Wheeler P, Dinno A. FSA: Fisheries Stock Analysis. R package version 0.8.32, 2021. https://github.com/droglenc/FSA.
24. Fonseca AM, Porto G, Uchida K, Arosa FA: Red blood cells inhibit activation-induced cell death and oxidative stress in human peripheral blood T lymphocytes. Blood, 97(10):3152–3160, 2001.
25. Fonseca AM, Pereira CF, Porto G, Arosa FA: Red blood cells upregulate cytoprotective proteins and the labile iron pool in dividing human T cells despite a reduction in oxidative stress. Free Radic Biol Med, 35(11):1404–1416, 2003.
26. Platts KE, Lawry J, Hancock BW, Rees RC: Phenotypic and cell cycle analysis of human peripheral blood mononuclear cells activated with interleukin-2 and/or OKT3. Exp Cell Res, 208(1):154–160, 1993.
27. Hoffmann W, Schmitz-Feuerhake I: How radiation-specific is the dicentric assay? J Expo Anal Environ Epidemiol, 9(2):113–133, 1999.
28. Gotoh E: Drug-induced premature chromosome condensation (PCC) protocols: cytogenetic approaches in mitotic chromosome and interphase chromatin. Methods Mol Biol, 1288:53–66, 2015.
29. Miura T, Nakata A, Kasai K, Nakano M, Abe Y, Tsushima E, Ossetrova NI, Yoshida MA, Blakely WF: A novel parameter, cell-cycle progression index, for radiation dose absorbed estimation in the premature chromosome condensation assay. Radiat Prot Dosimetry, 159(1-4):52–60, 2014.
30. Romm H, Barnard S, Boulay-Greene H, De Amicis A, De Sanctis S, Franco M, Herodin F, Jones A, Kulka U, Lista F, et al.: Laboratory intercomparison of the cytokinesis-block micronucleus assay. Radiat Res, 180(2):120–128, 2013.
31. Depuydt J, Baeyens A, Barnard S, Beinke C, Benedek A, Beukes P, Buraczewska I, Darroudi F, De Sanctis S, Dominguez I, et al.: RENEB intercomparison exercises analyzing micronuclei (Cytokinesis-block Micronucleus Assay). Int J Radiat Biol, 93(1):36–47, 2017.

32. Rodrigues MA, Beaton-Green LA, Wilkins RC: Validation of the cytokinesis-block micronucleus assay using imaging flow cytometry for high throughput radiation biodosimetry. Health Phys, 110(1):29–36, 2016.
33. Yin X, Tian W, Wang L, Wang J, Zhang S, Cao J, Yang H: Radiation quality-dependence of bystander effect in unirradiated fibroblasts is associated with TGF-β1-Smad2 pathway and miR-21 in irradiated keratinocytes. Sci Rep, 5:11373, 2015.
34. Shao C, Furusawa Y, Aoki M, Matsumoto H, Ando K: Nitric oxide-mediated bystander effect induced by heavy-ions in human salivary gland tumour cells. Int J Radiat Biol, 78(9):837–844, 2002.
35. Anzenberg V, Chandiramani S, Coderre JA: LET-dependent bystander effects caused by irradiation of human prostate carcinoma cells with X rays or alpha particles. Radiat Res, 170(4):467–476, 2008.
36. Kaźmierczak U, Banaś D, Braziewicz J, Buraczewska I, Czub J, Jaskóła M, Kaźmierczak Ł, Korman A, Kruszewski M, Lankoff A, et al.: Investigation of the bystander effect in CHO-K1 cells. Rep Pract Oncol Radiother, 19(Suppl):S37–S41, 2014.
37. Ji X, Ji J, Shan F, Zhang Y, Chen Y, Lu X: Cancer-associated fibroblasts from NSCLC promote the radioresistance in lung cancer cell lines. Int J Clin Exp Med, 8(5):7002–7008, 2015.
38. Saeed Y, Rehman A, Xie B, Xu J, Hong M, Hong Q, Deng Y: Astroglial U87 cells protect neuronal SH-SY5Y cells from indirect effect of radiation by reducing DNA damage and inhibiting Fas mediated apoptotic pathway in coculture system. Neurochem Res, 40(8):1644–1654, 2015.
39. De Simone U, Caloni F, Gribaldo L, Coccini T: Human co-culture model of neurons and astrocytes to test acute cytotoxicity of neurotoxic compounds. Int J Toxicol, 36(6):463–477, 2017.

Chapter 4:

「Shortened 48 h cytokinesis-block micronucleus assay for triage assessment in a radiological mass-casualty accident」

「大規模放射線災害時におけるトリアージのための細胞質分裂阻害微小核法の培養時間短縮」

弘前大学大学院保健学研究科保健学専攻

提出者氏名：Valerie Goh Swee Ting

所　　属：　生体検査科学領域

指導教員：　三浦富智

List of Abbreviations (Chapter 4)

% BNC: percentage of BNC in all cells

BNC: binucleated cell(s)

CBMN: cytokinesis-block micronucleus

CM: complete medium

Cyt-B: cytochalasin B

DCA: dicentric chromosome assay

Dic: dicentric chromosome(s)

IAEA: International Atomic Energy Agency

ISO: International Organization for Standardization

MN: micronucleus/micronuclei

NDI: nuclear division index

PBMC(s): peripheral blood mononuclear cells

PHA: phytohemagglutinin

RABiT: Rapid Automated Biodosimetry Technology

WB: whole blood

Introduction (Chapter 4)

In a radiological mass-casualty accident, a fast and reliable triage identification of individuals exposed to ≥ 2 Gy acute whole-body equivalent radiation from the worried well is essential for immediate medical treatment, as recommended by the U.S. Department of Health and Human Services Radiation Emergency Medical Management[1]. Multiple biomarkers assessed in human peripheral blood such as γH2AX[2-3], proteins[4-6], gene expression[7-9] and miRNA[10] were evaluated for triage as these biomarkers bypassed the need for peripheral blood lymphocyte culture to evaluate DNA damage. However, standardized radiological triage guidelines by the International Organization for Standardization (ISO) are only available for cytogenetic endpoints scored in cultured lymphocytes. Both dicentric chromosomes (Dic) and micronuclei (MN) can be used for cytogenetic triage, as seen in ISO 21243:2008[11] and ISO 17099:2014[12] respectively.

For triage assessment, 50 metaphases/30 Dic are scored for dicentric chromosome assay (DCA)[11], while 200 BNC are scored for cytokinesis-block micronucleus (CBMN) assay[12-13]. In contrast, conventional dose assessment requires 1000 metaphases/100 Dic to be scored for DCA[14], and 1000 BNC to be scored for CBMN assay[12] for reliable dose estimation. In manual Dic scoring for one individual by experienced scorers, conventional triage assessment can take up to 150 min[11] or 30 min with the Quickscan method[15]. However, MN scoring is much quicker than Dic scoring as the criteria for MN scoring is much simpler than Dic and requires no prior knowledge of chromosome karyotypes[16]. Despite the much longer scoring time, DCA is preferred over CBMN assay for dose estimation as Dic is considered as the "gold standard" due to its high radiation-sensitivity and low background frequency[14, 17]. In contrast, background MN frequency is affected by a variety of factors, including age, sex and lifestyle[18]. Furthermore, cell culture for DCA can be completed in 48 h, much faster than the conventional CBMN assay culture of 72 h.

To increase the feasibility of CBMN assay over DCA in radiological triage, previous efforts were made to reduce CBMN assay culture time to 64 h[19], 60 h[20], 54 h[21-22] and 48 h[23-24]. Similarly, technological advancements for high throughput assessment of MN were also developed for faster scoring and multiple sample handling. Semi-automated and automated MN scoring were developed for Giemsa[25], DAPI[26], DAPI/Fast

Green[27] and PI[28]-stained cells spread on microscope slides. For direct imaging with fixed cell solutions, imaging flow cytometry coupled with Rapid Automated Biodosimetry Technology (RABiT) was also developed to handle multiple low volume blood samples[29-30]. The RABiT system also allowed direct cell culture and fixation, cell imaging and automated MN scoring of cells from multiple donors on glass-bottomed microplates[21-22].

Furthermore, triage MN scoring is often performed only in whole blood (WB) cultures[13, 19, 21-24, 28, 30-32]. Despite ISO recommending both cultures of WB and peripheral blood mononuclear cells (PBMCs) isolated from WB for CBMN assay as the target cells analyzed are assumed to be phytohemagglutinin (PHA)-stimulated T lymphocytes, plasma and other cellular components present in WB but absent in PBMCs could influence DNA damage induction and repair. As previously shown in Chapters 2 and 3, differences in CBMN parameters were seen between WB and PBMC cultures. To the best of our knowledge, this study is the first to compare triage MN scoring for WB and PBMC cultures. In addition, as the separation of PBMCs from WB is required for γH2AX[3] and miRNA[33] analysis, a multi-parametric approach for triage assessment with γH2AX, miRNA and CBMN assay could also be performed with PBMCs directly isolated with CPT tubes or Histopaque.

In this study, we reduced the culture period of CBMN assay from 72 h to 48 h and evaluated various parameters with manual scoring of Giemsa-stained cells as a low-cost alternative. Firstly, cell proliferation indicators of nuclear division index (NDI)[34] and percentage of BNC in all cells (% BNC), conventional and triage MN frequency (MN/1000 BNC, MN/200 BNC) and time taken for triage MN scoring were compared in 0, 2 and 4 Gy WB and PBMC cultures from 3 donors in three conditions, varying in culture period and time of cytochaslin B (Cyt-B) addition [48 h culture (24 h @ Cyt-B), 72 h culture (24 h @ Cyt-B), 72 h culture (44 h @ Cyt-B)]. In the second part, DRCs using induced MN/BNC from another 3 donors were constructed for WB and PBMCs in the shortened [48 h culture (24 h @ Cyt-B)] and conventional [72 h culture (44 h @ Cyt-B)] CBMN assay. Dose estimation with the Method A was performed using induced MN frequencies after triage and conventional scoring from the first part of the study. As the analysis is still ongoing, preliminary results will be discussed in this chapter.

Materials & Methods (Chapter 4)

Blood collection and irradiation conditions

3 healthy donors (F, 26 y.o.; M, 34 y.o.; M, 52 y.o.) were used for 48 and 72 h CBMN assays in the first part, while another 3 healthy donors (F, 23 y.o.; M, 25 y.o.; M, 29 y.o.) were used for DRC construction in the second part of the study. Peripheral blood was collected in 6 ml lithium-heparin tubes (BD, Franklin Lakes, NJ) with their informed consent. The informed consent form was approved by the Committee of Medical Ethics in Hirosaki University Graduate School of Health Sciences (Approval number: 2012-278). The 52 y.o. male donor is a smoker.

X-ray dose-rate was first calibrated with either 6 ml lithium-heparin tubes or 5 ml round bottom polystyrene tubes containing water in an angled tube rack. Blood in lithium-heparin tubes was then directly irradiated with 2 Gy X-ray at 1 Gy/min (150 kVp, 20 mA, 0.5 mm Al + 0.3 mm Cu filter; MBR-1520R-3, Hitachi Power Solutions, Tokyo, Japan). For 0 Gy blood, tubes were placed in the X-ray generator without irradiation. The cumulative radiation dose and dose-rate were monitored in real-time with a thimble ionization chamber (TN31013, PTW, Freiburg, Germany) connected to a dosimeter (MZ-BD-3 [Type 153], Hitachi Medical Corporation, Tokyo, Japan). The X-ray generator automatically stops once the radiation dose has reached its desired value. The detector and dosimeter are annually calibrated by the Japan Quality Assurance Organization, satisfying national standard traceability and ISO/IEC 17025 requirements.

To stimulate DNA repair, blood was incubated in 37 °C water bath for 2 h after irradiation. PBMCs were isolated with Histopaque 1077 according to manufacturer's instructions (Sigma-Aldrich, St. Louis, MO), by layering a 1:1 dilution of 3 ml blood and 3 ml washing medium (RPMI 1640 [Thermo Fisher Scientific, Waltham, MA], 2 % heat-inactivated fetal bovine serum (FBS) [Sigma-Aldrich], 1 × kanamycin sulfate [Thermo Fisher Scientific]) on 3 ml Histopaque. After washing twice with washing medium, PBMCs were suspended in 3 ml complete medium (CM) (RPMI 1640, 20 % heat-inactivated FBS, 1 × kanamycin sulfate).

CBMN culture, harvest and fixation for WB and PBMCs

1:10 WB:CM and 1:5 PBMCs:CM were used in 5 ml cell culture in loosely capped 15 ml polypropylene Falcon® conical centrifuge tubes. A final concentration of 180 μg/ml PHA

was added to stimulate T lymphocyte proliferation. Duplicate cultures were prepared only for first part of the study.

In the first part of the study, 0, 2 and 4 Gy WB and PBMCs from 3 donors were cultured in three different conditions, differing in culture period and time of Cyt-B addition (48 h culture [Cyt-B @ 24 h], 72 h culture [Cyt-B @ 24 h], 72 h culture [Cyt-B @ 44 h]). A final concentration of 4.5 or 6 µg/ml Cyt-B (Sigma-Aldrich) was added to PBMC and WB cultures respectively, as the different Cyt-B concentrations are required to obtain optimal BNC frequencies in each type of cell culture[35)].

In the second part of the study, DRCs were constructed with peripheral blood from another 3 donors irradiated with X-rays at 1 Gy/min, at doses of 0, 0.15, 0.3, 0.5, 0.75, 1, 1.5, 2, 3, 4 Gy. Due to a high number of dose points, blood initially collected in lithium-heparin tubes was distributed to smaller volumes in 5 ml polystyrene tubes. The type of cell culture (WB versus PBMC) and type of CBMN assay (shortened 48 h culture [24 h @ Cyt-B] versus conventional 72 h culture [44 h @ Cyt-B]) were compared.

After the end of cell culture, WB was harvested with the modified IAEA 2011 + 1 % formaldehyde (Sigma-Aldrich) protocol while PBMCs were harvested with the CRG protocol as described previously in Chapter 2.

CBMN cell spreading and Giemsa staining for WB and PBMCs

High humidity spreading was performed with cells from PBMC cultures, on microscope sldies placed on a moist Kimwipe™ as seen in Chapter 2. Cells from WB cultures were spread directly on the slides as fixed WB cells were more susceptible to cell rupture in higher humidity. A minimum of 2 two-spot slides were prepared for each culture.

For consistency in cell concentrations for triage MN scoring, PBMCs were diluted in 300 and 500 µl fixative in 48 and 72 h cultures respectively, while WB were diluted in 500 and 800 µl fixative for 48 and 72 h cultures respectively. 15 µl was used for each spot.

After drying, slides were stained with 5 % Giemsa (Merck Millipore, Burlington, MA) in pH 6.8 Gurr Buffer (Thermo Fisher Scientific) for 12 min and mounted with malinol (Muto Pure Chemicals, Tokyo, Japan).

Analysis of CBMN endpoints (NDI, % BNC, conventional and triage MN scoring)

CBMN endpoint analysis was manually performed by a single experienced scorer. Cells were scored with Olympus CX31 (Olympus Co., Tokyo, Japan) at 400 × magnification for NDI, % BNC and MN. For NDI and % BNC, ≥ 125 viable cells were scored per spot for a total of ≥ 500 cells. Equations for NDI[34] and % BNC are provided below. M_1, M_2, M_3, and M_4 indicate the number of cells with one, two, three or four daughter nuclei respectively, and N is the total number of cells analyzed.

$$NDI = \frac{M_1 + 2M_2 + 3M_3 + 4M_4}{N}$$

$$\%\ BNC\ in\ all\ cells = \frac{M_2}{N} \times 100\ \%$$

BNC identification and MN scoring were performed in accordance to the standardized criteria compiled by the Human MicroNucleus project[16]. In conventional MN scoring for 0 and 2 Gy samples, ≥ 250 BNC were scored per spot per slide, for a total of 1000 BNC. In conventional MN scoring for 4 Gy samples, ≥ 125 BNC were scored per spot per slide, for a total of 500 BNC. In triage MN scoring for 0 and 2 Gy samples, ≥ 200 BNC were scored per spot. In triage MN scoring for 4 Gy samples, ≥ 100 BNC were scored per spot.

DRCs constructed with shortened 48 h and conventional 72 h CBMN assay

Due to a limited number of donors available for DRC construction, a modified approach was used instead of the recommended approach of multiple DRCs constructed for 3 age groups separately for males and females by ISO 17099[12]. In our DRC construction, induced MN/BNC (MN/BNC at 0 Gy – MN/BNC at irradiated doses) was used instead of observed MN/BNC, to account for the donor-specific background MN frequency in males and females of different ages. To reduce the risk of upper and lower dose over-estimation in the 95 % confidence limit (CL), a pooled induced MN/BNC from the 3 donors was used for DRC construction as previously discussed in Chapter 1.

For increased statistical reliability, 10,000 BNC for 0, 0.15 and 0.3 Gy, 5000 BNC for 0.5 and 0.75 Gy, 3000 BNC for 1, 1.5, 2 Gy, 1500 BNC for 3 Gy and 1000 BNC for 4 Gy were manually scored in Giemsa-stained slides per donor and condition at 400 ×.

Poisson distribution was first verified in observed MN distributions with GOF Poisson R files kindly provided by M Higueras. The R files are based on the same Shiny R application developed by Fernández-Fontelo *et al.*[36] and Higueras *et al.*[37]. Over-dispersion tests (*u*, *D*, *L*-tests), zero-inflated Poisson (ZIP) tests (*CR*, *Z*-tests) and Bayesian test (ZIP versus Poisson) and dispersion index were calculated[38-42].

As the observed MN distributions showed mixed conclusions after Poisson validation, with lower doses often showing over-dispersion, a Quasipoisson model was used for generalized linear modelling. DRCs were constructed using Biodose Tools[43], with iteratively reweighted least squares. Linear-quadratic DRC coefficients (C, α, β), their standard errors and *p*-values calculated with F-test were reported.

Dose estimation with "radir" package in R

Dose estimation was performed in WB and PBMC cultures of 48 h culture (24 h @ Cyt-B) and 72 h culture (44 h @ Cyt-B), using conventional induced MN frequency scored in 1000 BNC and triage induced MN frequency scored in 200 BNC. Due to mixed conclusions seen in observed MN distributions in all donors after Poisson validation, dose and its lower and upper 95 % CL was estimated using Method A[44], with Dose Estimate ver 5.2[45].

Other statistical analysis

As the coefficient of variance (CV) was within 20 %[12] in 2 and 4 Gy MN frequency (MN/1000 BNC) in duplicate cultures of the first part of the study, average values of NDI, MN frequency and NPB frequency were used in the figures. Graphical representation and statistical analyses were carried out with R ver 4.0.3[46], RStudio ver 1.3.1093[47], and "tidyverse" package[48]. p-values < 0.05 were significant.

Results (Chapter 4)

Cell-cycle progression in 48 h (24 h @ Cyt-B), 72 h (24 h @ Cyt-B) and 72 h (44 h @ Cyt-B)

NDI and % BNC were first compared in the three culture conditions (Figure 1A). As expected, NDI and % BNC were much lower in 48 h than 72 h cultures for 0, 2 and 4 Gy cells. Comparing 72 h cultures, similar NDI and % BNC were seen for 24 h @ Cyt-B and 44 h @ Cyt-B. Likewise, as seen in Figure 1B, 48 h cultures showed many mono and bi-nucleated cells while 72 h cultures showed many multi-nucleated cells.

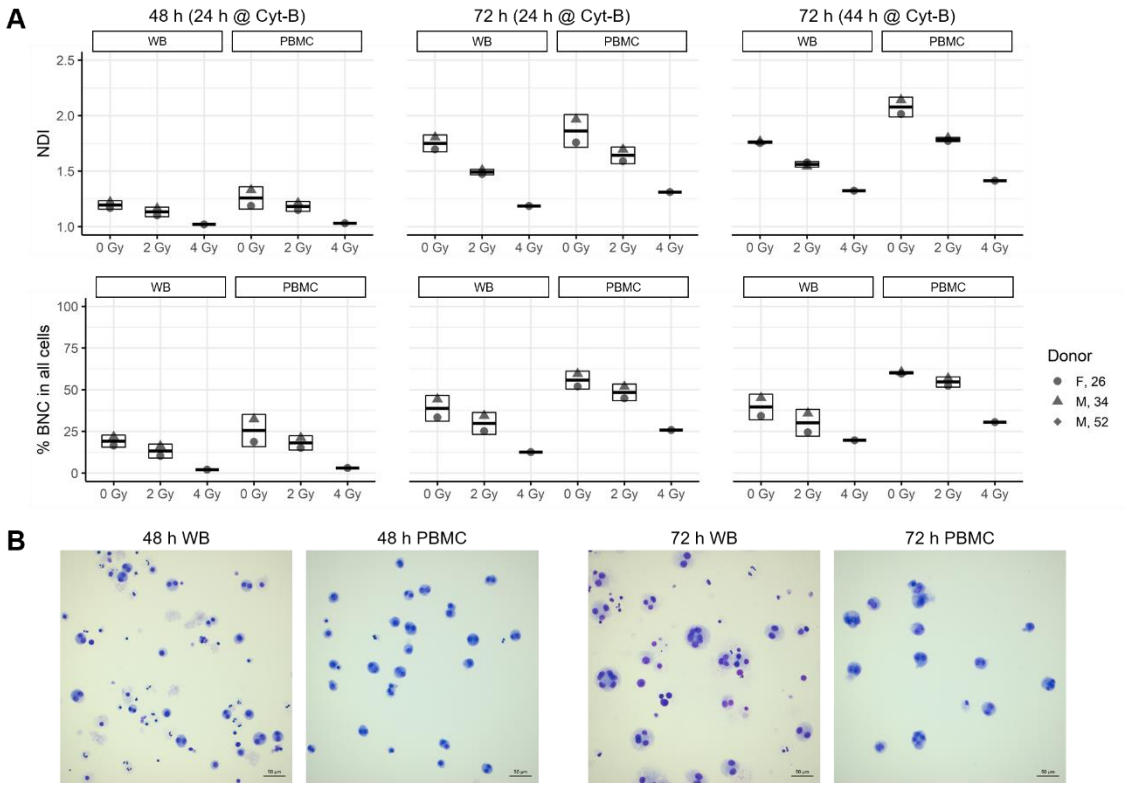

Figure 1: (A) NDI and % BNC for WB and PBMCs of three culture conditions. Preliminary results showed a lower NDI and % BNC for 48 h than 72 h cultures, and for increasing radiation dose. Similar NDI and % BNC were seen in 72 h cultures with different lengths of Cyt-B treatment. (B) Representative images of Giemsa-stained cells at 200 ×. Cells were mostly mono or bi-nucleated in 48 h cultures, while many multi-nucleated cells were seen in 72 h cultures. (Scale bar: 50 µm).

Conventional MN frequency (MN/1000 BNC) in 48 h (24 h @ Cyt-B), 72 h (24 h @ Cyt-B) and 72 h (44 h @ Cyt-B)

In Figure 2, conventional MN frequencies (MN/1000 BNC) in both WB and PBMCs were compared in three culture conditions. A similar MN frequency was seen in 0 Gy cells. For 2 and 4 Gy cells, MN frequency was higher in 48 h (24 h @ Cyt-B) and 72 h (24 h @ Cyt-B) than 72 h (44 h @ Cyt-B), showing a possible effect in culture period and length of Cyt-B treatment. In all conditions, MN frequency in 2 and 4 Gy WB was higher than PBMCs.

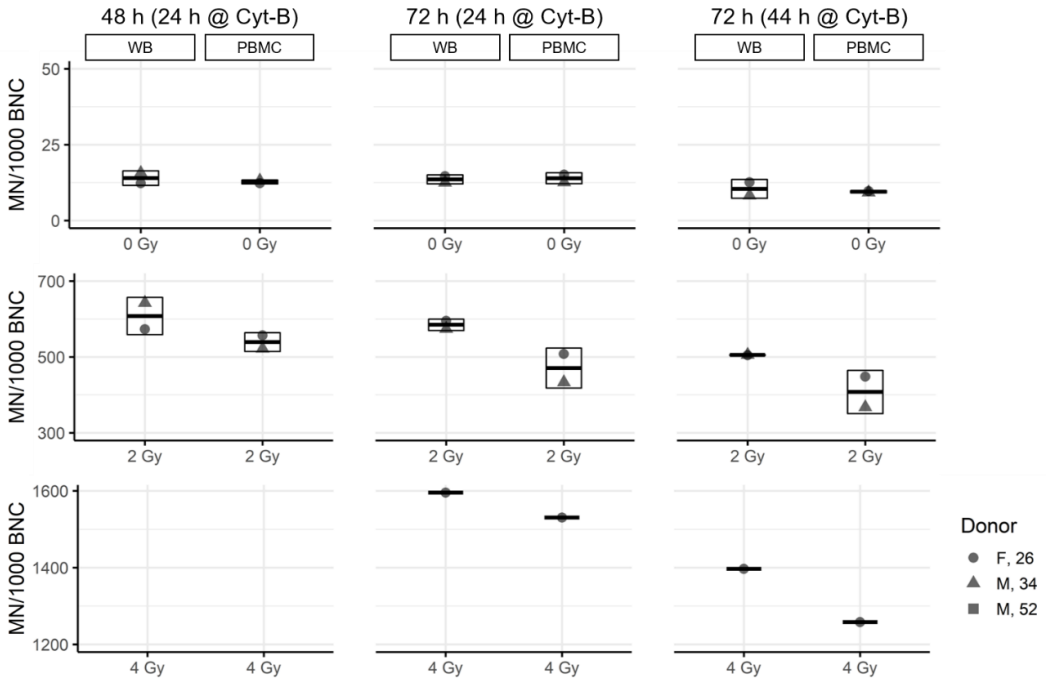

Figure 2: MN frequency (MN/1000 BNC) for WB and PBMCs of three culture conditions. Preliminary results showed similar MN frequency at 0 Gy and higher MN frequency at 2 and 4 Gy in 48 h than 72 h cultures. In all three culture conditions, MN frequency in irradiated samples was higher in WB than PBMCs.

Triage MN frequency (MN/200 BNC), MN distributions and scoring time in 48 h (24 h @ Cyt-B), 72 h (24 h @ Cyt-B) and 72 h (44 h @ Cyt-B)

As seen in Table 1, preliminary results in triage MN frequency were similar to conventional MN frequency, where a higher MN frequency for 2 and 4 Gy samples was seen with shorter culture period (48 h versus 72 h) and elongated Cyt-B treatment (24 h @ Cyt-B versus 44 h @ Cyt-B). Irradiated 2 and 4 Gy samples of three donors were also able to be easily distinguished from 0 Gy in both WB and PBMCs (i.e. 0 Gy: 1–5 MN/200 BNC, 2 Gy: 100–120 MN/200 BNC, 4 Gy: 300–400 MN/200 BNC).

For 48 h cultures in both WB and PBMCs, scoring time was within 7 min for 0 Gy, and 14 min for 2 Gy. For 72 h cultures in both WB and PBMCs, scoring time was within 5 min for 0 Gy, 9 min for 2 Gy and 12 min for 4 Gy.

Table 1: Preliminary results of triage MN frequency and time taken for scoring for F, 26 donor

Culture condition	Cells, Dose	Triage MN frequency	Scoring time (min:s)
48 h culture (24 h @ Cyt-B)	WB, 0 Gy	2.08 ± 1.42	6:32 ± 0:37
	PBMC, 0 Gy	1.86 ± 1.71	5:39 ± 0:40
	WB, 2 Gy	114.91 ± 16.26	12:59 ± 0:48
	PBMC, 2 Gy	114.15 ± 7.46	9:49 ± 0:46
72 h culture (24 h @ Cyt-B)	WB, 0 Gy	2.54 ± 2.14	4:38 ± 0:32
	PBMC, 0 Gy	3.16 ± 2.21	3:04 ± 0:21
	WB, 2 Gy	120.25 ± 19.47	7:54 ± 0:31
	PBMC, 2 Gy	101.79 ± 5.44	5:34 ± 1:03
	WB, 4 Gy	328.54 ± 30.97	9:46 ± 1:40
	PBMC, 4 Gy	301.06 ± 23.17	7:58 ± 0:57
72 h culture (44 h @ Cyt-B)	WB, 0 Gy	2.55 ± 2.00	3:34 ± 0:14
	PBMC, 0 Gy	2.21 ± 1.37	2:40 ± 0:21
	WB, 2 Gy	100.91 ± 17.37	8:53 ± 0:34
	PBMC, 2 Gy	89.53 ± 18.44	4:51 ± 0:34
	WB, 4 Gy	271.47 ± 37.72	11:34 ± 0:55
	PBMC, 4 Gy	249.85 ± 21.96	7:39 ± 0:24

Triage MN scoring was performed for 200 BNC in each spot of the slide for 0 and 2 Gy cultures (total 8 spots for 4 slides in duplicate cultures). MN frequency for 4 Gy cultures was scored in 100 BNC due to a reduced BNC frequency. MN frequency and time taken were expressed in Mean ± SD, averaged from 8 spots.

Figure 3 shows the observed triage MN distributions in 2 and 4 Gy WB and PBMC cultures. MN distribution patterns differed greatly between 2 and 4 Gy cultures. In addition, the overall distribution pattern was similar in the three culture conditions for 2 Gy and 4 Gy cultures.

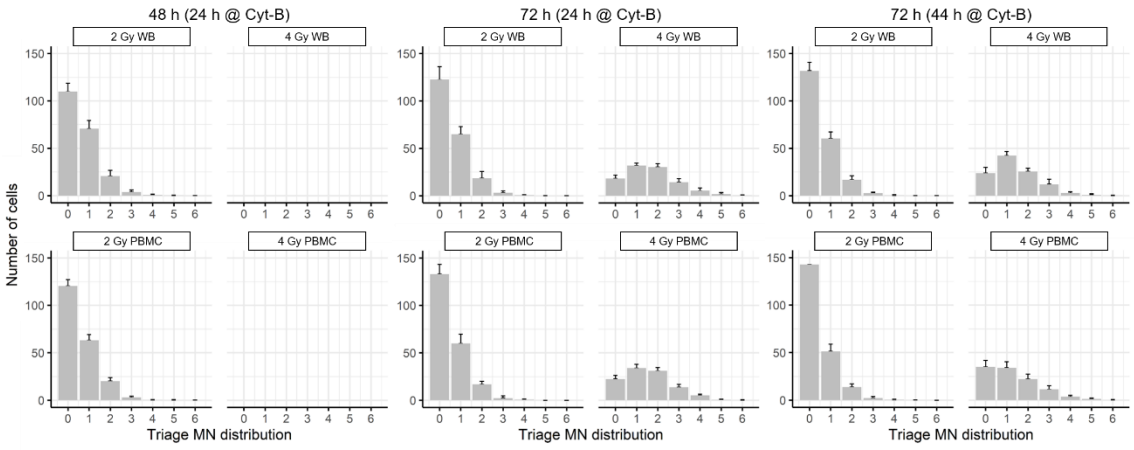

Figure 3: Observed triage MN distributions of 2 and 4 Gy WB and PBMCs of three culture conditions, pooled from three donors and 8 spots scored for triage. 200 BNC was scored for 2 Gy while 100 BNC was scored for 4 Gy. MN distribution patterns were very different between 2 and 4 Gy cultures.

DRCs of shortened 48 h (24 h @ Cyt-B) and conventional 72 h (44 h @ Cyt-B) CBMN assay

DRCs were constructed with pooled induced MN/BNC to account for the different age and sex of the 3 donors. Four different conditions were evaluated: shortened 48 h culture (24 h @ Cyt-B) for WB and PBMCs, and conventional 72 h culture (44 h @ Cyt-B) for WB and PBMCs (Figure 4). DRC coefficients, their *p*-values and SE were shown in Table 2.

DRCs were very similar for WB cultures of 48 and 72 h, while some differences were seen in PBMC cultures of 48 and 72 h, especially in the higher doses. In particular, DRCs differed greatly depending on the type of cell culture performed.

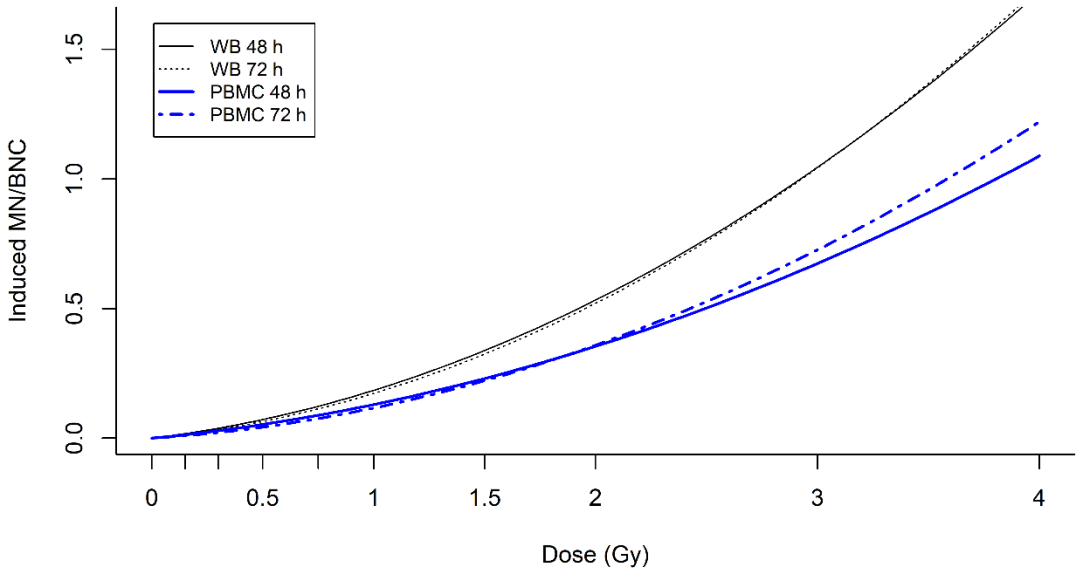

Figure 4: Preliminary DRCs of the four conditions constructed with Biodose Tools with pooled data from three donors.

Table 2: Preliminary DRC coefficients ($Y = C + \alpha D + \beta D^2$) and their *p*-values and SE

Culture condition	C (± SE_C)	α (± SE_α)	β (± SE_β)	*p*-value (C)	*p*-value (α)	*p*-value (β)
WB, 48 h (24 h @ Cyt-B)	7.85e-08 ± 0.009	0.103 ± 0.036	0.082 ± 0.017	2	0.047	0.004
WB, 72 h (44 h @ Cyt-B)	8.88e-08 ± 0.005	0.085 ± 0.019	0.087 ± 0.009	2	0.006	5.78e-05
PBMC, 48 h (24 h @ Cyt-B)	8.67e-08 ± 0.005	0.082 ± 0.019	0.048 ± 0.009	2	0.008	0.002
PBMC, 72 h (44 h @ Cyt-B)	8.50e-08 ± 0.003	0.053 ± 0.012	0.063 ± 0.005	2	0.005	1.19e-05

Values smaller than 3 decimal places are shown in scientific notation.

Dose estimation with triage (MN/200 BNC) and conventional (MN/1000 BNC) MN frequency

As the observed MN distributions of 2 and 4 Gy cultures showed mixed results after Poisson validation with GOF Poisson in both triage and conventional modes (Table 3), dose estimation was performed with Method A (Table 4). Estimated doses in all conditions were within ± 0.7 Gy of actual doses.

Table 3: Verification of Poisson assumption in observed MN distributions scored in triage and conventional modes for F, 26 donor

Culture condition	Cells, Dose	Reject Poisson?	
		Triage MN distri.	Conventional MN distri.
48 h culture (24 h @ Cyt-B)	WB, 2 Gy	Mixed (5), Yes (3)	No (1), Mixed (1)
	PBMC, 2 Gy	No (8)	No (2)
72 h culture (44 h @ Cyt-B)	WB, 2 Gy	No (8)	No (2)
	PBMC, 2 Gy	No (6), Yes (2)	No (1), Yes (1)
	WB, 4 Gy	No (4), Mixed (4)	Mixed (2)
	PBMC, 4 Gy	No (5), Mixed (1), Yes (2)	Mixed (1), Yes (1)

Detailed results from the statistical tests (D, L, CR, Z, Bayesian vs ZIP tests) performed in GOF Poisson for each MN distribution were not explicity shown. Final results of Poisson verification were compiled in the "Reject Poison?" column. No: Poisson was validated for all tests, Mixed: Poisson was rejected for some tests, Yes: Poisson was rejected for all tests. A maximum of 8 spots were analyzed for triage MN scoring, while duplicate cultures were analyzed for conventional MN scoring.

Table 4: Preliminary dose estimation with induced MN frequency scored in triage and conventional modes in F, 26 donor

Culture condition	Cells, Actual dose	Triage (100/200 BNC)			Conventional (500/1000 BNC)		
		Ind. MN/BNC	Est. dose (Gy)	Est. dose range (Gy)	Ind. MN/BNC	Est. dose (Gy)	Est. dose range (Gy)
48 h culture (24 h @ Cyt-B)	WB, 2 Gy	0.564	2.071	1.602 – 2.540	0.561	2.064	1.646 – 2.482
	PBMC, 2 Gy	0.561	2.680	2.050 – 3.309	0.544	2.629	2.069 - 3.189
72 h culture (44 h @ Cyt-B)	WB, 2 Gy	0.492	1.934	1.642 – 2.226	0.492	1.934	1.726 – 2.141
	PBMC, 2 Gy	0.437	2.243	1.919 – 2.566	0.438	2.248	2.035 – 2.461
	WB, 4 Gy	1.345	3.464	3.040 – 3.888	1.384	3.521	3.212 - 3.829
	PBMC, 4 Gy	1.238	3.521	3.212 – 3.829	1.245	4.049	3.728 – 4.370

Induced MN frequency was obtained by subtracting the average background MN frequency at 0 Gy from the average MN frequency at 2 and 4 Gy. Dose estimation was performed with Method A at 95 % CL, with Dose Estimate ver 5.2. For triage estimation, cell number was fixed at 200 for 2 Gy and 100 for 4 Gy. For conventional estimation, cell number was fixed at 1000 for 2 Gy and 500 for 4 Gy

Discussion (Chapter 4)

Triage scoring and dose estimation with cytogenetic markers during a radiation mass-casualty needs to be efficient and reliable, such that individuals exposed to ≥ whole-body equivalent 2 Gy can be quickly distinguished from the worried well for immediate medical treatment. The current gold standard of DCA requires only 48 h for cell culture, but is limited by the long scoring time and prior knowledge of chrosome karyotypes for scoring. On the other hand, CBMN assay is conventionally cultured for 72 h, but scoring is much faster. Recent attempts in reducing reporting time for estimated doses involve automated scoring and robotics for high throughput analysis, but they can be very costly. In our preliminary study, we have showed that a shortened 48 h CBMN culture is feasible for triage assessment for both WB and PBMC cultures up to 2 Gy, even in individuals with low NDI. Acute radiation syndrome symptoms such as skin erythema, nausea, diarrhea and low blood cell counts can also be used simultaneously to identify individuals exposed to higher doses up to 4 Gy. Using manual triage scoring of 200 BNC with light microscopy, 0 Gy samples can be identified within 7 min and 2 Gy samples can be scored within 15 min, in slides with appropriate cell concentrations.

72 h (44 h @ Cyt-B) CBMN culture is often used and recommended as it was shown to obtain an optimal frequency of BNC for both WB and PBMC cultures[14, 35], although 68 – 70 h cultures were also used by multiple laboratories[49]. In our 72 h cultures, a high % BNC of 40–60 % in unirradiated and 30–50 % in 2 Gy cells was obtained. Our results also showed that the length of Cyt-B treatment did not significantly affect NDI and % BNC for 72 h cultures. In addition, while our results showed PBMCs with higher NDI and % BNC than WB cultures, the opposite was instead seen in Ellard and Parry's study as % BNC was higher in WB than PBMCs[50]. It is thus important to evaluate the optimal CBMN culture conditions in WB and PBMCs for multiple individuals in each population as differences in individual susceptibility to Cyt-B had been shown even within the same age group[51].

Moreover, in Köksal *et al.*'s study, reducing CBMN culture time from 72 h to 48 h led to a conclusion that 48 h was too short to obtain desirable BNC frequencies for MN scoring[52]. While this is undeniably true as a much lower % BNC was seen in our 48 h cells (0 Gy: 25–30 %, 2 Gy: 12–20 %), a sufficient number of BNC was able to be

obtained for MN scoring of more than 10,000 BNC for a 5 ml culture (500 µl WB). Likewise, as shown by Rodrigues *et al.* for 48 h cultures of 2 ml (200 µl WB), up to 2000 BNC was scored with imaging flow cytometry[23]. Even though more time is needed to score MN in cultures showing low % BNC, a shorter CBMN culture is highly applicable for triage as a reduced number of BNC is scored to account for the lower % BNC. In addition, by personal observation, locating BNC for MN scoring was much easier in 48 h cultures as cells were mostly mono- and bi-nucleated.

We also saw a similar/higher MN frequency in 48 h than 72 h cultures in manually scored WB and PBMCs. As MN contains unstable chromosome aberrations such as acentric fragments and whole chromosomes formed by mis-segregation[35], the elongated culture time could have induced apoptosis in cells with many unstable aberrations, hence decreasing MN frequency. This is also similar in DCA, where a 48 h culture and first metaphase analysis are required to accurately represent Dic frequency, as Dic is an unstable chromosome aberration which could decrease up to 50 % with each cell division[53]. In contrast, Rodrigues *et al.* showed a lower MN frequency in 48 h (24 h @ Cyt-B) than 72 h (24 h @ Cyt-B) WB cultures in automatically scored cells with imaging flow cytometry, which could be due to damaged cells dividing slower than healthy cells[23]. In Köksal *et al.*'s study comparing 48 h (24 h @ Cyt-B) and 72 h (44 h @ Cyt-B) CBMN assay, a lower MN frequency was also seen in 48 than 72 h WB cultures in manually scored cells[52]. This finding was also supported other studies by Lee *et al.*[20] and Almássy *et al.*[54], where an increasing MN frequency was seen in elongated culture periods. Although our results did not agree with previous studies, differences in donor population could have contributed to MN frequency variability[55]. Nevertheless, a 48 h CBMN culture period was still able to easily distinguish irradiated from unirradiated samples, thus supporting the use of a shortened CBMN assay for radiation triage as results are able to be reported at a much quicker time. It also reinforces the recommendation that the same culture protocols should be used DRC construction and dose estimation.

Moreover, our observation of a higher MN frequency in 72 h (24 h @ Cyt-B) than 72 h (44 h @ Cyt-B) was also seen by Lee *et al.*[20] and Köksal *et al.*[52], although no clear increasing relationship between MN frequency and Cyt-B treatment time in 72 h cultures was seen[53]. On the other hand, in RENEB's CBMN intercomparison study, a much lower

MN frequency in lab 3 [72 h (24 h @ Cyt-B)] than lab 6 [72 h (44 h @ Cyt-B)] was observed[49], which could be attributed to different visual interpretations of the MN scoring criteria by different scorers. As very few tri and tetra-nucleated cells were seen in our 48 h cultures, it was possible that MN was mostly scored in BNC arrested after the first cell division for 72 h (24 h @ Cyt-B) while MN was scored in both BNC arrested after the first cell division if mitosis was delayed and the second cell division for 72 h (44 h @ Cyt-B). As a result, this observation might show that MN is likely unstable and could decrease with multiple cell divisions. As stated in EPR-Biodosimetry, Cyt-B should be preferably added at 24 h for "biological dosimetry to ensure only first division cells are captured"[14]. Further study is thus required to analyze if MN scored during first division arrest is necessary for a reliable dose estimation, by using DNA conjugates such as BrdU or CFSE to differentiate first and second cell divisions. Nonetheless, the length of Cyt-B treatment could be an important factor affecting MN frequency and hence consistency in CBMN protocols for DRC construction and dose estimation is important.

MN scoring in 200 BNC had been shown by McNamee *et al.*[13] to reliably identify individuals exposed to ≥ 1 Gy gamma irradiation with manual scoring on acridine orange-stained cells, and thus 200 BNC is recommended by ISO 17099[12] for initial triage assessment. For higher doses, 200 total MN can be scored[12]. In our study, we have showed that 2 and 4 Gy WB and PBMC cultures was easily distinguished with total MN frequency (2 Gy: 100–120 MN/200 BNC, 4 Gy: 120–160/100 BNC) and observed MN distributions, for both 48 and 72 h cultures. However, depending on the spot analyzed by the same scorer, triage MN scored showed differences of up to 70 MN in 2 Gy and 60 MN in 4 Gy cultures. Morever, in Chapter 3, we also showed differences of up to 60 MN in MN/1000 BNC between 3 scorers for the same slides in 2 Gy cultures. As such, if irradiated individuals were identified with CBMN triage, we highly recommend multiple scorers to score the same 2-spot slide and report average MN frequency for more reliable dose estimation.

Furthermore, to the best of our knowledge, this is the first time CBMN DRCs were constructed for the same donors comparing WB and PBMC cultures of 48 h (24 h @ Cyt-B) and 72 h (44 h @ Cyt-B). We have shown that with preliminary data, WB cultures of 48 h and 72 h were very similar while some differences especially in higher

doses were seen in 48 and 72 h PBMC cultures. As cell cycle arrest and delay is often seen at higher doses, some cells in PBMC cultures might have been unable to proceed to telophase in 48 h. As a result, the MN frequency at 48 h was slightly lower than at 72 h. This was in direct contrast with Rodrigues *et al.*'s study, where a much lower DRC was seen in 48 h than 72 h WB cultures[23]. Moreover, we also showed that due to the lower MN frequency seen in PBMCs, the DRCs in both 48 and 72 h cultures were much lower in PBMCs than WB. This phenomenon was also seen in the DRCs in Sioen *et al.*'s study, which compared 70 h (23 h @ Cyt-B) WB and fresh PBMC cultures of up to 2 Gy[56]. On the contrary, in Lue *et al.*'s study comparing 70 h (44 h @ Cyt-B) 50 µl WB and 500 µl PBMC cultures, DRCs in both types of cultures were very similar up to 6 Gy[57]. Once again, population differences could have influenced dose-response relationships observed, and hence CBMN assays of multiple conditions should be separately evaluated in each laboratory. Despite the differences in DRCs seen, triage and conventional dose estimation with our donor population of both 48 and 72 h WB and PBMC cultures were within ± 0.7 Gy of actual doses.

In conclusion, our study showed that with a low cost method of manual MN scoring on Giemsa-stained cells, and shortening the CBMN assay to 48 h (24 h @ Cyt-B) for both WB and PBMCs, radiation triage identification of individuals exposed to a whole-body equivalent dose of ≥ 2 Gy can be easily performed. In our donor population, triage MN scoring was completed in 7 min for 0 Gy and in 14 min for 2 Gy samples. Individuals of ≥ 2 Gy can also be identified with MN frequency and observed MN distributions. Triage dose estimates were also within ± 0.7 Gy of actual doses. We thus highly recommend the 48 h CBMN assay for initial triage in a radiation mass-casualty accident. If more reliable dose estimates are required, dose estimation with 1000 BNC in CBMN assay or 1000 metaphases in DCA can be additionally performed on selected individuals.

References (Chapter 4)

1. Coleman CN, Weinstock DM, Casagrande R, Hick JL, Bader JL, Chang F, Nemhauser JB, Knebel AR: Triage and treatment tools for use in a scarce resources-crisis standards of care setting after a nuclear detonation. Disaster Med Public Health Prep, 5 Suppl 1:S111-21, 2011.

2. Moquet J, Barnard S, Rothkamm K: Gamma-H2AX biodosimetry for use in large scale radiation incidents: comparison of a rapid '96 well lyse/fix' protocol with a routine method. PeerJ, 2:e282, 2014.
3. Viau M, Testard I, Shim G, Morat L, Normil MD, Hempel WM, Sabatier L: Global quantification of γH2AX as a triage tool for the rapid estimation of received dose in the event of accidental radiation exposure. Mutat Res Genet Toxicol Environ Mutagen, 793:123–131, 2015.
4. Ossetrova NI, Sandgren DJ, Blakely WF: C-reactive protein and serum amyloid A as early-phase and prognostic indicators of acute radiation exposure in nonhuman primate total-body irradiation model. Radiat Meas, 46(9):1019–1024, 2011.
5. Lee Y, Pujol Canadell M, Shuryak I, Perrier JR, Taveras M, Patel P, Koller A, Smilenov LB, Brenner DJ, Chen EI, et al.: Candidate protein markers for radiation biodosimetry in the hematopoietically humanized mouse model. Sci Rep, 8:13557, 2018.
6. Balog RP, Bacher R, Chang P, Greenstein M, Jammalamadaka S, Javitz H, Knox SJ, Lee S, Lin H, Shaler T, et al.: Development of a biodosimeter for radiation triage using novel blood protein biomarker panels in humans and non-human primates. Int J Radiat Biol, 96(1):22–34, 2020.
7. Macaeva E, Mysara M, De Vos WH, Baatout S, Quintens R: Gene expression-based biodosimetry for radiological incidents: assessment of dose and time after radiation exposure. Int J Radiat Biol, 95(1):64–75, 2019.
8. Port M, Ostheim P, Majewski M, Voss T, Haupt J, Lamkowski A, Abend M: Rapid high-throughput diagnostic triage after a mass radiation exposure event using early gene expression changes. Radiat Res, 192(2):208–218, 2019.
9. Wang Q, Lee Y, Shuryak I, Pujol Canadell M, Taveras M, Perrier JR, Bacon BA, Rodrigues MA, Kowalski R, Capaccio C, et al.: Development of the FAST-DOSE assay system for high-throughput biodosimetry and radiation triage. Sci Rep, 10:12716, 2020.
10. Małachowska B, Tomasik B, Stawiski K, Kulkarni S, Guha C, Chowdhury D, Fendler W: Circulating microRNAs as biomarkers of radiation exposure: A systematic review and meta-analysis. Int J Radiat Oncol Biol Phys, 106(2):390–402, 2020.

11. International Organization for Standardization: Radiation protection – Performance criteria for laboratories performing cytogenetic triage for assessment of mass casualties in radiological or nuclear emergencies – General principles and application to dicentric assay. ISO 21243, 2008.
12. International Organization for Standardization: Radiological protection – Performance criteria for laboratories using the cytokinesis block micronucleus (CBMN) assay in peripheral blood lymphocytes for biological dosimetry. ISO 17099, 2014.
13. McNamee JP, Flegal FN, Greene HB, Marro L, Wilkins RC: Validation of the cytokinesis-block micronucleus (CBMN) assay for use as a triage biological dosimetry tool. Radiat Prot Dosimetry. 135(4):232–242, 2009.
14. International Atomic Energy Agency. Cytogenetic dosimetry: applications in preparedness for and response to radiation emergencies. EPR-Biodosimetry. IAEA, Vienna, Austria, 2011.
15. Flegal FN, Devantier Y, Marro L, Wilkins RC: Validation of QuickScan dicentric chromosome analysis for high throughput radiation biological dosimetry. Health Phys, 102(2):143–153, 2012.
16. Bonassi S, Fenech M, Lando C, Lin YP, Ceppi M, Chang WP, Holland N, Kirsch-Volders M, Zeiger E, Ban S, et al.: HUman MicroNucleus project: international database comparison for results with the cytokinesis-block micronucleus assay in human lymphocytes: I. Effect of laboratory protocol, scoring criteria, and host factors on the frequency of micronuclei. Environ Mol Mutagen, 37(1):31–45, 2001.
17. Hoffmann W, Schmitz-Feuerhake I: How radiation-specific is the dicentric assay? J Expo Anal Environ Epidemiol, 9(2):113–133, 1999.
18. Fenech M, Bonassi S. The effect of age, gender, diet and lifestyle on DNA damage measured using micronucleus frequency in human peripheral blood lymphocytes. Mutagenesis, 26(1):43–49, 2011.
19. Lee T-K, Johnson J, Wiley AL Jr, Means JA: Assessment of two protocols for the human lymphocyte cytokinesis-blocked micronucleus assay. Mutagenesis, 10(4):375–377, 1995.
20. Lee TK, Wiley AL Jr, Esinhart JD, Blackburn LD: Radiation dose-dependent variations of micronuclei production in cytochalasin B-blocked human lymphocytes.

Teratog Carcinog Mutagen, 14(1):1–12, 1994.

21. Repin M, Pampou S, Garty G, Brenner DJ: RABiT-II: A fully-automated micronucleus assay system with shortened time to result. Radiat Res, 191(3):232–236, 2019.
22. Repin M, Pampou S, Brenner DJ, Garty G: The use of a centrifuge-free RABiT-II system for high-throughput micronucleus analysis. J Radiat Res, 61(1):68–72, 2020.
23. Rodrigues MA, Beaton-Green LA, Wilkins RC: Validation of the cytokinesis-block micronucleus assay using imaging flow cytometry for high throughput radiation biodosimetry. Health Phys, 110(1):29–36, 2016.
24. Rodrigues MA, Probst CE, Beaton-Green LA, Wilkins RC: The effect of an optimized imaging flow cytometry analysis template on sample throughput in the reduced culture cytokinesis-block micronucleus assay. Radiat Prot Dosimetry, 172(1-3):223–229, 2016.
25. Decordier I, Papine A, Plas G, Roesems S, Vande Loock K, Moreno- Palomo J, Cemeli E, Anderson D, Fucic A, Marcos R, et al.: Automated image analysis of cytokinesis-blocked micronuclei: an adapted protocol and a validated scoring procedure for biomonitoring. Mutagenesis, 24(1):85–93, 2008.
26. Varga D, Johannes T, Jainta S, Schuster S, Schwarz-Boeger U, Kiechle M, Patino Garcia B, Vogel W: An automated scoring procedure for the micronucleus test by image analysis. Mutagenesis, 19(5):391–397, 2004.
27. François M, Hochstenbach K, Leifert W, Fenech MF: Automation of the cytokinesis-block micronucleus cytome assay by laser scanning cytometry and its potential application in radiation biodosimetry. Biotechniques, 57(6):309–312, 2014.
28. Tamizh Selvan G, Chaudhury NK, Venkatachalam P: Comparison of results of the manual and automated scoring of micronucleus frequencies in 60Co-irradiated peripheral blood lymphocytes for triage dosimetry. Appl Radiat Isot, 97:70–77, 2015.
29. Rodrigues MA, Beaton-Green LA, Wilkins RC, Fenech MF: The potential for complete automated scoring of the cytokinesis block micronucleus cytome assay using imaging flow cytometry. Mutat Res Genet Toxicol Environ Mutagen, 836(Pt A):53–64, 2018.
30. Wang Q, Rodrigues MA, Repin M, Pampou S, Beaton-Green LA, Perrier J, Garty G, Brenner DJ, Turner HC, Wilkins RC: Automated triage radiation biodosimetry:

Integrating imaging flow cytometry with high-throughput robotics to perform the cytokinesis-block micronucleus assay. Radiat Res, 191(4):342–351, 2019.

31. Thierens H, Vral A, Vandevoorde C, Vandersickel V, de Gelder V, Romm H, Oestreicher U, Rothkamm K, Barnard S, Ainsbury E, et al.: Is a semi-automated approach indicated in the application of the automated micronucleus assay for triage purposes? Radiat Prot Dosimetry, 159(1-4):87–94, 2014.
32. Willems P, August L, Slabbert J, Romm H, Oestreicher U, Thierens H, Vral A: Automated micronucleus (MN) scoring for population triage in case of large scale radiation events. Int J Radiat Biol, 86(1):2–11, 2010.
33. Knops K, Boldt S, Wolkenhauer O, Kriehuber R: Gene expression in low- and high-dose-irradiated human peripheral blood lymphocytes: possible applications for biodosimetry. Radiat Res, 178(4):304–312, 2012.
34. Fenech M: Cytokinesis-block micronucleus cytome assay. Nat Protoc. 2(5):1084–1104, 2007.
35. Eastmond DA, Tucker JD: Identification of aneuploidy-inducing agents using cytokinesis-blocked human lymphocytes and an antikinetochore antibody. Environ Mol Mutagen, 13(1):34–43, 1989.
36. Fernández-Fontelo A, Puig P, Ainsbury EA, Higueras M: An exact goodness-of-fit test based on the occupancy problems to study zero-inflation and zero-deflation in biological dosimetry data. Radiat Prot Dosimetry, 179(4):317–326, 2018.
37. Higueras M, González JE, Di Giorgio M, Barquinero JF: A note on Poisson goodness-of-fit tests for ionizing radiation induced chromosomal aberration samples. Int J Radiat Biol, 94(7):656–663, 2018.
38. Rao CR, Chakravarti IM: Some small sample tests of significance for a Poisson distribution. Biometrics, 12(3):264–282, 1956.
39. Merkle W: Poisson goodness-of-fit tests for radiation-induced chromosome aberrations. Int J Radiat Biol Relat Stud Phys Chem Med, 40(6):685–692, 1981.
40. van den Broek J: A score test for zero inflation in a Poisson distribution. Biometrics, 51(2):738–743, 1995.
41. Bayarri MJ, Berger JO, Datta GS: Objective Bayes testing of Poisson versus inflated Poisson models. In: Clarke B and Ghosal S (eds) Pushing the limits of contemporary statistics: contributions in honor of Jayanta K. Ghosh, pp. 105–121, Institute of

Mathematical Statistics, Beachwood, Ohio, USA, 2008.

42. Higueras M, Puig P, Ainsbury EA, Vinnikov VA, Rothkamm K: A new Bayesian model applied to cytogenetic partial body irradiation estimation. Radiat Prot Dosimetry, 168(3):330–336, 2016.
43. Hernández A, Endesfelder D, Einbeck J, Puig P, Benadjaoud A, Higueras M, Ainsbury E, Gruel G, Kulka U, Barrios L, et al.: Biodose Tools: An R Shiny application for biological dosimetry, 2020. URL https://biodosetools-team.github.io/biodosetools/.
44. Savage JRK, Papworth DG: Constructing a 2B calibration curve for retrospective dose reconstruction. Radiat Prot Dosim, 88(1):69–76, 2000.
45. Ainsbury EA, Lloyd DC: Dose estimation software for radiation biodosimetry. Health Phys, 98(2):290–295, 2010.
46. R Core Team: R: a language and environment for statistical computing. R Foundation for Statistical Computing, Vienna, Austria, 2020.
47. RStudio Team: RStudio: integrated development for R. RStudio, Inc., Boston, MA, USA, 2020.
48. Wickham H, Averick M, Bryan J, Chang W, McGowan L, François R, Grolemund G, Hayes A, Henry L, Hester J, et al. Welcome to the Tidyverse. JOSS, 4(43):1686, 2019.
49. Depuydt J, Baeyens A, Barnard S, Beinke C, Benedek A, Beukes P, Buraczewska I, Darroudi F, De Sanctis S, Dominguez I, et al.: RENEB intercomparison exercises analyzing micronuclei (Cytokinesis-block Micronucleus Assay). Int J Radiat Biol, 93(1):36–47, 2017.
50. Ellard S, Parry EM: A modified protocol for the cytochalasin B in vitro micronucleus assay using whole human blood or separated lymphocyte cultures. Mutagenesis, 8(4):317–320, 1993.
51. Surrallés J, Carbonell E, Marcos R, Degrassi F, Antoccia A, Tanzarella C: A collaborative study on the improvement of the micronucleus test in cultured human lymphocytes. Mutagenesis, 7(6):407–410, 1992.
52. Köksal G, Lloyd DC, Edwards AA, Prosser JS: The dependence of the micronucleus yield in human lymphocytes on culture and cytokinesis blocking times. Radiat Prot Dosimetry, 29(3): 209–212, 1989.
53. Kaddour A, Colicchio B, Buron D, El Maalouf E, Laplagne E, Borie C, Ricoul M,

Lenain A, Hempel WM, Morat L, et al.: Transmission of induced chromosomal aberrations through successive mitotic divisions in human lymphocytes after in vitro and in vivo radiation. Sci Rep, 7:3291, 2017.

54. Almássy Z, Krepinsky AB, Bianco A, Koteles GJ: The present status and perspectives of micronucleus assay in radiation protection. A review. Int J Rad Appl Instr A, 38(4):241–249, 1987.
55. Thierens H, Vral A, de Ridder L: Biological dosimetry using the micronucleus assay for lymphocytes: interindividual differences in dose response. Health Phys, 61(5):623-630, 1991.
56. Sioen S, Cloet K, Vral A, Baeyens A: The cytokinesis-block micronucleus assay on human isolated fresh and cryopreserved peripheral blood mononuclear cells. J Pers Med, 10(3):125, 2020.
57. Lue SW, Repin M, Mahnke R, Brenner DJ: Development of a high-throughput and miniaturized cytokinesis-block micronucleus assay for use as a biological dosimetry population triage tool. Radiat Res, 184(2):134–142, 2015.

Chapter 5:

「The short and long-term effects in spleen histology and chromosome aberrations after low and high dose-rate gamma irradiation on neonatal B6C3F1 mice」

「低線量率および高線量率γ線照射新生児 B6C3F1 マウスにおける脾臓組織の再構築および染色体異常動態の短期的および長期的解析」

弘前大学大学院保健学研究科保健学専攻

提出者氏名：Valerie Goh Swee Ting

所　　属：　生体検査科学領域

指導教員：　三浦富智

List of Abbreviations (Chapter 5)

Ace: acentric fragment(s)

AML: acute myeloid leukemia

Dic: dicentric chromosome(s)

FBS: fetal bovine serum

H&E: hematoxylin and eosin

HDR-IR: high dose-rate ionizing radiation

L marker: large marker

LDR-IR: low dose-rate ionizing radiation

Q-banding: quinacrine banding

S marker: small marker

Introduction (Chapter 5)

The effects after high dose-rate ionizing radiation (HDR-IR) are well-studied and understood to be biologically damaging, as seen from acute radiation syndrome development[1)] and increased risks of secondary cancer development after primary tumor radiotherapy[2)]. In contrast, the effects after low dose-rate ionizing radiation (LDR-IR), which is a dose-rate equal to and less than 6 mSv/h as defined by the United Nations Scientific Committee on the Effects of Atomic Radiation[3)], are not as clear-cut. Studies have shown various beneficial effects of LDR-IR, such as radio-adaptive responses of LDR-IR conditioning to better respond to higher doses of radiation[4-6)], increased life span in mouse models of type II diabetes[7)] and accelerated ageing[8)], and decreased cancer incidence and mortality rates in individuals living in natural high background radiation areas than control areas[9-10)]. On the other hand, chronic LDR-IR also showed increased neoplasm development, increased chromosome aberration frequency and lifespan reduction in mice[11)], and possible increased risk of breast cancer[12)] and leukemia[13)] in occupationally exposed workers.

LDR-IR exposure can come from sources such as cosmic, terrestrial and occupational exposures, nuclear testing and radiation accidents. Furthermore, the uncertainty of LDR-IR biological effects has led to a conservative approach in radiation protection. The current model for radiation protection, the Linear No-Threshold hypothesis, is primarily extrapolated from the Life-Span Study of HDR-IR Japanese atomic bomb victims, and states that there is a linear increase of excess relative cancer risk even in low doses[14-15)]. However, there are also many studies that dispute the linear relationship of cancer risk and radiation dose, arguing that other models of hypersensitivity, threshold and even hormesis might better represent LDR-IR effects[16-17)]. In particular, animal experiments greatly contributed to the understanding of such effects after LDR-IR exposure in adult mice[11, 18-21)], trans-generational effects in the offspring after parental exposure[11, 22)] and fetal effects after *in utero* exposure in pregnant mice[23-24)]. On the contrary, there were much fewer studies analyzing the effects after LDR-IR exposure on neonatal mice[25)].

Furthermore, there is an increasing concern over the effects of LDR-IR in neonates and children as they have a higher risk of developing cancers due to their longer

lifespan after the initial radiation exposure than adults[26]. Little or no association[27] and positive association[28] have both been shown in studies analyzing the risk of childhood cancers and background ionizing radiation, although concerns were raised over the validity of results in the latter study. In another LDR-IR study comparing the heights of children who had lived in radio-contaminated apartments in Taiwan, a clear dose-related decrease in height was seen only in boys with a cumulative dose of more than 60 mSv, but not in girls. The authors speculated that as girls usually enter puberty earlier than boys, hormones produced during puberty could have compensated or reduced LDR-IR effects on physical height[29]. As such, biological changes during organ maturation and puberty in neonates and children could potentially affect radiation responses as compared to adults. In a HDR-IR study performed by Sasaki and Fukuda[30], mice irradiated from the neonatal to juvenile period also showed a more likely reduction of lifespan and an increased development of various solid tumors than those irradiated as adults.

In the event of radiation exposure, organs with high proliferative potential such as the spleen and bone marrow are highly radio-sensitive[14]. As a result, differences in immune system capability could potentially vary radiation responses between neonates and adults. Multiple studies have previously shown that the immune system differs between neonates and adults in both mice[31-32] and humans[33-35]. In our study, we comprehensively compared splenic responses during and after LDR-IR and HDR-IR exposure in neonates of both sexes at 7 days old. The mice were sacrificed at various time points at 14, 21, 28, 35, 42, 75, 100, 200, 300, 400 and 500 days old. For short-term effects, mice at 14 to 35 days old were compared. For long-term effects, mice at 14 to 500 days old were compared. Physical parameters of their body weight, absolute spleen mass and spleen index were monitored. Spleen morphology was analyzed with hematoxylin and eosin (H&E) staining. Chromosome aberrations of unstable dicentric chromosomes, excess fragments and stable translocation marker chromosomes were examined on Giemsa-stained splenocyte metaphases. Q-banding was also performed for additional chromosome karyotyping.

Materials & Methods (Chapter 5)

Mice and irradiation

Pregnant B6C3F1 mice were purchased from Oriental Yeast Co. Ltd. (Tokyo, Japan) and housed under specific pathogen conditions in the radiation facility in the National Institutes for Quantum and Radiological Science and Technology (QST), Chiba, Japan. Five to six 7 days old pups with the least amount of weight differences from each mother were used in the experiment.

A minimum of five mice of each sex were irradiated for each experimental condition. For the mice exposed to HDR-IR (dose rate: 30 Gy/h, source: ^{137}Cs, Gammacell 40, MDS Nordion, Ottawa, Canada), pups were irradiated to 4 Gy at 7 d, and continued to be housed with their mother before weaning at 28 d. For the mice exposed to LDR-IR (dose rate: 6 mGy/h, source: ^{137}Cs, Pony Industry Co. Ltd., Osaka, Japan), pups were housed with their mother in the same cage during the 4 weeks of irradiation, on a rack of height 0.48 m and 3.35 m away from the 1.11 TBq ^{137}Cs source. After weaning at 28 d, the mice continued to be exposed up to a total of 4 Gy. As a result, the LDR-IR mice at 14 d were irradiated to 1 Gy, mice at 21 d were irradiated to 2 Gy, and so forth. For the control mice, the pups were housed with their mother in the same cage until weaning. After weaning, the irradiated mice were housed together in cages of five and separated by sex. Mice were examined at 14, 21, 28, 35, 42, 75, 100, 200, 300, 400 and 500 d (Figure 1).

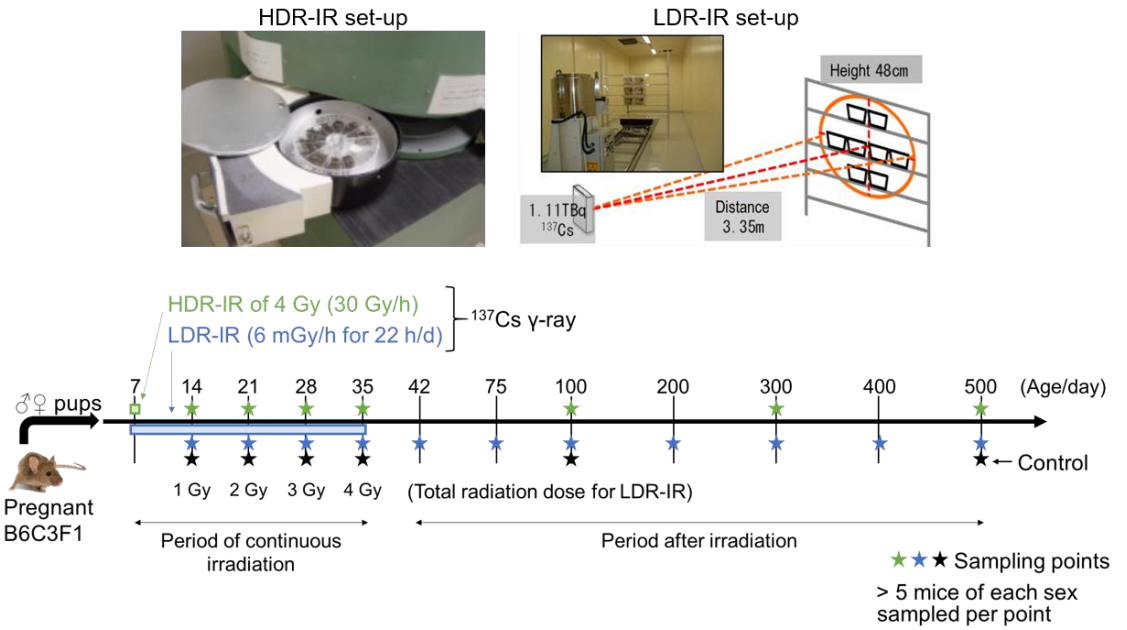

Figure 1: Experimental set-up for Control, LDR-IR and HDR-IR mice. Male and female pups at 7 days old were irradiated to a total dose of 4 Gy with LDR-IR (6 mGy/h for 22 h/d) or HDR-IR (30 Gy/h). Mice were sampled at different time points from 14 to 500 d.

Body weight, absolute spleen mass, spleen index

The body weight of each mice was measured immediately before sacrifice, while the absolute spleen mass was measured immediately after spleen collection. Spleen index was calculated with the equation below, which accounted for the increase in body weight with increasing age.

$$Spleen\ index\ = \frac{Spleen\ mass\ (g)}{Body\ weight\ (g)} \times\ 100\ \%$$

Spleen cell culture, cell harvest and chromosome aberration analysis

Spleen samples were shipped cold from QST to Hirosaki University, and arrived the next day after spleen collection for cell culture. The spleens were first washed in RPMI 1640 (Thermo Fisher Scientific, MA, USA) supplemented with 1 × kanamycin sulfate (Thermo Fisher Scientific) and 2 % heat-inactivated fetal bovine serum (FBS) (Sigma-Aldrich, MO, USA), then mashed through a 40 µm Falcon™ cell strainer (Corning Inc., NY, USA). After washing, spleen cells were cultured in 15 ml conical centrifuge tubes with RPMI 1640, kanamycin, 20 % heat-inactivated FBS and three mitogens, phytohemagglutinin HA-15 (Remel Europe, Dartford, UK; final conc: 248.4 µg/ml), lipopolysaccharide (Sigma-Aldrich; final conc: 10 µg/ml) and concavalin A (Sigma-Aldrich; final conc: 3 µg/ml), in a 5 % CO_2 incubator at 37 °C. Colcemid (Thermo Fisher Scientific; final conc:

0.2 g/ml) was added 24 h after the start of culture for metaphase arrest. Spleen cells were harvested after a total of 46 h in culture.

Spleen cells were hypotonically treated with 75 mM KCl for 20 min at 37 °C, then fixed in three rounds of cold fresh fixative (3:1 methanol: acetic acid). Automated chromosome spreading was performed in a humidified chamber using HANABI-PIV (ADSTEC Co., Tokyo, Japan). Chromosomes were stained with 5 % Giemsa (Merck Millipore, MA, USA) diluted in pH 6.2 Gurr's buffer (Thermo Fisher Scientific), then mounted in malinol (Muto Pure Chemicals, Tokyo, Japan). Images of metaphase spreads were captured with 63 × oil AutoCapt mode, using AXIOImager Z.2 microscopes (Carl Zeiss AG, Oberkochen, Germany) equipped with CCD cameras and Metafer 4 (MetaSystems GmbH, Altlussheim, Germany).

Wherever possible, more than 200 metaphases with 39 or 40 well-defined chromosomes were analyzed per mouse for dicentric chromosomes (chromosomes with 2 centromeres), excess acentrics (fragments formed by deletions or other origins) and translocation marker chromosomes (chromosomes which are much larger [L marker] or smaller than normal [S marker]) (Figure 2). For mice which showed very low mitotic index (MI) (i.e. Control 21 d; LDR-IR 400 d, 500 d; HDR-IR 14 d, 21 d, 35 d, 300 d, 500 d), all of the cells were analyzed, with the number of metaphases analyzed ranging from 34 to 189. Moreover, due to the extreme cold weather from January to March 2018 in Hirosaki, some of spleens received were partially frozen, and hence were excluded from analysis.

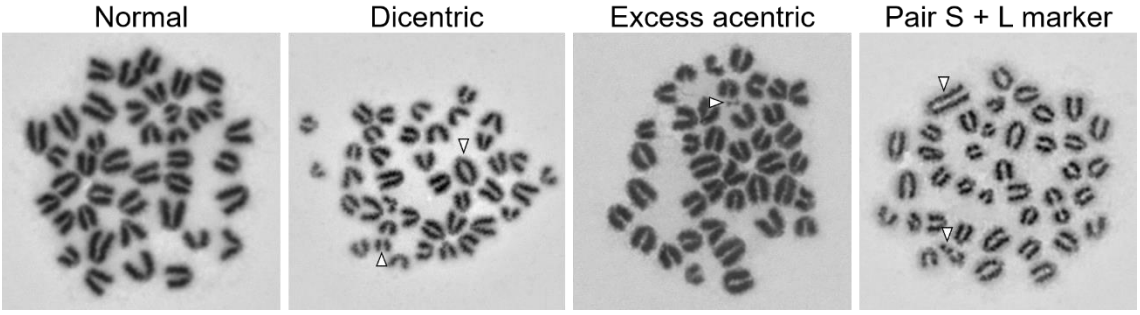

Figure 2: Chromosome aberrations (white arrows) analyzed in primary murine splenocyte metaphases. A normal metaphase contains 40 acrocentric chromosomes. In a metaphase with Dic, a chromosome with 2 centromeres (Dic) and an accompanying acentric fragment (Ace) is present. In a metaphase with excess Ace, an excess Ace is present. In a metaphase with marker chromosomes, chromosomes which are much larger than normal (L marker) and chromosomes which are much smaller than normal (S marker) are present. In the image, a pair of S + L markers is present.

MI, an indicator of the percentage of cells in mitosis, was calculated with Equation 2[36]. For mice with high enough MI, MI was between 2.26 to 18.82 %.

$$MI = \frac{\#\ Metaphases}{\#\ Metaphases\ and\ Blast\ cells} \times 100\ \%$$

Spleen histology

Tissues were fixed in 10 % formalin overnight before transferring to 70 % ethanol for long-term storage. 5 μm thick paraffin-embedded sections were then stained with H&E. Whole slide images were captured with Nanozoomer S360 (Hamamatsu Photonics K. K., Hamamatsu, Japan), and images were shared using NDP.view2 (Hamamatsu Photonics).

Karyotyping with Q-banding

Quinacrine banding (Q-banding) was performed on air-dried metaphase spreads. Slides were first washed in McIlvaine buffer (2.54 g Na_2HPO_4 and 0.437 g citric acid dissolved in 100 ml distilled water), then stained in Hoescht 33258 (final conc: 0.5 μg/ml in McIlvaine buffer) at 37 °C for 10 min. After rinsing the slides in water, slides were stained with Quinacrine staining solution (dissolve quinacrine mustard [Sigma-Aldrich] in McIlvaine buffer to a final concentration of 100 μg/ml) for 10 min. Slides were washed with two rounds of McIlvaine buffer. Finally, air-dried slides were mounted with 1:1 VECTASHIELD HardSet™ Antifade Mounting Medium with and without DAPI (Vector Laboratories, Inc., Burlingame, CA). Q-bands were imaged with AXIOImager Z.2 and Metafer 4 at 1000 ×, and processed with Ikaros Karyotyping System (Ver 5.4, MetaSystems GmbH).

Statistical tests

Data representation and statistical analysis were carried out with R 4.0.3[37], RStudio 1.3.1093[38] and an additional package of "tidyverse"[39]. Data was represented as Mean ± SD where appropriate. No outliers were removed from the data set.

Results (Chapter 5)

Changes in body weight from 14 to 500 d

In Figure 3, the body weight of Control, LDR-IR and HDR-IR mice from 14 to 500 d was measured. The mice showed a general increase in body weight in all three irradiation conditions. HDR-IR mice showed the lowest body weight from 21 to 35 d, and a plateau in body weight from 300 to 500 d, in comparison to LDR-IR and Control mice.

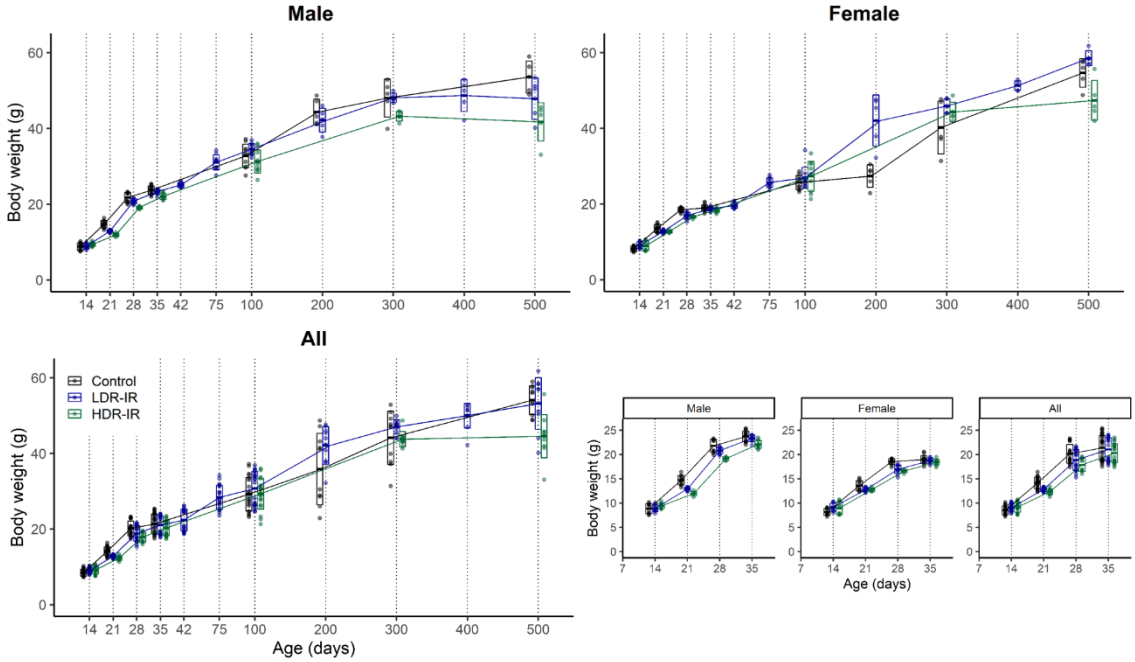

Figure 3: Body weight of control, LDR-IR and HDR-IR mice from 14 to 500 d. A general increase was seen in all three irradiation conditions. From 21 to 35 d, HDR-IR mice showed the lowest body weight than LDR-IR and Control mice. From 300 to 500 d, HDR-IR mice showed a plateau in body weight while some increase was seen in LDR-IR and LDR-IR mice.

Changes in absolute spleen mass from 14 to 500 d

In Figure 4, the kinetics of spleen mass was significantly different in the three irradiation conditions during the early phase (14 to 35 d), where a large spleen mass increase was seen only in HDR-IR 14 d mice. A plateau in HDR-IR spleen mass was seen from 14 to 28 d, before a decrease was seen at 35 and 100 d. In contrast, the trend in spleen mass was similar between Control and LDR-IR mice, where an increase in spleen mass was seen from 14 to 28 d, before decreasing at 35 d and plateauing until 300 d. Despite the same trend seen, spleen mass of LDR-IR mice was lower than Control mice in the early phase. At 500 d, a large variance in spleen mass was seen in all three irradiation conditions, especially in LDR-IR and HDR-IR mice.

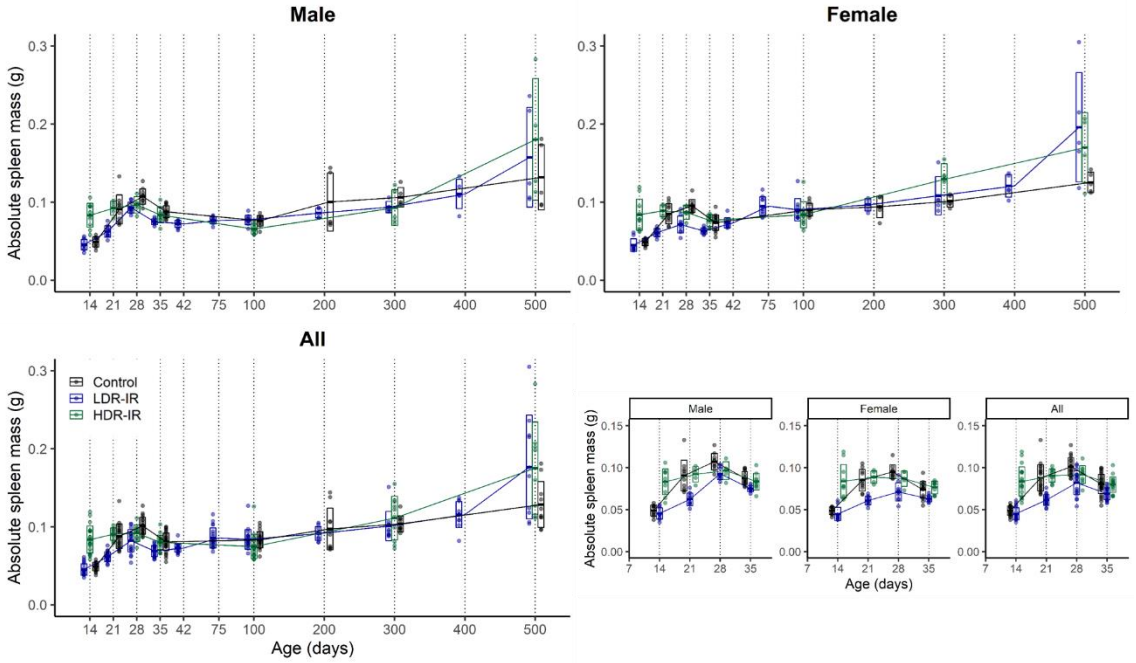

Figure 4: Absolute spleen mass of control, LDR-IR and HDR-IR mice from 14 to 500 d. Spleen mass of one HDR-IR male mouse with suspected AML and one HDR-IR female mouse with spleen mass of 0.546 g were omitted. Changes in spleen mass were significantly different between the three irradiation conditions in the early phase (14 to 35 d), especially in HDR-IR mice. In addition, a large variance in spleen mass was seen at 500 d, particularly in LDR-IR and HDR-IR mice.

Changes in spleen index from 14 to 500 d

In Figure 5, similar to the changes in absolute spleen mass, spleen index kinetics were significantly different in the early phase from 14 to 35 d. Spleen enlargement was only seen 7 days after 4 Gy HDR-IR (HDR-IR 14 d). However, with increasing time, spleen index of HDR-IR mice decreased to similar levels with LDR-IR and Control mice. On the other hand, spleen index of LDR-IR mice showed a trend largely similar to Control mice, but consistently showed a lower spleen index than Control mice. A slight peak in spleen index was seen at 21 d in Control mice, but this was absent in LDR-IR mice.

In contrast, HDR-IR, LDR-IR and Control mice at 100 to 300 d showed a similar spleen index. At 500 d, a wide variance in spleen index was seen in LDR-IR and HDR-IR mice, but was absent in Control mice. No clear differences between males and females were seen.

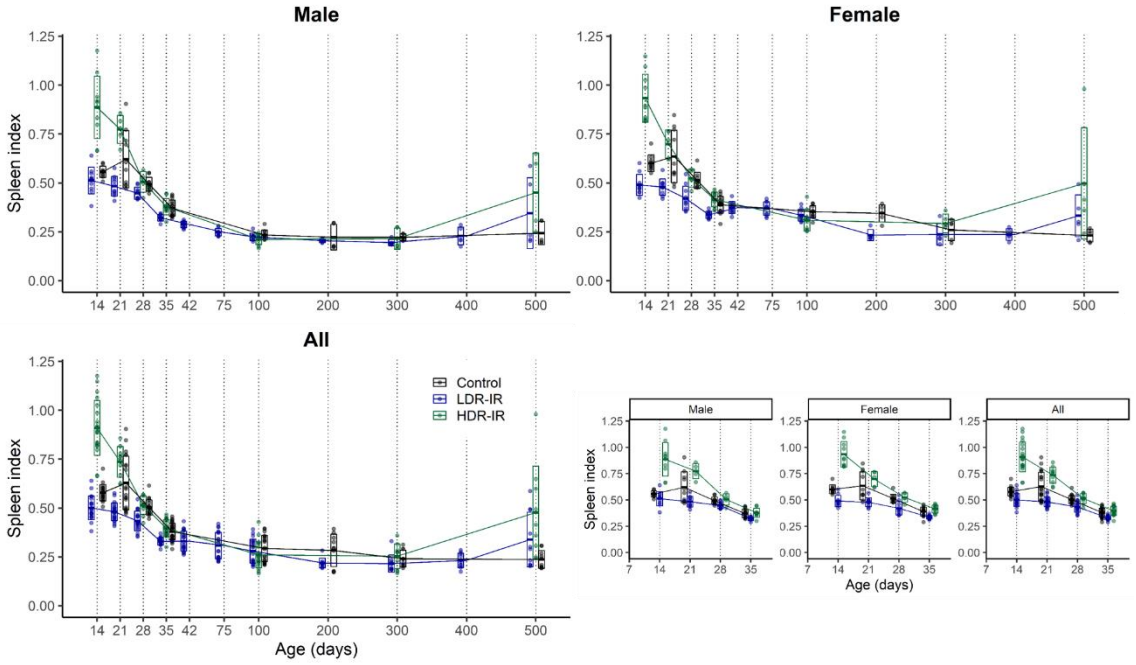

Figure 5: Spleen index of control, LDR-IR and HDR-IR mice from 14 to 500 d. Spleen index of one HDR-IR male mouse with suspected AML was omitted. Changes in spleen index were the most different from 14 to 35 d in the three irradiation conditions, especially in HDR-IR mice. Moreover, a large variance in spleen index was seen at 500 d, particularly in LDR-IR and HDR-IR mice.

Spleen histology from 14 to 35 d

As significant differences in absolute spleen mass and spleen index were seen in the early phase (14 to 35 d), spleen histology with H&E was performed to elucidate differences in spleen morphology in the three irradiation conditions. In Figure 6, low magnification images of spleen H&E sections were compared. 7 days after 4 Gy HDR-IR, HDR-IR 14 d mice showed the greatest loss of white pulp, but was able to recover at 21 d. No visible differences in white pulp staining intensity were seen for LDR-IR and Control mice from 14 to 35 d. Similar spleen morphology was seen for both male and female mice.

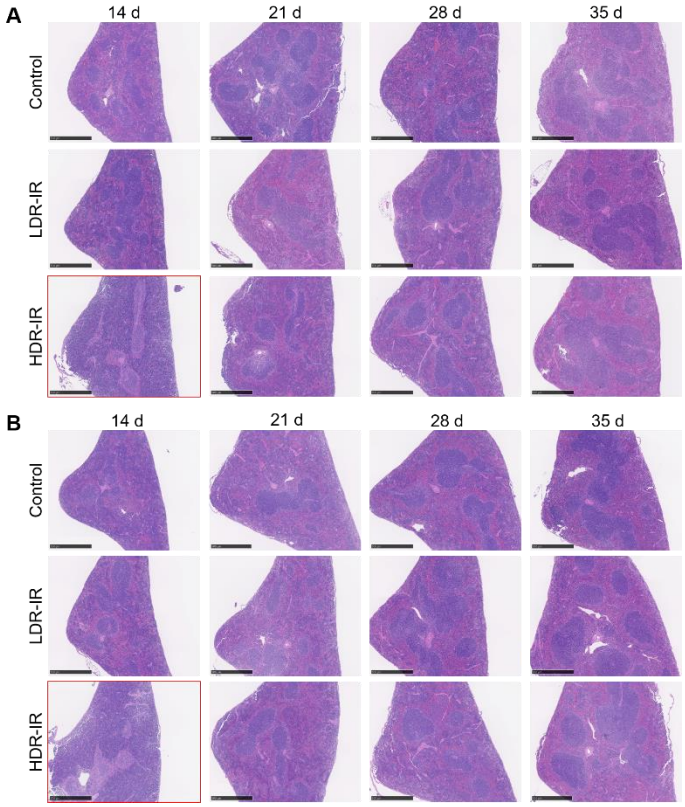

Figure 6: Low magnification spleen H&E sections of Control, LDR-IR and HDR-IR mice from 14 to 35 d. (A) Male mice. (B) Female mice. HDR-IR 14 d male and female mice both showed the greatest white pulp loss (red box), and a recovery to normal spleen morphology was seen at 21 d. (Scale bars: 500 µm).

At higher magnifications in Figure 7, severe lymphocyte loss was seen in the white pulp for both male and female HDR-IR 14 d, and recovery was seen at 21 d. The red pulp of HDR-IR 14 d mice was infiltrated with lymphocytes and showed a huge reduction of erythrocytes. This abnormality was also recovered at 21 d.

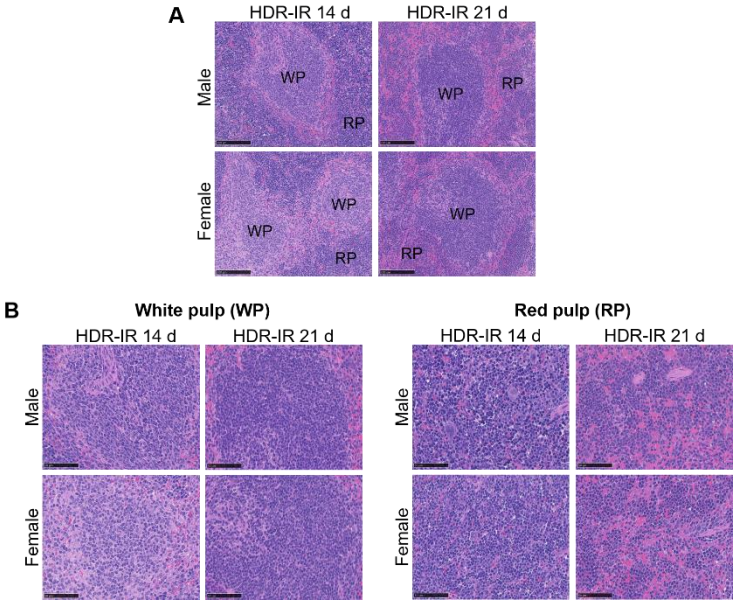

Figure 7: Spleen histology of HDR-IR mice at 14 and 21 d, at (A) 200 × and (B) 400 × magnification. Severe white pulp loss and lymphocyte infiltration in the red pulp were seen in both male and female mice. Normal spleen morphology was recovered at 21 d. (Scale bars: 100 and 50 μm).

Dic kinetics from 14 to 500 d

In Figure 8, Dic frequency in LDR-IR mice showed a peak at 28 to 35 d, before decreasing to baseline frequency at 200 d. In contrast, HDR-IR mice showed some increase in 14, 21 d and 35 d, before decreasing to baseline frequency. A large variability in Dic kinetics was seen in HDR-IR 21 d F mice, but it was most likely due to a lower number of metaphases analyzed. Control mice showed baseline Dic frequency in almost all time points. Dic kinetics were clearly different between LDR-IR and HDR-IR mice.

Based on the peak Dic frequency seen at 35 d in all LDR-IR mice, the Dic half-lives calculated from 35 d to 200 d and 35 d to 500 d were 42.5 and 109.4 days respectively.

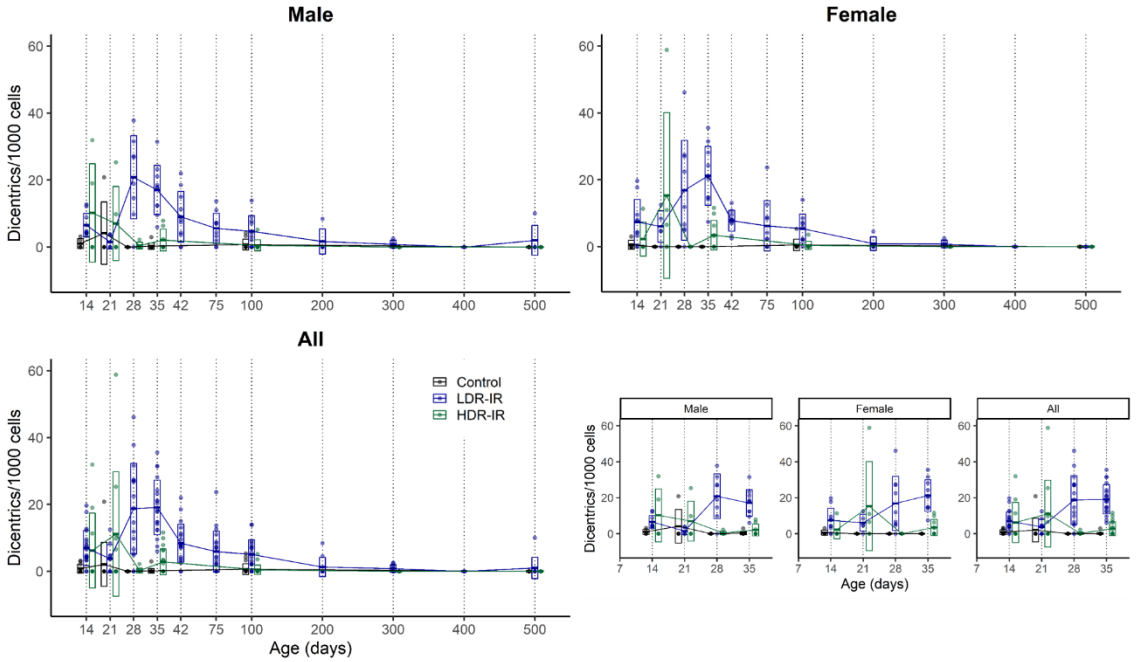

Figure 8: Dic frequency of Control, LDR-IR and HDR-IR mice from 14 to 500 d. Dic kinetics differed greatly between LDR-IR and HDR-IR mice.

Excess Ace kinetics from 14 to 500 d

In Figure 9, excess Ace frequency in LDR-IR mice increased to a peak at 35 d, then decreased to baseline frequency at 200 d. In contrast, HDR-IR mice showed an increase to a peak at 28 d, then sharply decreased to near baseline frequency ar 35 and 42 d. Control mice only showed some variability in excess Ace frequency at 21 d. Excess Ace kinetics were clearly different between LDR-IR and HDR-IR mice. Some correlation between Dic and Excess Ace frequency in LDR-IR mice was also seen.

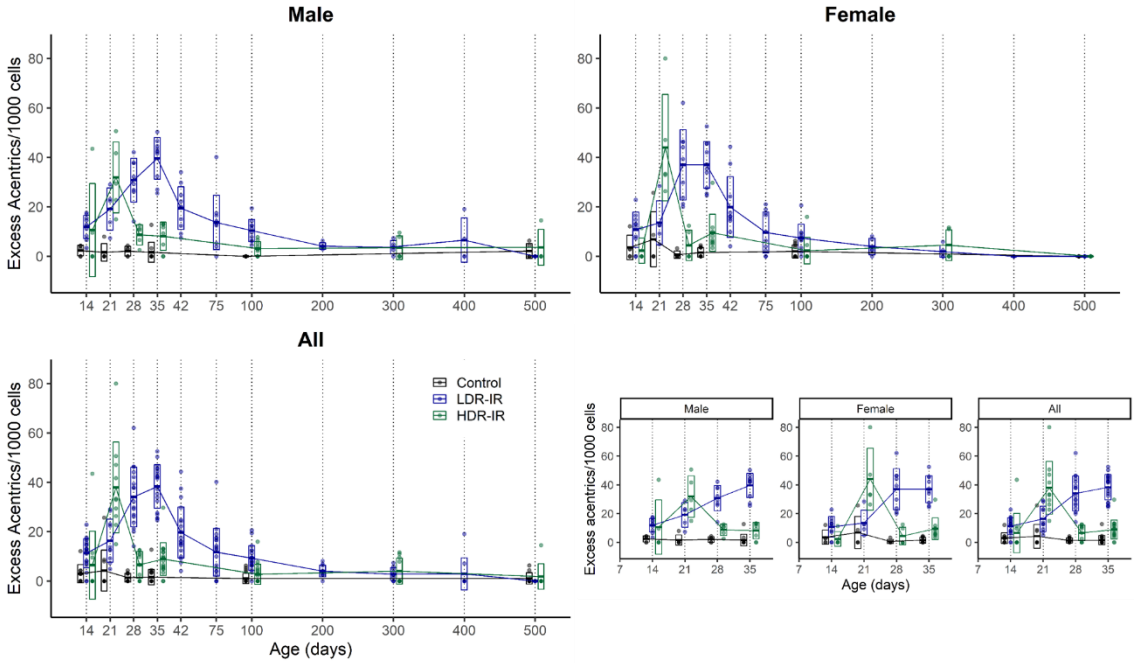

Figure 9: Excess Ace frequency of Control, LDR-IR and HDR-IR mice from 14 to 500 d. Excess Ace kinetics differed greatly between LDR-IR and HDR-IR mice.

Marker chromosome kinetics from 14 to 500 d

In Figure 10, both total and pair S+L marker chromosome frequency were higher in HDR-IR than LDR-IR mice from 14 to 500 d. Pair S+L marker chromosomes were also more specific to HDR-IR mice due to the almost baseline frequency seen in both LDR-IR and Control mice.

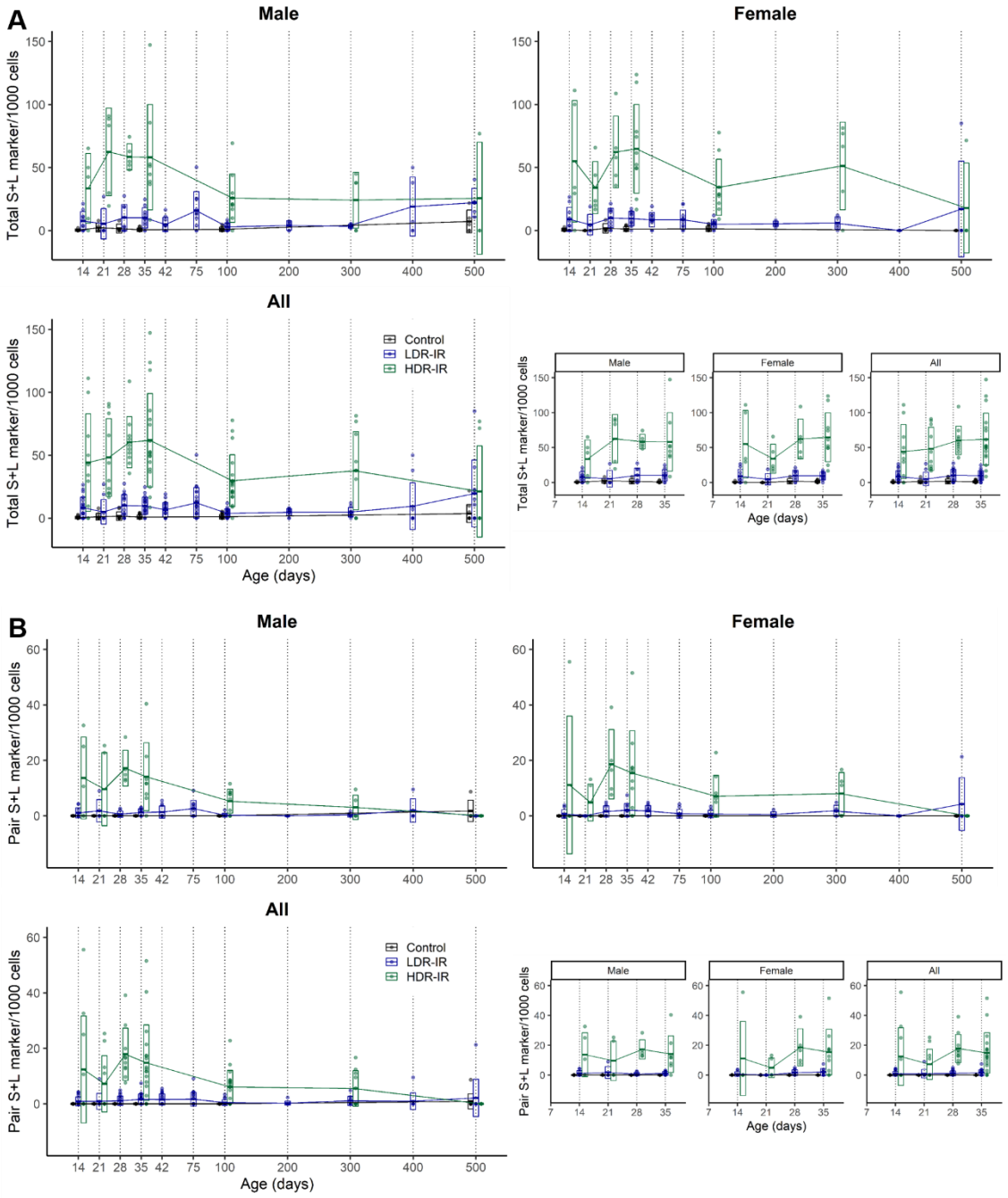

Figure 10: (A) Total marker and (B) pair marker chromosome frequency of Control, LDR-IR and HDR-IR mice from 14 to 500 d. HDR-IR mice showed a consistently higher frequency of marker chromosomes than LDR-IR mice.

Suspected AML in one male HDR-IR 500 d mouse

In one of the male HDR-IR 500 d mouse, splenomegaly was observed. Q-banding karyotypes showed consistent chromosome 2 deletion in cells cultured without PHA stimulation, which is an established marker of AML[40]. Other abnormalities such as chromosome 7 trisomy, chromosome 15 trisomy and chromosome 17 tri/tetrasomy were also similarly seen in the three metaphases, which was highly indicative of tumor cells proliferating clonally (Figure 11).

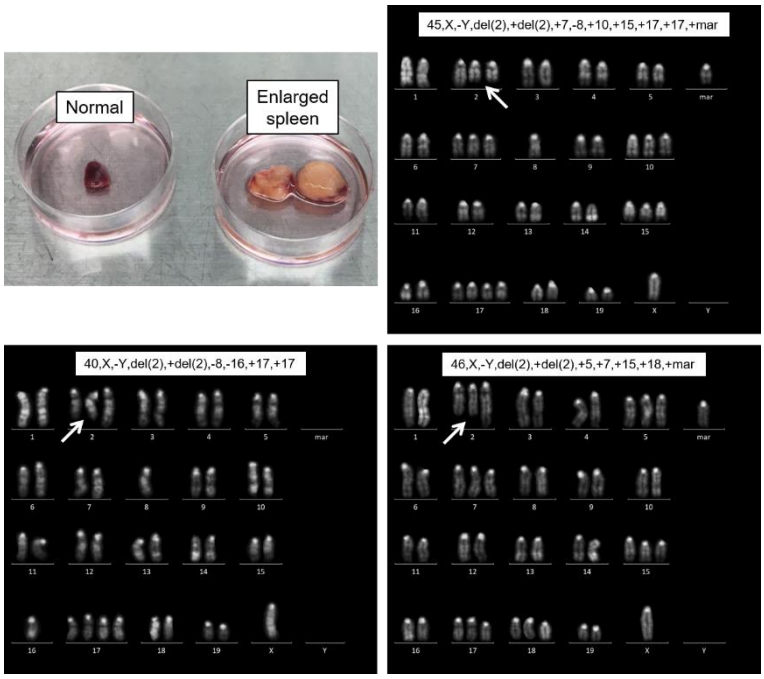

Figure 11: Image of the enlarged spleen from one male HDR-IR 500 d mouse, and Q-banding karyotypes from three metaphases cultured without PHA stimulation. Chromosome 2 deletion (white arrow), a biomarker of AML, was seen.

Discussion (Chapter 5)

It is widely accepted that HDR-IR is biologically harmful while LDR-IR have shown both bio-positive and harmful effects in multiple studies. To better understand LDR-IR effects, various mouse studies have analyzed the long-term effects after LDR-IR in adults[11, 18-21], possible developmental issues in offspring after *in utero* LDR-IR in pregnant mice[23-24] and trans-generational effects after LDR-IR in F_0 generation[11, 22], in contrast to the very limited studies in neonatal mice[25]. In this study, neonatal B6C3F1 mice were irradiated with HDR-IR (30 Gy/h) or LDR-IR (6 mGy/h for 22 h/d) at 7 d and monitored for up to 500 d. This allowed for a comparison of radiation responses in the radio-sensitive spleen during immune system development and maturation in the early phase of continuous LDR-IR (14 to 35 d), and to monitor long-term changes in the late phase. A

comprehensive analysis of physical parameters (body weight, absolute spleen mass, spleen index), histology and chromosome aberration analysis (Dic, excess Ace, marker chromosomes) was performed.

In the Control B6C3F1 mice from 14 to 500 d, a slight peak in spleen index was seen at 21 d, before slowly decreasing for up to 500 d. The slight peak could signify some rapid cell increase only at 21 d, although general H&E spleen histology did not show any significant differences between HDR-IR, LDR-IR and Control mice. Similarly in Forni's study of C57BL/6 mice [41], the increase in the ratio of total spleen cells at 21 d to 7 d was the highest. Likewise, 3 Gy X-ray HDR-IR at 21 d than 7 d in neonatal C57BL/6 mice also showed spleens were more sensitive to radiation damage, as a higher leukemic incidence was seen in 21 d mice[42]. In contrast for adult mice, as seen from our results and Iwata *et al.*'s study[43], spleen index of Control B6C3F1 mice were consistent as adults from 14 to 71 weeks, while slight increases in spleen index were seen as the mice grew older for up to 109 weeks.

Moreover, our HDR-IR mice showed a sharp increase in spleen index due to splenomegaly 7 days after 4 Gy HDR-IR, then a decrease in spleen index to similar levels as control at 100 d. However, a different spleen index kinetics was seen in adult HDR-IR mice, as multiple studies showed an immediate decrease in spleen index, an increase back to baseline after several days, another increase higher than control at 17 days before returning back to baseline again[44-46]. As for LDR-IR neonates, our results showed similar spleen index kinetics as Control mice, although their spleen index was consistently lower than Control mice during continuous irradiation up to 35 d.

In terms of spleen histology, HDR-IR neonatal mice at 14 d showed a significant loss of cells in the white pulp, while many lymphocytes were instead seen in the red pulp. At 21 d, HDR-IR spleens recovered back to a similar morphology as the Control mice. Conversely, after 4 Gy HDR-IR in adult mice, a severe depletion of cells was seen in both red and white pulps 2 days after HDR-IR. Instead of a high lymphocyte population evenly distributed in the red pulp, the red pulp of adult mice showed areas of darkly stained blast cells and differentiated cells at 18 days after HDR-IR[45]. From these studies, the neonatal spleen was probably the most sensitive at 21 d, and the period of radiation exposure as

neonates or as adults most likely influenced the different splenic radiation responses seen after LDR-IR or HDR-IR.

As for chromosome aberration kinetics after radiation exposure in neonates, our results showed that dose-rate played a more significant role in the type of chromosome aberrations accumulated rather than total dose. Unstable aberrations of Dic and excess Ace showed a higher frequency in LDR-IR than HDR-IR mice, especially in the earlier periods up to 200 d. As for stable aberrations of marker chromosomes, a higher frequency was seen in HDR-IR than LDR-IR mice, and marker chromosomes persisted for up to 300 d. Likewise, in Nakano *et al.*'s study[47], 2.5 – 11.5 translocations/1000 cells were detected with fluorescence *in situ* hybridization in 2 Gy HDR-IR B6C3F1 neonates at 20 weeks of age (140 d). However, when chromosome aberrations were analyzed 24 and 48 h after HDR-IR without *in vitro* cell culture, unstable aberrations such as chromosome breaks and Dic decreased to almost 0 at 48 h, while translocations still persisted in low frequencies. Both our and Nakano *et al.*'s results showed some persistence of stable aberrations, while unstable aberrations rapidly decreased after HDR-IR in neonatal mice.

Furthermore, differences in chromosome aberrations were also seen between our HDR-IR neonates and other studies of HDR-IR adult mice. In our study, Dic and excess Ace frequency in HDR-IR neonates showed the highest increase at 21 d, before decreasing rapidly at 28 d. This trend in Dic kinetics was not seen in studies of 3 Gy HDR-IR adult mouse splenocytes, as only a decline of Dic frequency with increasing time was seen, with a return to baseline frequency at 56 to 224 d[48-49]. A similar trend of Ace kinetics with Dic kinetics was also seen[49]. As for stable chromosome aberrations, our results showed marker chromosomes persisting in HDR-IR neonates, although a large variance was seen at each time point. In Nakano *et al.*'s study, translocations in neonates decreased with increasing time after HDR-IR, but the decline was not observed in HDR-IR adults when they were at 20 weeks (140 d) of age[47]. However, with increasing time after the initial exposure, a 30 to 40 % decrease of total translocations was seen at 224 days after 3 Gy HDR-IR in Hande and Natarajan's study[49]. By comparing HDR-IR exposure in neonates to adults, unstable chromosome aberrations clearly showed different kinetics as postnatal splenocyte increase at 21 d possibly increased Dic frequency at 21 d in our HDR-IR neonates, and such an increase was not seen in HDR-IR adult mice. In

contrast, stable chromosome aberration kinetics were similar in HDR-IR neonates and adult mice, as a decrease in stable aberrations was seen with increasing time after the initial exposure.

Some similarities and differences in chromosome aberration kinetics were also seen in neonates exposed to LDR-IR in our study and adult mice exposed to LDR-IR in other studies. In Tanaka *et al.*'s study of LDR-IR adult C3H/HeN mice, during the period of continuous irradiation up to 4 Gy for 200 mGy/d (0.9 mGy/h) and 400 mGy/d (1.8 mGy/h), a consistent increase in Dic frequency was seen in splenocytes for 19 and 9 days after LDR-IR respectively[50]. An increase in Dic and excess Ace frequencies were also seen in our LDR-IR neonatal mice from 14 to 35 d continuously irradiated at 6 mGy/h. Moreover, even in the period of continuous irradiation of very low LDR-IR of 20 mGy/d (0.091 mGy/h), an increase in translocation frequency was also seen in adult mice[51]. In contrast, our LDR-IR neonates showed similar low marker chromosome frequency from 14 to 35 d. (Dic half-life for HDR-IR neonates/adults versus LDR-IR neonates). Once again, unstable and stable chromosome aberration kinetics could also be affected depending on the age of exposure during LDR-IR.

Furthermore, suspected AML was only present in one male HDR-IR 500 d, based on chromosome 2 deletion in Q-banding karyotypes. In Braga-Tanaka *et al.*'s study, a very low incidence of myeloid leukemia was developed only in LDR-IR males irradiated as adults at 20 mGy/d[11]. In Sasaki and Fukuda's study, HDR-IR neonatal B6C3F1 mice (0.87 Gy/min) did not develop excess myeloid leukemia[30].

In conclusion, our results showed differences in spleen index and histology between HDR-IR and LDR-IR neonatal mice, especially in the early phase. Dose-rate also played a more significant role in the type of chromosome aberrations accumulated after irradiation in neonates, as HDR-IR mice showed a higher frequency of stable chromosome aberrations while LDR-IR mice showed a higher frequency of unstable chromosome aberrations. Furthermore, as compared to other HDR-IR and LDR-IR studies in adult mice, differences in spleen index and chromosome aberration kinetics were also seen. This study thus highlights the importance of evaluating radiation responses separately for adults and newborns/children, as radiation exposure during postnatal immune system development could affect cell damage and recovery.

References (Chapter 5)

1. Macià I Garau M, Lucas Calduch A, López EC: Radiobiology of the acute radiation syndrome. Rep Pract Oncol Radiother, 16(4):123–130, 2011.
2. Kamran SC, Berrington de Gonzalez A, Ng A, Haas-Kogan D, Viswanathan AN: Therapeutic radiation and the potential risk of second malignancies. Cancer. 122(12):1809–1821, 2016.
3. United Nations Scientific Committee on the Effects of Atomic Radiation: Biological mechanisms of radiation actions at low doses. A white paper to guide the Scientific Committee's future programme of work. Report V.12-57831. NY, USA, 2012.
4. Wang B, Ohyama H, Shang Y, Tanaka K, Aizawa S, Yukawa O, Hayata I: Adaptive response in embryogenesis: V. Existence of two efficient dose-rate ranges for 0.3 Gy of priming irradiation to adapt mouse fetuses. Radiat Res, 161(3):264–272, 2004.
5. Ina Y, Tanooka H, Yamada T, Sakai K: Suppression of thymic lymphoma induction by life-long low-dose-rate irradiation accompanied by immune activation in C57BL/6 mice. Radiat Res, 163:153–158, 2005.
6. Sakai K, Nomura T, Ina Y: Enhancement of bio-protective functions by low dose/dose-rate radiation. Dose Response, 4:327–332, 2016.
7. Nomura T, Li XH, Ogata H, Sakai K, Kondo T, Takano Y, Magae J: Suppressive effects of continuous low-dose-rate γ irradiation on diabetic nephropathy in type II diabetes mellitus model mice. Radiat Res, 176:356–365, 2011.
8. Nomura T, Sakai K, Ogata H, Magae J: Prolongation of life span in the accelerated aging Klotho mouse model, by low-dose-rate continuous γ irradiation. Radiat Res. 179:717–724, 2013.
9. Nambi KSV, Soman SD: Environmental radiation and cancer in India. Health Phys, 52(5):653–657, 1987.
10. Wei LX, Zha YR, Tao ZF: Epidemiological investigation of radiological effects in high background radiation areas of Yangjiang, China. Radiat Res, 31(1):119–136, 1990.
11. Braga-Tanaka I 3rd, Tanaka S, Kohda A, Takai D, Nakamura S, Ono T, Tanaka K, Komura JI: Experimental studies on the biological effects of chronic low dose-rate radiation exposure in mice: overview of the studies at the Institute for Environmental Sciences. Int J Radiat Biol, 94(5):423–433, 2018.

12. Preston DL, Kitahara CM, Freedman DM, Sigurdson AJ, Simon SL, Little MP, Cahoon EK, Rajaraman P, Miller JS, Alexander BH, Doody MM, Linet MS: Breast cancer risk and protracted low-to-moderate dose occupational radiation exposure in the US Radiologic Technologists Cohort, 1983-2008. Br J Cancer, 115(9):1105–1112, 2016.
13. Gillies M, Haylock R, Hunter N, Zhang W: Risk of leukemia associated with protracted low-dose radiation exposure: Updated results from the National Registry for Radiation Workers Study. Radiat Res, 192(5):527–537, 2019.
14. International Commission on Radiological Protection: The 2007 Recommendations of the International Commission on Radiological Protection. ICRP publication 103. Ann ICRP, 37(2-4):1–332, 2007.
15. Vaiserman A, Koliada A, Zabuga O, Socol Y: Health impacts of low-dose ionizing radiation: Current scientific debates and regulatory issues. Dose Response, 16(3):1559325818796331, 2018.
16. Cardarelli JJ 2nd, Ulsh BA: It is time to move beyond the Linear No-Threshold theory for low-dose radiation protection. Dose Response, 16(3):1559325818779651, 2018.
17. Tharmalingam S, Sreetharan S, Brooks AL, Boreham DR: Re-evaluation of the linear no-threshold (LNT) model using new paradigms and modern molecular studies. Chem Biol Interact, 301:54–67, 2019.
18. Okudaira N, Uehara Y, Fujikawa K, Kagawa N, Ootsuyama A, Norimura T, Saeki K, Nohmi T, Masumura K, Matsumoto T, et al.: Radiation dose-rate effect on mutation induction in spleen and liver of gpt delta mice. Radiat Res, 173(2):138–147, 2010.
19. Graupner A, Eide DM, Brede DA, Ellender M, Lindbo Hansen E, Oughton DH, Bouffler SD, Brunborg G, Olsen AK: Genotoxic effects of high dose rate X-ray and low dose rate gamma radiation in ApcMin/+ mice. Environ Mol Mutagen, 58(8):560–569, 2017.
20. Seawright JW, Samman Y, Sridharan V, Mao XW, Cao M, Singh P, Melnyk S, Koturbash I, Nelson GA, Hauer-Jensen M, Boerma M: Effects of low-dose rate γ-irradiation combined with simulated microgravity on markers of oxidative stress, DNA methylation potential, and remodeling in the mouse heart. PLoS One, 12(7):e0180594, 2017.

21. Yamauchi K, Ono T, Ayabe Y, Hisamatsu S, Yoneya M, Tsutsumi Y, Komura JI: Life-shortening effect of chronic low-dose-rate irradiation in calorie-restricted mice. Radiat Res, 192(4):451–455, 2019.
22. Mughal SK, Myazin AE, Zhavoronkov LP, Rubanovich AV, Dubrova YE: The dose and dose-rate effects of paternal irradiation on transgenerational instability in mice: a radiotherapy connection. PLoS One, 7(7):e41300, 2012.
23. Abramsson-Zetterberg L, Zetterberg G, Sundell-Bergman S, Grawé J: Absence of genomic instability in mice following prenatal low dose-rate gamma-irradiation. Int J Radiat Biol, 76(7):971–977, 2000.
24. Kato F, Ootsuyama A, Nomoto S, Kondo S, Norimura T: Threshold effect for teratogenic risk of radiation depends on dose-rate and p53-dependent apoptosis. Int J Radiat Biol, 77(1):13–19, 2001.
25. Spalding JF, Thomas RG, Tietjen GL: Life span of C57 mice as influenced by radiation dose, dose rate, and age at exposure. LA--9528. Los Alamos National Laboratory, New Mexico, USA, 1982.
26. United Nations Scientific Committee on the Effects of Atomic Radiation: UNSCEAR 2013 Report to the General Assembly, with scientific annexes. Volume II: Scientific Annex B. Effects of radiation exposure of children. NY, USA, 2013.
27. Evrard AS, Hémon D, Billon S, Laurier D, Jougla E, Tirmarche M, Clavel J: Childhood leukemia incidence and exposure to indoor radon, terrestrial and cosmic gamma radiation. Health Phys, 90(6):569–579, 2006.
28. Spycher BD, Lupatsch JE, Zwahlen M, Röösli M, Niggli F, Grotzer MA, Rischewski J, Egger M, Kuehni CE; Swiss Pediatric Oncology Group; Swiss National Cohort Study Group: Background ionizing radiation and the risk of childhood cancer: a census-based nationwide cohort study. Environ Health Perspect, 123(6):622–628, 2015.
29. Wang J-C, Lin Y-P, Hwang J-S, Hsieh W-H A, Tsai Y-J M, Chang WP: Physical heights of children with prolonged low dose-rate γ-radiation exposure in radiocontaminated buildings. Int J Radiat Biol, 77(1):117–125, 2001.
30. Sasaki S, Fukuda N: Dose-response relationship for induction of solid tumors in female B6C3F1 mice irradiated neonatally with a single dose of gamma rays. J Radiat Res, 40(3):229–241, 1999.

31. Astori M, Finke D, Karapetian O, Acha-Orbea H: Development of T–B cell collaboration in neonatal mice. Int Immunol, 11(3):445–451, 1999.
32. Higuchi Y, Zeng H, Ogawa M: CD38 expression by hematopoietic stem cells of newborn and juvenile mice. Leukemia, 17(1):171–174, 2003.
33. Rufer N, Brümmendorf TH, Kolvraa S, Bischoff C, Christensen K, Wadsworth L, Schulzer M, Lansdorp PM: Telomere fluorescence measurements in granulocytes and T lymphocyte subsets point to a high turnover of hematopoietic stem cells and memory T cells in early childhood. J Exp Med, 190(2):157–167, 1999.
34. Simon AK, Hollander GA, McMichael A: Evolution of the immune system in humans from infancy to old age. Proc Biol Sci, 282(1821):20143085, 2015.
35. Georgountzou A, Papadopoulos NG: Postnatal innate immune development: from birth to adulthood. Front Immunol, 8:957, 2017.
36. International Atomic Energy Agency: Cytogenetic dosimetry: applications in preparedness for and response to radiation emergencies. EPR-Biodosimetry. IAEA, Vienna, Austria, 2011.
37. R Core Team: R: a language and environment for statistical computing. R Foundation for Statistical Computing, Vienna, Austria, 2020.
38. RStudio Team: RStudio: integrated development for R. RStudio, Inc., Boston, MA, USA, 2020.
39. Wickham H, Averick M, Bryan J, Chang W, McGowan L, François R, Grolemund G, Hayes A, Henry L, Hester J, et al. Welcome to the Tidyverse. JOSS, 4(43):1686, 2019.
40. Trakhtenbrot L, Krauthgamer R, Resnitzky P, Haran-Ghera N: Deletion of chromosome 2 is an early event in the development of radiation-induced myeloid leukemia in SJL/J mice. Leukemia, 2(8):545–550, 1988.
41. Forni L: Strain differences in the postnatal development of the mouse splenic lymphoid system. Annales de l'Institut Pasteur / Immunologie, 139(3):257–266, 1988.
42. Maisin JR, Gerber GB, Vankerkom J, Wambersie A: Survival and diseases in C57BL mice exposed to X rays or 3.1 MeV neutrons at an age of 7 or 21 days. Radiat Res, 146(4):453–460, 1996.
43. Iwata H, Hagiwara T, Katoh M, Yamamoto S, Yamakawa S, Shiga A, Hirouchi Y, Kobayashi K, Inoue H, Enomoto M: Historical control data of organ weight and gross findings in F344/DuCrj rats and B6C3F1 mice. Jikken Dobutsu, 42(3):383–396,

1993.

44. Brues Am, Stroud AN: Quantitation of cellular responses in the mouse spleen after irradiation. Ann N Y Acad Sci, 114:557–570, 1964.
45. Takada A, Takada Y, Kim U, Ambrus JL: Bone marrow, spleen, and thymus regeneration patterns in mice after whole-body irradiation. Radiat Res, 45(3):522–535, 1971.
46. Pecaut MJ, Nelson GA, Gridley DS: Dose and dose rate effects of whole-body gamma-irradiation: I. Lymphocytes and lymphoid organs. In Vivo, 15(3):195–208, 2001.
47. Nakano M, Kodama Y, Ohtaki K, Nakashima E, Niwa O, Toyoshima M, Nakamura N: Chromosome aberrations do not persist in the lymphocytes or bone marrow cells of mice irradiated in utero or soon after birth. Radiat Res, 167(6):693–702, 2007.
48. Kligerman AD, Halperin EC, Erexson GL, Honoré G: The persistence of lymphocytes with dicentric chromosomes following whole-body X irradiation of mice. Radiat Res, 124(1):22–27, 1990.
49. Hande MP, Natarajan AT: Induction and persistence of cytogenetic damage in mouse splenocytes following whole-body X-irradiation analysed by fluorescence in situ hybridization. IV. Dose response. Int J Radiat Biol, 74(4):441–448, 1998.
50. Tanaka K, Kohda A, Satoh K, Toyokawa T, Ichinohe K, Ohtaki M, Oghiso Y: Dose-rate effectiveness for unstable-type chromosome aberrations detected in mice after continuous irradiation with low-dose-rate gamma rays. Radiat Res, 171(3):290–301, 2009.
51. Tanaka K, Kohda A, Satoh K: Dose-rate effects and dose and dose-rate effectiveness factor on frequencies of chromosome aberrations in splenic lymphocytes from mice continuously exposed to low-dose-rate gamma-radiation. J Radiol Prot, 3(1):61-70, 2013.

Conclusion (Overall thesis)

In conclusion, radiation-induced chromosome aberrations are useful for dose estimation with cytogenetic biodosimetry in humans, and to study radiation effects in mice. Even though cytogenetic biodosimetry has been established with more than 60 years of history, there are still improvements that could be made in DRC construction and dose estimation with multiple aberration markers, used conventionally and for triage in mass-casualty events. Likewise, the understanding of short and long-term LDR-IR effects was enhanced in our study of mice exposed to radiation in their neonatal period, as previous LDR-IR studies focused on LDR-IR effects in fetal mice, adult mice and mice in multiple generations. In Chapters 1 to 4, FISH-Tr analysis for retrospective dose estimation and CBMN analysis in both WB and PBMC cultures for conventional and triage applications were explored. In Chapter 5, both unstable and stable aberrations scored in splenocyte metaphases were compared during and after LDR-IR and HDR-IR in mice monitored from 14 d to 500 d. In addition, the change in physical parameters such as spleen index and spleen histology were analyzed together with chromosome aberration kinetics.

In Chapter 1, a R-script was developed to construct a FISH-Tr DRC with age-adjusted Tr/CE and radiation dose in Gy, which reported the DRC plot with 95 % upper and lower CL, DRC coefficients and their associated SE and *p*-values, and the goodness-of-fit results (df, χ^2, *p*-value) with chi-square. If Poisson distribution is rejected in the observed Tr distribution, the linear regression model and Poisson weights can be directly modified by the user to fit the DRC more reliably. The R-script also allowed for DRC construction with multiple donors. In addition, various considerations for FISH-Tr DRC construction was discussed. (1) Age-adjustment of Tr is crucial. Both the Sigurdson's and Lucas' equation were proposed for for Tr age-adjustment. Based on the larger sample size in Sigurdson's meta-analysis as compared to Lucas', Sigurdon's equation would be preferred and is ultimately recommended in ISO 20046:2019. (2) Cells scored should be converted to CE specific for males and females as the chromosome lengths are sex-specific. Moreover, as the choice of chromosome staining is lab-dependent, CE conversion allows FISH-Tr DRCs to be reliably compared among different labs. (3) The choice of chromosomes to stain is not an important concern. Despite previous studies showing certain chromosomes with higher Tr sensitivity than others, it is now generally

accepted that Tr yield is independent of chromosome number. (4) The type of radiation exposure should be considered for retrospective dosimetry. Partial-body exposures or complicated forms of exposure could reduce Tr half-life and affect dose estimation accuracy. (5) Simple one and two-way Tr in stable cells should be scored for correct Tr age-adjustment with Sigurdson's equation. (6) DRCs should be constructed with multiple donors (≥ 3) for higher chances of successfully modelling and to better represent the population for reliable dose estimation. (7) As multiple donors are recommended, DRCs should be constructed with a pooled dataset to prevent dose overestimation, especially in higher doses of > 1 Gy. (8) Clones should be excluded from Tr scoring, especially in higher doses. This will prevent dose overestimation and reduce the chances of overdispersion in observed Tr distribution. Finally, in such a comprehensive review of factors and the development of R-script for FISH-DRC construction, we hope that future constructions of FISH-Tr DRC will allow for a more reliable retrospective dosimetry to be performed.

Chapter 2 established a CBMN harvest and fixation protocol for isolated PBMC cultures using equipment and reagents commonly used in cytogenetic biodosimetry. The CRG protocol is an alternative to the current recommended method of PBMC harvest, cytocentrifugation. In our method, a fixed cell suspension can be stored long-term in -30 °C, and fixed cells can be used in downstream experiments such as FISH with pan-centromeric probes. Cell suspensions from many donors can be easily stored in cryovials, as opposed to post-fixed slides with cells spread with cytocentrifugation, which is especially useful for mass-casualty events. Furthermore, our method was easily replicated in multiple laboratories, who used their own equipment and reagents, and only had the CRG protocol as a reference. Our method also showed good staining for Giemsa, DAPI and acridine orange. WB and PBMC cultures fixed with IAEA and CRG protocols respectively were also compared in the CBMN assay, as both protocols used hypotonic treatment and fixatives with methanol and acetic acid for cell harvest. In our donor set of males and females in their 20s to 50s, > 94 % of BNC were scorable when harvested with CRG protocol, in contrast to 14 – 89 % in IAEA protocols. Higher NDI and lower induced MN frequency were also seen in 2 Gy PBMC than 2 Gy WB cultures. Background MN frequency was higher in WB than PBMCs, and was age-dependent. Furthermore, even though humidity during cell spreading did not significantly affect NDI and MN frequency,

humidity should be optimized depending on the donor, type of cell culture and how strongly the cells are fixed. For example, PBMCs fixed with CRG protocol can withstand high to very high humidity regardless of donor age and sex. NDI should only be evaluated in viable cells with intact cytoplasm, especially in WB cultures, due to the difficulty in differentiating mononuclear T cells from unstimulated cells with only nuclear stains such as DAPI. Lastly, WB and PBMC cultures should be separately performed for DRC construction and dose estimation in CBMN assay, even though the target cells analyzed are assumed to be PHA-stimulated T lymphocytes.

Due to the differences in NDI and MN frequency observed between WB and PBMC 15 ml single cultures in Chapter 2, it was hypothesized that soluble factors present in WB but absent in PBMCs could affect CBMN parameters. As a result, Chapter 3 investigated NDI and MN frequency in 0 and 2 Gy WB and PBMCs (WB, WB-IR, PBMC, PBMC-IR) in a 6-well transwell co-culture assay. The experimental set-up only allowed soluble factors to pass through, but not cells. As some differences in NDI and MN frequency were seen between upper and lower wells, though not significant, wells of the same level were compared. In the absence of direct cell contact, cell cycle progression was more affected than DNA damage repair/induction as NDI in only PBMC and PBMC-IR co-cultured with WB and WB-IR was higher than mono-cultures of PBMC and PBMC-IR. No radiation-induced bystander effect was also observed in WB and PBMCs co-cultured with PBMC-IR or WB-IR respectively. Furthermore, different types of culture vessels also showed some differences in MN frequency, as a higher MN frequency was seen in single 15 ml cultures than mono-cultures of both WB-IR and PBMC-IR. Thus, unlike our hypothesis in Chapter 2 where co-cultures of PBMCs with WB were expected to show higher MN frequency, soluble factors in WB were not responsible for the higher MN frequency seen. In a future study, to investigate the effect of direct cell contact in CBMN assay, separated components of WB (plasma, erythrocytes, platelets, neutrophils) will be directly cultured with PBMCs to evaluate NDI and MN frequency. Lastly, similar to Chapter 2, MN frequency in all configurations of WB-IR was higher than PBMC-IR, thus CBMN assay should be separately evaluated in each type of cell culture.

In Chapter 4, a shortened 48 h CBMN assay for both WB and PBMC cultures was shown to be feasible for triage assessment in the event of a mass-casualty radiation

accident, in a low-cost method of manual scoring in Giemsa-stained cells with light microscopy. Individuals exposed to 2 Gy and 4 Gy were easily distinguished from the unirradiated worried well after MN scoring in 200 BNC, based on total MN frequency and observed MN distributions. In our donor population, 0 Gy cells were identified in 7 min while 2 and 4 Gy cells were identified within 15 min with triage scoring. Likewise, dose estimation with triage MN frequency was comparable to conventional MN frequency. Furthermore, MN frequency was higher in 48 h than 72 h cultures, and higher in 72 h (24 h @ Cyt-B) than 72 h (44 h @ Cyt-B), showing that length of culture and Cyt-B treatment could influence MN frequency.

Lastly, in Chapter 5, a large-scale mouse experiment was performed to compare short and long-term splenic effects in three irradiation conditions (LDR-IR, HDR-IR and Control mice) in neonatal B6C3F1 mice from 14 to 500 d. The mice were irradiated at 7 days old such that different radiation responses were compared during immune system development and maturation. During the early phase (14 to 35 d), the spleen was greatly affected due to some spleen enlargement seen only in HDR-IR 14 d mice. Histological analysis revealed a large lymphocyte loss in the white pulp and lymphocyte infiltration in the red pulp of HDR-14 d mice, and the spleen recovered to normal after an additional 7 days. No differences were seen between LDR-IR and Control mice up to 35 d. Kinetics of unstable (Dic, excess Ace) and stable (S and L marker) chromosome aberrations were also different between HDR-IR and LDR-IR mice. LDR-IR mice showed a higher frequency and longer persistence of Dic and excess Ace than HDR-IR mice. In contrast, HDR-IR showed a higher frequency and much longer persistence of marker chromosomes than LDR-IR mice. As such, dose-rate instead of total dose played a more significant role in spleen damage and chromosome aberration kinetics in our experiment. Moreover, the time of radiation exposure most likely affected the differences in spleen damage/recovery and chromosome aberration kinetics seen in our experiment and other experiments of adult mice exposed to LDR-IR. These results could provide a new insight in understanding different radiation responses in the radio-sensitive spleen between neonates/children and adults.

Acknowledgements (Overall thesis)

This research was kindly funded by the Armed Forces Radiobiology Research Institute under work units RBB4352319 (Chapter 1), RAB4AM and AFR-B4-4313 (Chapter 2), JSPS KAKENHI Grant Number 19K08142 (Chapters 3 and 4), and the Nuclear Energy Science & Technology and Human Resource Development Project (through concentrating wisdom) from the Ministry of Education, Culture, Sports, Science and Technology of Japan (Chapter 5).

This research would not have been possible without the help of other researchers and students: Prof. Tomisato Miura, Dr. Yohei Fujishima, Ms. Kai Takebayashi, Mr. Ryo Nakayama, Dr. Mitsuaki A. Yoshida, Dr. Kosuke Kasai, Dr. Kentaro Ariyoshi, Dr. Yu Abe, Dr. Akifumi Nakata, Prof. Akira Sakai, Dr. Daisuke Iizuka, Dr. Yi Shang, Dr. Chizuru Tsuruoka, Dr. Shizuka Kakinuma, Dr. Hideaki Yamashiro, Prof. William F. Blakely, Dr. Ruth C. Wilkins, Dr. Christelle Chua En Lin, Ms. Chew Zi Huai, Mr. Kaito Yanagidate and Mr. Yura Hayasaka. We also like to extend our gratitude to our laboratory staff: Mr Yuki Sato and Ms Naomi Sasaki.

We would also like to thank the donors for the blood samples, and the Committee of Medical Ethics in Hirosaki University Graduate School of Medicine for approving the use of human blood for experimental research with informed consent.

We declare that there is no conflict of interest. The opinions, conclusions and recommendations expressed or implied do not necessarily reflect the views of the Armed Forces Radiobiology Research Institute, Uniformed Services University of the Health Sciences, Department of Defense or any other department or agency of the U.S. Federal Government.

Lastly, we would like to express our gratitude to the publisher, Taylor and Francis and the journal, International Journal of Radiation Biology, for allowing us to include published data in this thesis.

Abstract in Japanese (Overall thesis)

「細胞遺伝学的線量評価法の改善のためのヒトとマウスにおける放射線誘発染色体異常に関する研究および低線量率電離放射線のさらなる理解」

Valerie Goh Swee Ting
弘前大学大学院保健学研究科、生体検査科学領域

この論文は、ヒトとマウスの両方のさまざまな研究で使用される放射線誘発性染色体異常の解析を報告する。ヒト末梢血を用いた生物学的線量評価では、プロトコル、染色体異常スコアリング法、および解析結果の解釈において、さまざまな評価技術を改善し、線量推定の信頼性向上に貢献した。これについては、第 1 章から第 4 章で詳細に述べる。大規模なマウスモデルにおける生物影響研究では、新生児マウスに対する高線量率および低線量率の電離放射線（HDR-IR、LDR-IR）の影響の短期的および長期的影響を解析した。新生児/小児期と成熟期における放射線応答の違いを解明するため、発達期マウスにおける放射線被ばく影響を評価した。これについては第 5 章で述べる。

第 1 章では、信頼性の高い線量推定のための FISH-転座（Tr）用線量反応曲線（DRC）の構築法について述べる。本研究では、1、2、および 4 番染色体蛍光標識により検出された Tr 頻度の DRC は、二動原体染色体（Dic）用の修正 R スクリプトを使用して、一般化線形モデリングで構築した。FISH-Tr-DRC は、少なくとも 3 人のドナーと 1 Gy 未満の少なくとも 5 つの線量ポイントで作成する必要があり、自然発生的な Tr は、Sigurdson 等の年齢補正式で差し引く必要があり、スコアリングされた細胞は、相対ゲノム量から等価細胞数あたりの Tr 数に変換する必要があることを明らかにした。

第 2 章では、細胞遺伝学的線量評価で一般的に使用される試薬および機器を使用して、分離末梢血単核球（PBMC）を培養し、細胞懸濁液として長期間保存できる CBMN 法の代替プロトコルを提案した。本研究で提案されたプロトコルでは、IAEA が推奨するプロトコルとは対照的に、ドナーの年齢、性別、

細胞展開中の湿度に関係なく、解析対象と判断される二核細胞を 94% 以上の頻度で得ることが可能でる。さらに、代替プロトコルでは、2 Gy X 線照射血を用いた全血（WB）培養と PBMC 培養の比較において、WB 培養では有意に核分裂指数（NDI）が高く、また、微小核（MN）頻度低いことが明らかとなった。このことから、CBMN 法では、線量評価の際、培養システムに応じた検量線を用いることが推奨される。

第 3 章では、0 および 2 Gy 照射した WB と PBMC の 6 ウェルトランスウェル共培養および単一培養をさまざまな組み合わせで検証した研究を述べる。0 および 2 Gy 照射した WB と PBMC の共培養では、WB 培養に由来する何らかの可溶性因子が NDI を大幅に増加させたが、PBMC 培養由来の可溶性因子は NDI を増加させなかった。これは、MN 頻度の増加を期待した最初の仮説とは対照的だった。一方、すべての組み合わせで、2 Gy WB の MN 頻度は 2 Gy PBMC よりも一貫して高かった。これは、CBMN 法において WB および PBMC 培養を別々に評価する必要があるという第 2 章の提言を支持する。

第 4 章では、大量の死傷者による放射線事故が発生した場合のトリアージ線量評価のために、48 時間の細胞培養の短縮 CBMN 法の開発について述べる。IAEA と ISO は、培養時間が 48 時間と短いため、Dic 法によるトリアージ評価を推奨している。しかし、トリアージのために 50 分裂中期像の解析に要する時間は、スコアラー1 人あたり 150 分かかる場合がある。対照的に、MN 解析は、染色体核型の事前知識がなくても迅速に実行可能である。この研究では、従来の 72 時間の培養時間は 48 時間に短縮され、経験豊富なスコアラーが患者あたり 200 個の二核細胞解析を 15 分以内に完了できるトリアージ評価のための CBMN 法代替プロトコルが提案された。

第 5 章では、量子科学技術研究開発機構（QST）と共同で大規模なマウス実験を実施した研究を述べる。7 日齢オスおよびメス B6C3F1 マウスに、6 mGy/h または 30 Gy/h の ^{137}Cs γ線を総線量 4 Gy 照射した。14、21、28、35、42、75、100、200、300、400 および 500 日齢にマウスを安楽死処理した。体重、脾

臓質量および脾臓指数をモニターするとともに、脾細胞培養後に染不安定型染色体異常および安定型染色体異常を解析した。この研究では、被ばく線量よりも線量率が脾臓における放射線障害や染色体異常の動態に影響を及ぼした。さらに、我々の実験における新生児のLDR-IR中のDic動態は、他の成体マウス実験とは異なり、放射線照射後の Dic の生物学的半減期に違いがある可能性を示している。これらの結果は、発達期マウスと成熟マウス間の脾臓における異なる放射線応答を理解する上での新しい洞察を提供する。